CHAPTER

EIGHT

NUMERICAL METHODS FOR THE "PARABOLIZED" NAVIER-STOKES EQUATIONS

The computational fluid dynamics (CFD) "frontier" has advanced from the simple to the complex. Generally, the simple methods taxed the available computational power when they occupied the frontier. The evolution proceeded from methods for various forms of the potential and boundary-layer equations to the Euler equations and then to various "parabolized" forms of the Navier-Stokes equations that are the subject of this chapter. Most of the schemes were developed at a time when the use of the full Navier-Stokes equations was prohibitive for many problems because of the large computer memory or CPU time required. If such parabolized schemes were considered economical of computer resources when they were introduced, they are still so. However, the need to save CPU time has diminished in a relative sense because of the incredible reduction in cost per operation experienced in recent times. Numerous numerical strategies will be discussed in this chapter. They all share the common characteristic that the steady form of the governing equations is employed, and the solution is "marched" in space. Some of the solution strategies to be described in this chapter share aspects in common with methods for the full Navier-Stokes equations discussed in Chapter 9.

8.1 INTRODUCTION

The boundary-layer equations can be utilized to solve many viscous flow problems, as discussed in Chapter 7. There are, however, a number of very

important viscous flow problems that cannot be solved by using the boundary-layer equations. In these problems, the boundary-layer assumptions are not valid. For example, if the inviscid flow is fully merged with the viscous flow, the two flows cannot be solved independently of each other, as required by boundary-layer theory. As a result, it becomes necessary to solve a set of equations that is valid in both the inviscid and viscous flow regions.

Examples of viscous flow fields where the boundary-layer equations are not the appropriate governing equations are shown in Figs. 8.1(a)–(d). The hypersonic rarefied flow near the sharp leading edge of a flat plate [Fig. 8.1(a)] is a classic example of a viscous flow field that cannot be solved by the boundary-layer equations. In fact, very near the leading edge, the flow is not a continuum, so that the Navier-Stokes equations are invalid. In the merged-layer region, where the flow can first be considered a continuum, the shock layer and the viscous layer are fully merged and indistinguishable from each other. Further downstream, the shock layer coalesces into a discontinuity, and a distinct inviscid layer develops between the shock wave and the viscous layer. This is the beginning of the interaction region, which is further divided into the strong- and weak-interaction regions. The weak-interaction region eventually evolves into the classic Prandtl boundary-layer flow further downstream. Obviously, the boundary-layer equations cannot be used in the merged-layer region because the viscous layer and the shock layer are completely merged. At the beginning of the strong-interaction region, the viscous flow cannot be solved independently of the inviscid flow because of the strong interaction. In the weak-interaction region, it is possible to solve the inviscid and viscous portions of the flow separately, but this must be done in an iterative fashion, as discussed in Chapter 7. That is, the boundary-layer equations can be computed initially using approximate edge conditions. With the computed displacement thickness, the inviscid portion of the flow field can then be determined. This provides new edge conditions for the recomputation of the boundary layer. This procedure can be repeated until the solution for the entire flow field does not change between iterations. Unless the interaction is very weak, it has been observed that this iterative procedure is often inferior to solving a set of equations that is valid in both the inviscid and viscous flow regions (Davis and Rubin, 1980).

Figure 8.1(b) illustrates a mixing layer problem for which the boundary-layer (thin-shear-layer) equations are not applicable. Across the mixing layer, a strong normal pressure gradient exists. Consequently, the usual boundary-layer (thin-shear-layer) equations, which contain the normal momentum equation

$$\frac{\partial p}{\partial y} = 0 \tag{8.1}$$

are not valid. In this case, a more complete normal momentum equation is required. Another example of a flow field where the boundary-layer equations may not be applicable is the supersonic flow around a blunt body at high altitude, as seen in Fig. 8.1(c). In the region between the shock wave and the

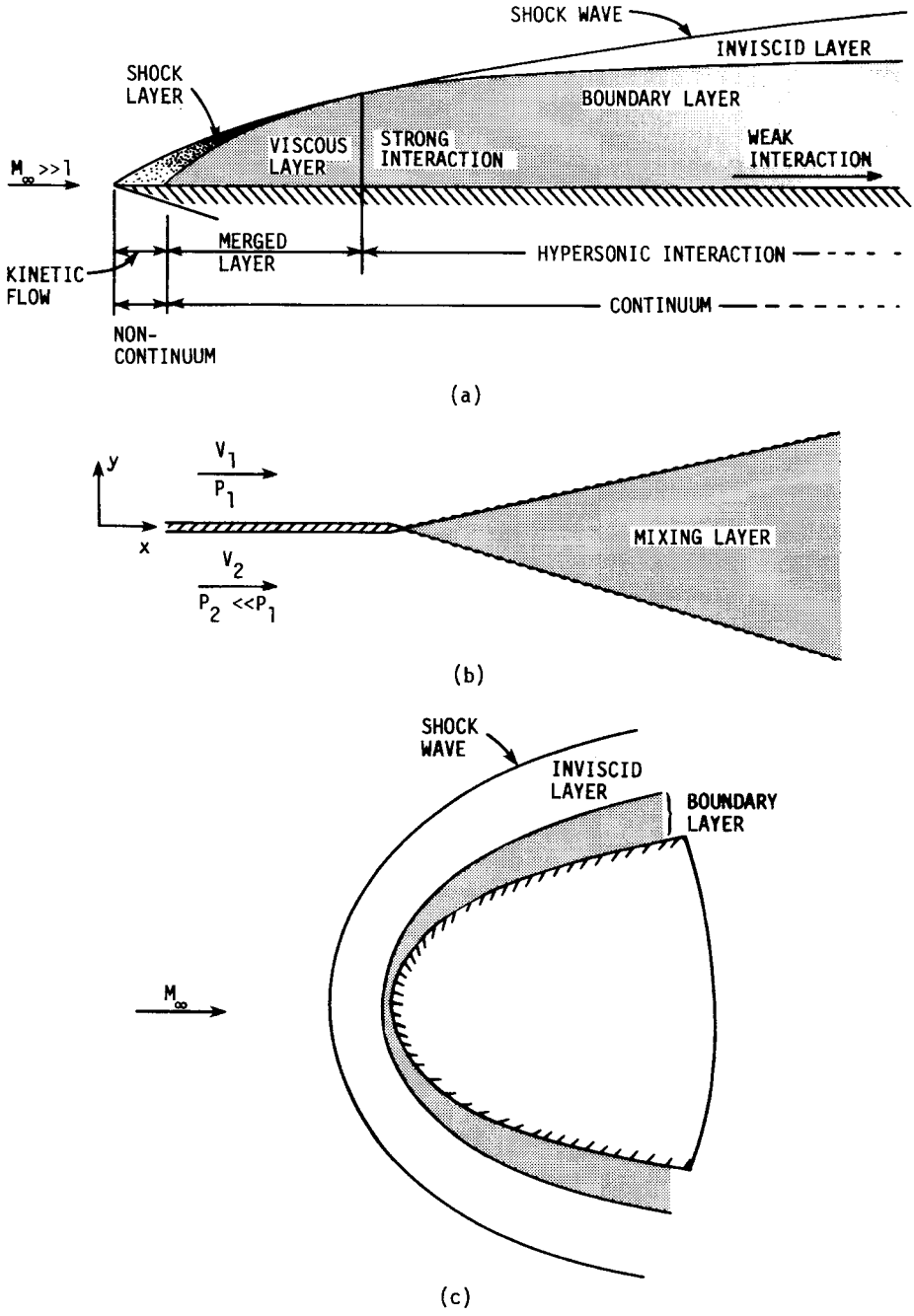

Figure 8.1 Examples of flow fields where the boundary-layer equations are not applicable. (a) Leading edge of a flat plate in a hypersonic rarefied flow. (b) Mixing layer with a strong transverse pressure gradient. (c) Blunt body in a supersonic flow at high altitude.

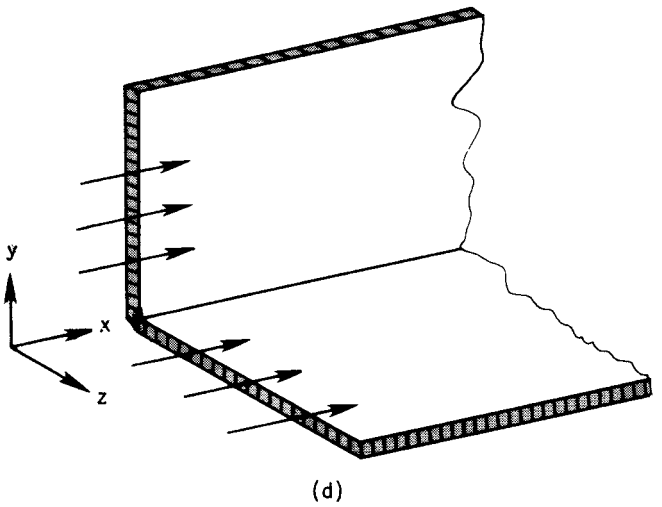

Figure 8.1 Examples of flow fields where the boundary-layer equations are not applicable (*Cont.*). (d) Flow along a streamwise corner.

body (i.e., the shock layer) there exists a strong interaction between the boundary layer and the inviscid flow region. As a result, sets of equations that are valid in both the inviscid and viscous regions are normally used to compute this type of flow field.

The flow along the corner formed by two intersecting surfaces, illustrated in Fig. 8.1(d), provides a final example of a flow for which the boundary-layer equations are not applicable. As pointed out in Chapter 7, the boundary-layer equations only include viscous derivatives with respect to a single "normal" coordinate direction. Very near the corner, viscous derivatives with respect to *both* "normal" directions will be important. Such a flow configuration occurs often in applications, as for example, near wing-body junctures and in rectangular channels.

The complete Navier-Stokes equations are an obvious set of equations that can be used to solve the flow fields in Fig. 8.1 as well as all other viscous flow fields for which the boundary-layer equations are not applicable. In some cases they are the only equations that apply. Unfortunately, the Navier-Stokes equations are very difficult to solve in their complete form. In general, a very large amount of computer time and storage is necessary to obtain a solution with these equations. This is particularly true for the compressible Navier-Stokes equations, which are a mixed set of elliptic-parabolic equations for a steady flow and a mixed set of hyperbolic-parabolic equations for an unsteady flow. The time-dependent solution procedure is normally used when a steady flow field is computed. That is, the unsteady Navier-Stokes equations are integrated in time until a steady-state solution is achieved. Thus, for a three-dimensional (3-D) flow field, a four-dimensional (4-D) (three space, one time) problem must be

solved when the compressible Navier-Stokes equations are employed. Methods for solving the complete Navier-Stokes equations are discussed in Chapter 9.

Fortunately, for many of the viscous flow problems where the boundary-layer equations are not applicable, it is possible to solve a reduced set of equations that fall between the complete Navier-Stokes equations and the boundary-layer equations in terms of complexity. These reduced equations belong to a class of equations that is often referred to as the "thin-layer" or "parabolized" Navier-Stokes equations. There are several sets of equations that fall within this class:

1. thin-layer Navier-Stokes (TLNS) equations
2. parabolized Navier-Stokes (PNS) equations
3. reduced Navier-Stokes (RNS) equations
4. partially parabolized Navier-Stokes (PPNS) equations
5. viscous shock-layer (VSL) equations
6. conical Navier-Stokes (CNS) equations

The sets of equations in this class are characterized by the fact that they are applicable to both inviscid and viscous flow regions. In addition, the equations all contain a nonzero normal pressure gradient. This is a necessary requirement if viscous and inviscid regions are to be solved simultaneously. Finally, the equations in this class omit all viscous terms containing derivatives in the streamwise direction.

There are two very important advantages that result when these equations are used instead of the complete Navier-Stokes equations. First, there are fewer terms in the equations, which leads to some reduction in the required computation time. Second, and by far the most important advantage, is the fact that for a steady flow all of the equations in this class, except the TLNS equations, are a mixed set of hyperbolic-parabolic equations in the streamwise direction (provided that certain conditions are met). In other words, the Navier-Stokes equations are "parabolized" in the streamwise direction. As a consequence, the equations can be solved using a boundary-layer type of marching technique, so that a typical problem is reduced from four dimensions to three spatial dimensions. A substantial reduction in computation time and storage is thus achieved. In this chapter we will discuss the derivation of the equations in the "thin-layer Navier-Stokes" class and present a number of methods for solving them.

8.2 THIN-LAYER NAVIER-STOKES EQUATIONS

The unsteady boundary-layer equations can be formally derived from the complete Navier-Stokes equations by neglecting terms of the order of $1/(\mathrm{Re}_L)^{1/2}$ and smaller. As a consequence of this order-of-magnitude analysis, all viscous terms containing derivatives parallel to the body surface are dropped, since they are substantially smaller than viscous terms containing derivatives normal to the wall. In addition, the normal momentum equation is reduced to a simple equation [i.e., Eq. (8.1) for a Cartesian coordinate system] that indicates that the

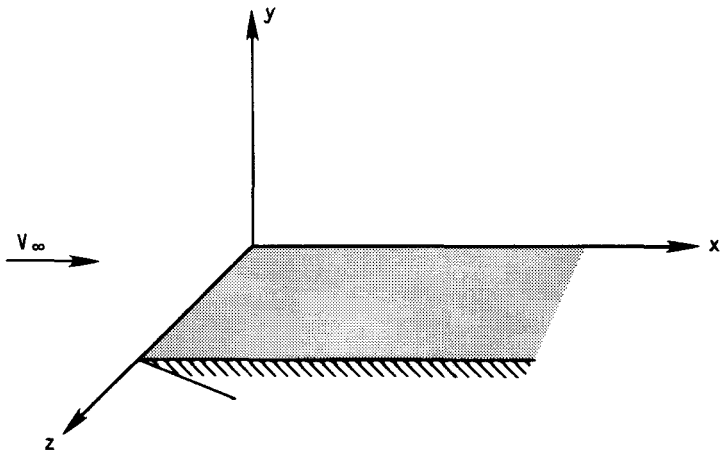

Figure 8.2 Flow over a flat plate.

normal pressure gradient is negligible. In the thin-layer approximation to the Navier-Stokes equations, the viscous terms containing derivatives in the directions parallel to the body surface are again neglected in the unsteady Navier-Stokes equations, but all other terms in the momentum equations are retained. One of the principal advantages of retaining the terms that are normally neglected in boundary-layer theory is that separated and reverse flow regions can be computed in a straightforward manner. Also, flows that contain a large normal pressure gradient, such as those shown in Fig. 8.1, can be readily computed.

The concept of the thin-layer approximation also arises from a detailed examination of typical high Reynolds number computations involving the complete Navier-Stokes equations (Baldwin and Lomax, 1978). In these computations, a substantial fraction of the available computer storage and time is expended in resolving the normal gradients in the boundary layer, since a highly stretched grid is required. As a result, the gradients parallel to the body surface are usually not resolved in an adequate manner even though the corresponding viscous terms are retained in the computations. Hence, for many Navier-Stokes computations it makes sense to drop those terms that are not being adequately resolved, provided that they are reasonably small. This naturally leads to the use of the thin-layer Navier-Stokes equations.

Upon simplifying the complete Navier-Stokes equations using the thin-layer approximation for the flow geometry shown in Fig. 8.2, the TLNS equations in Cartesian coordinates become as follows:

continuity:

$$\frac{\partial \rho}{\partial t} + \frac{\partial \rho u}{\partial x} + \frac{\partial \rho v}{\partial y} + \frac{\partial \rho w}{\partial z} = 0 \tag{8.2}$$

x momentum:

$$\frac{\partial \rho u}{\partial t} + \frac{\partial}{\partial x}(p + \rho u^2) + \frac{\partial}{\partial y}\left(\rho uv - \mu \frac{\partial u}{\partial y}\right) + \frac{\partial}{\partial z}(\rho uw) = 0 \tag{8.3}$$

y momentum:

$$\frac{\partial \rho v}{\partial t} + \frac{\partial}{\partial x}(\rho uv) + \frac{\partial}{\partial y}\left(p + \rho v^2 - \frac{4}{3}\mu \frac{\partial v}{\partial y}\right) + \frac{\partial}{\partial z}(\rho vw) = 0 \tag{8.4}$$

z momentum:

$$\frac{\partial \rho w}{\partial t} + \frac{\partial}{\partial x}(\rho uw) + \frac{\partial}{\partial y}\left(\rho vw - \mu \frac{\partial w}{\partial y}\right) + \frac{\partial}{\partial z}(p + \rho w^2) = 0 \tag{8.5}$$

energy:

$$\frac{\partial E_t}{\partial t} + \frac{\partial}{\partial x}(E_t u + pu) + \frac{\partial}{\partial y}\left(E_t v + pv - \mu u \frac{\partial u}{\partial y} - \frac{4}{3}\mu v \frac{\partial v}{\partial y} - \mu w \frac{\partial w}{\partial y} - k \frac{\partial T}{\partial y}\right) + \frac{\partial}{\partial z}(E_t w + pw) = 0 \tag{8.6}$$

These equations are written for a laminar flow, but they can be readily modified to apply to a turbulent flow using the techniques of Section 5.4.

For more complicated body geometries it becomes necessary to map the body surface into a transformed coordinate surface in order to apply the thin-layer approximation. Suppose we apply the general transformation given by

$$\begin{aligned} \xi &= \xi(x, y, z, t) \\ \eta &= \eta(x, y, z, t) \\ \zeta &= \zeta(x, y, z, t) \\ t &= t \end{aligned} \tag{8.7}$$

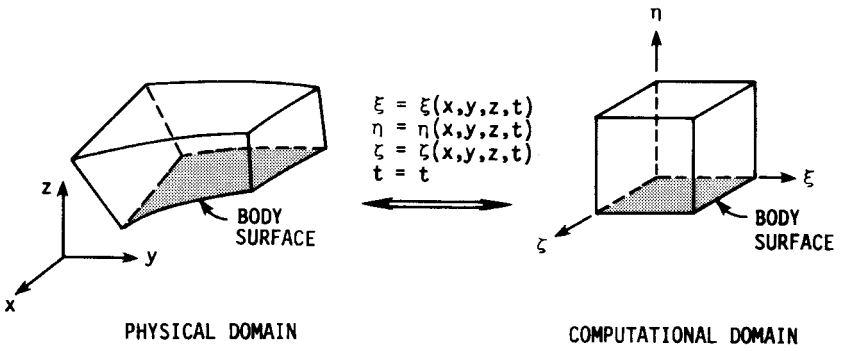

Figure 8.3 Generalized transformation. (a) Physical domain. (b) Computational domain.

to the complete Navier-Stokes equations (see Section 5.6.2) and let the body surface be defined as $\eta = 0$, as seen in Fig. 8.3. The transformed Navier-Stokes equations in strong conservation-law form become

$$\left(\frac{\mathbf{U}}{J}\right)_t + \left(\frac{\mathbf{U}\xi_t + \mathbf{E}\xi_x + \mathbf{F}\xi_y + \mathbf{G}\xi_z}{J}\right)_\xi + \left(\frac{\mathbf{U}\eta_t + \mathbf{E}\eta_x + \mathbf{F}\eta_y + \mathbf{G}\eta_z}{J}\right)_\eta + \left(\frac{\mathbf{U}\zeta_t + \mathbf{E}\zeta_x + \mathbf{F}\zeta_y + \mathbf{G}\zeta_z}{J}\right)_\zeta = 0 \tag{8.8}$$

where J is the Jacobian of the transformation and **U**, **E**, **F**, and **G** are defined by Eqs. (5.44). We now apply the thin-layer approximation to the transformed Navier-Stokes equations. This approximation allows us to drop all viscous terms containing partial derivatives with respect to ξ and ζ. The resulting thin-layer equations may be written as (Pulliam and Steger, 1978):

$$\frac{\partial \mathbf{U}_2}{\partial t} + \frac{\partial \mathbf{E}_2}{\partial \xi} + \frac{\partial \mathbf{F}_2}{\partial \eta} + \frac{\partial \mathbf{G}_2}{\partial \zeta} = \frac{\partial \mathbf{S}_2}{\partial \eta} \tag{8.9}$$

where

$$\begin{aligned}
\mathbf{U}_2 &= \frac{\mathbf{U}}{J} \\
\mathbf{E}_2 &= \frac{1}{J}\begin{bmatrix} \rho U \\ \rho u U + \xi_x p \\ \rho v U + \xi_y p \\ \rho w U + \xi_z p \\ (E_t + p)U - \xi_t p \end{bmatrix} \\
\mathbf{F}_2 &= \frac{1}{J}\begin{bmatrix} \rho V \\ \rho u V + \eta_x p \\ \rho v V + \eta_y p \\ \rho w V + \eta_z p \\ (E_t + p)V - \eta_t p \end{bmatrix} \\
\mathbf{G}_2 &= \frac{1}{J}\begin{bmatrix} \rho W \\ \rho u W + \zeta_x p \\ \rho v W + \zeta_y p \\ \rho w W + \zeta_z p \\ (E_t + p)W - \zeta_t p \end{bmatrix}
\end{aligned} \tag{8.10}$$

and all the viscous terms are contained in

$$\mathbf{S}_2 = \frac{1}{J}\begin{bmatrix} 0 \\ \mu\left(\eta_x^2 + \eta_y^2 + \eta_z^2\right)u_\eta + \dfrac{\mu}{3}(\eta_x u_\eta + \eta_y v_\eta + \eta_z w_\eta)\eta_x \\ \mu\left(\eta_x^2 + \eta_y^2 + \eta_z^2\right)v_\eta + \dfrac{\mu}{3}(\eta_x u_\eta + \eta_y v_\eta + \eta_z w_\eta)\eta_y \\ \mu\left(\eta_x^2 + \eta_y^2 + \eta_z^2\right)w_\eta + \dfrac{\mu}{3}(\eta_x u_\eta + \eta_y v_\eta + \eta_z w_\eta)\eta_z \\ \left(\eta_x^2 + \eta_y^2 + \eta_z^2\right)\left[\dfrac{\mu}{2}(u^2 + v^2 + w^2)_\eta + kT_\eta\right] \\ + \dfrac{\mu}{3}(\eta_x u + \eta_y v + \eta_z w)(\eta_x u_\eta + \eta_y v_\eta + \eta_z w_\eta) \end{bmatrix} \tag{8.11}$$

For compactness, Eqs. (8.10) are written in terms of the contravariant velocity components (U, V, W), which are defined by

$$\begin{aligned} U &= \xi_t + \xi_x u + \xi_y v + \xi_z w \\ V &= \eta_t + \eta_x u + \eta_y v + \eta_z w \\ W &= \zeta_t + \zeta_x u + \zeta_y v + \zeta_z w \end{aligned} \tag{8.12}$$

The contravariant velocity components U, V, W are in directions normal to constant ξ, η, ζ surfaces, respectively.

Although the TLNS equations are considerably less complicated than the complete Navier-Stokes equations, a substantial amount of computer effort is still required to solve these equations. The TLNS equations are a mixed set of hyperbolic-parabolic PDEs in time. As a consequence, the "time-dependent" approach can be applied in an identical manner to the procedure normally used to solve the compressible Navier-Stokes equations. Thus we will postpone our discussion of methods for solving the TLNS equations until Chapter 9, where the methods for solving the complete Navier-Stokes equations are discussed.

8.3 "PARABOLIZED" NAVIER-STOKES EQUATIONS

The "parabolized" Navier-Stokes (PNS) equations have steadily gained popularity because they can be used to predict complex 3-D steady supersonic viscous flow fields in an efficient manner. This efficiency is achieved because the equations can be solved using a space-marching technique as opposed to the time-marching technique that is normally employed for the complete Navier-Stokes equations. As a result, the computational effort required to solve the PNS equations for an entire supersonic flow field is similar to the effort required to solve either the inviscid portion of the flow field using the Euler equations or the viscous portion of the flow field using the boundary-layer equations. Furthermore, since the PNS equations are valid in both the inviscid

and viscous portions of the flow field, the interaction between these regions of the flow field is automatically taken into account.

The term "parabolized" Navier-Stokes equations is somewhat of a misnomer, since the equations are actually a mixed set of hyperbolic-parabolic equations, provided that certain conditions are met. These conditions include the requirements that the inviscid outer region of the flow be supersonic and the streamwise velocity component be everywhere positive. Note that the last requirement excludes streamwise flow separation, but crossflow separation is permitted. An additional constraint is caused by the presence of the streamwise pressure gradient in the streamwise momentum equation. If this term is included everywhere in the flow field, then upstream influence can occur in the subsonic portion of the boundary layer and a single-pass space-marching method of solution is not well posed. This leads to exponentially growing solutions, which are often called *departure solutions*. Several techniques have been proposed to circumvent this difficulty, and they are discussed in Section 8.3.2.

8.3.1 Derivation of PNS Equations

The derivation of the PNS equations from the complete Navier-Stokes equations is, in general, not as rigorous as the derivation of the boundary-layer equations. Because of this, slightly different versions of the PNS equations have appeared in the literature. These versions differ in some cases because of the type of flow problem being considered. However, in all cases the normal pressure gradient term is retained, and the second derivative terms with respect to the streamwise direction are omitted.

One of the earliest studies involving the use of the PNS equations was by Rudman and Rubin (1968). In their study, the hypersonic laminar flow near the leading edge of a flat plate [see Fig. 8.1(a)] was computed using a set of PNS equations. Rudman and Rubin derived their PNS equations from the complete Navier-Stokes equations using a series expansion technique. This method for reducing the complexity of the Navier-Stokes equations is an alternative to the order-of-magnitude analysis used in Chapter 5 to derive the boundary-layer equations. In the series expansion method, the flow variables are first nondimensionalized with respect to local reference conditions in order to estimate the magnitude of the various terms in the Navier-Stokes equations. The flow variables are then expanded in an appropriate series. Rudman and Rubin assumed the following form:

$$
\begin{aligned}
u &= V_\infty(u_0^* + \epsilon u_1^* + \cdots) \\
v &= V_\infty \delta^*(v_0^* + \epsilon v_1^* + \cdots) \\
p &= p_\infty p_{\text{ref}}^*(p_0^* + \epsilon p_1^* + \cdots) \\
\rho &= \rho_\infty \rho_{\text{ref}}^*(\rho_0^* + \epsilon \rho_1^* + \cdots) \\
T &= T_\infty T_{\text{ref}}^*(T_0^* + \epsilon T_1^* + \cdots)
\end{aligned}
\tag{8.13}
$$

$$\mu = \mu_\infty \mu_{\text{ref}}^* (\mu_0^* + \epsilon \mu_1^* + \cdots)$$
$$x = x^* L \qquad y = y^* \delta \qquad \delta = \delta^* L$$

where the superscript asterisk denotes a nondimensional quantity, the subscript ref represents the local reference value of a flow variable nondimensionalized with respect to the free stream value, L is the characteristic length in the x direction, and δ is the characteristic length in the y direction. The first term in the series expansion (denoted with a subscript zero) is used to obtain the zeroth-order solution, while both the first and second terms are needed to obtain the first-order solution. The relative magnitude of the coefficient ϵ is determined later in the analysis. For the relatively thin disturbed region shown in Fig. 8.1(a), the gradients normal to the surface are much greater than the gradients parallel to the surface, and δ^* can be assumed to be small.

When the expansions are substituted into the 2-D steady Navier-Stokes equations, the following nondimensional equations result (for convenience the subscript zero has been dropped):

continuity:

$$\frac{\partial \rho^* u^*}{\partial x^*} + \frac{\partial \rho^* v^*}{\partial y^*} = O(\epsilon) \tag{8.14}$$

x momentum:

$$\rho^* u^* \frac{\partial u^*}{\partial x^*} + \rho^* v^* \frac{\partial u^*}{\partial y^*} = -\Delta^2 \frac{\partial p^*}{\partial x^*} + \frac{1}{(\delta^*)^2 \operatorname{Re}_{\text{ref}}} \frac{\partial}{\partial y^*} \left(\mu^* \frac{\partial u^*}{\partial y^*} \right) + O\left[\epsilon, (\operatorname{Re}_{\text{ref}})^{-1} \right] \tag{8.15}$$

y momentum:

$$\rho^* u^* \frac{\partial v^*}{\partial x^*} + \rho^* v^* \frac{\partial v^*}{\partial y^*} = -\left(\frac{\Delta}{\delta^*} \right)^2 \frac{\partial p^*}{\partial y^*} + \frac{1}{(\delta^*)^2 \operatorname{Re}_{\text{ref}}} \left[\frac{4}{3} \frac{\partial}{\partial y^*} \left(\mu^* \frac{\partial v^*}{\partial y^*} \right) + \frac{\partial}{\partial x^*} \left(\mu^* \frac{\partial u^*}{\partial y^*} \right) - \frac{2}{3} \frac{\partial}{\partial y^*} \left(\mu^* \frac{\partial u^*}{\partial x^*} \right) \right] + O\left[\epsilon, (\operatorname{Re}_{\text{ref}})^{-1} \right] \tag{8.16}$$

energy:

$$\Delta^2 \left[\rho^* u^* \frac{\partial T^*}{\partial x^*} + \rho^* v^* \frac{\partial T^*}{\partial y^*} + (\gamma - 1) p^* \left(\frac{\partial u^*}{\partial x^*} + \frac{\partial v^*}{\partial y^*} \right) - \frac{\gamma}{\text{Pr}} \frac{1}{(\delta^*)^2 \operatorname{Re}_{\text{ref}}} \frac{\partial}{\partial y^*} \left(\mu^* \frac{\partial T^*}{\partial y^*} \right) \right]$$

$$= \frac{\gamma - 1}{(\delta^*)\,\mathrm{Re}_{\mathrm{ref}}} \left\{ \mu^* \left(\frac{\partial u^*}{\partial y^*} \right)^2 + (\delta^*)^2 \left[\frac{4}{3}\mu^* \left(\frac{\partial u^*}{\partial x^*} \right)^2 + \frac{4}{3}\mu^* \left(\frac{\partial v^*}{\partial y^*} \right)^2 - \frac{4}{3}\mu^* \frac{\partial u^*}{\partial x^*} \frac{\partial v^*}{\partial y^*} + 2\mu^* \frac{\partial v^*}{\partial x^*} \frac{\partial u^*}{\partial y^*} \right] + \epsilon \left[\mu_1^* \left(\frac{\partial u^*}{\partial y^*} \right)^2 + 2\mu^* \frac{\partial u^*}{\partial y^*} \frac{\partial u_1^*}{\partial y^*} \right] \right\}$$

$$+ O\left[\Delta^2 (\mathrm{Re}_{\mathrm{ref}})^{-1}, (\delta^*)^2 (\mathrm{Re}_{\mathrm{ref}})^{-1}, \frac{\epsilon^2 (\mathrm{Re}_{\mathrm{ref}})^{-1}}{(\delta^*)^2} \right] \tag{8.17}$$

In the above equations, $\mathrm{Re}_{\mathrm{ref}} = (\rho_\infty V_\infty L/\mu_\infty)(\rho^*_{\mathrm{ref}}/\mu^*_{\mathrm{ref}})$, $\Delta^2 = T^*_{\mathrm{ref}}/M_\infty^2\gamma$, and a perfect gas is assumed.

The next step in the process is to determine which terms can be neglected in comparison to other terms in Eqs. (8.14)–(8.17). In order to do this, we need to obtain estimates for the magnitudes of $\mathrm{Re}_{\mathrm{ref}}$, Δ^2, and $(\Delta/\delta^*)^2$ in the various regions of the flow field. From our previous discussions on boundary layers, we know that for a thin viscous layer, $\mathrm{Re}_{\mathrm{ref}}$ is of order $1/(\delta^*)^2$. Also, near the edge of the viscous layer, Δ^2 is proportional to $(M_\infty^2)^{-1}$, since $T^*_{\mathrm{ref}} = 1$ in this region. From compressible boundary-layer theory (Schlichting, 1968) it is known that Δ^2 can achieve a maximum value of the order of $(\gamma - 1)/2A\gamma$, where A varies between $\mathrm{Pr}^{-1/2}$ for an adiabatic wall to about 4 in the cold wall limit. Hence for most cases, we can assume $\Delta^2 \ll 1$, provided that $M_\infty \geqslant 5$. Rudman and Rubin (1968) have shown that $(\Delta/\delta^*)^2$ is of order unity in the merged-layer region. Further downstream in the strong-interaction region, they have shown that $(\Delta/\delta^*)^2$ is very large near the wall but decreases in value to order unity at the edge of the boundary layer. Using the above information for the relative magnitudes of $\mathrm{Re}_{\mathrm{ref}}$, Δ^2, and $(\Delta/\delta^*)^2$ in the various regions of the flow field, we can now simplify Eqs. (8.14)–(8.17). For the set of equations valid to zeroth-order ($M_\infty \geqslant 5$), we can neglect terms of order $(\delta^*)^2$, Δ^2, and ϵ; but we must retain terms of order $(\Delta/\delta^*)^2$. As a result, the continuity equation and the y momentum equation cannot be reduced further. On the other hand, the x momentum equation is simplified, since the streamwise pressure gradient term can be dropped and the energy equation reduces to

$$\frac{\partial u^*}{\partial y^*} = 0 \tag{8.18}$$

If we combine Eq. (8.18) with the x momentum equation, we find that

$$u^* = \text{const} = 1 \tag{8.19}$$

or

$$u = V_\infty$$

Obviously, this is a trivial result (applicable only in the free stream), and we are forced to retain higher-order terms [i.e., $(\delta^*)^2$, Δ^2, and ϵ] in order to obtain a meaningful energy equation. Note that we can eliminate many of the higher-order terms by employing Eq. (8.19). The final forms of the zeroth-order equations in dimensional form become

continuity:

$$\frac{\partial \rho u}{\partial x} + \frac{\partial \rho v}{\partial y} = 0 \tag{8.20}$$

x momentum:

$$\rho u \frac{\partial u}{\partial x} + \rho v \frac{\partial u}{\partial y} = \frac{\partial}{\partial y}\left(\mu \frac{\partial u}{\partial y}\right) \tag{8.21}$$

y momentum:

$$\rho u \frac{\partial v}{\partial x} + \rho v \frac{\partial v}{\partial y} = -\frac{\partial p}{\partial y} + \frac{4}{3}\frac{\partial}{\partial y}\left(\mu \frac{\partial v}{\partial y}\right) + \frac{\partial}{\partial x}\left(\mu \frac{\partial u}{\partial y}\right) - \frac{2}{3}\frac{\partial}{\partial y}\left(\mu \frac{\partial u}{\partial x}\right) \tag{8.22}$$

energy:

$$\rho u c_v \frac{\partial T}{\partial x} + \rho v c_v \frac{\partial T}{\partial y} = -p\left(\frac{\partial u}{\partial x} + \frac{\partial v}{\partial y}\right) + \frac{\partial}{\partial y}\left(k \frac{\partial T}{\partial y}\right) + \mu\left(\frac{\partial u}{\partial y}\right)^2 + \frac{4}{3}\mu\left(\frac{\partial v}{\partial y}\right)^2 \tag{8.23}$$

The zeroth-order equations are valid for leading edge flow fields when $M_\infty \geqslant 5$, while the first-order equations are applicable when $M_\infty \geqslant 2$. The zeroth-order equations were derived by neglecting terms of order $(\delta^*)^2$, Δ^2, and ϵ. Since ϵ is the coefficient of the first-order terms, its order is given by the largest of $(\delta^*)^2$ and Δ^2. Rudman and Rubin have shown that in order for $(\delta^*)^2$ to be very small (i.e., $\leqslant 0.05$) the zeroth-order equations are not valid upstream of the point at which

$$\frac{\chi_\infty}{M_\infty^2} \cong 2$$

where χ_∞ is the strong-interaction parameter defined by

$$\chi_\infty = \left(\frac{\mu_{\text{wall}} T_\infty}{\mu_\infty T_{\text{wall}}}\right)^{1/2} \left(M_\infty^3 \operatorname{Re}_{x_\infty}\right)^{-1/2}$$

Consequently, an initial starting solution is required for the present leading edge problem. The same is true for all other problems that are solved using the PNS equations. For the present problem it is permissible to employ an approximate starting solution located very close to the leading edge because it will have a small effect on the flow field further downstream. This is because

only a small amount of mass flow passes between the plate and the shock layer edge at this initial station as compared with the mass flow passing between the plate and the shock wave at stations further downstream. For other problems, however, the initial starting solution will have a definite effect on the downstream flow field, and in many cases, the starting solution must be determined accurately.

The set of PNS equations derived by Rudman and Rubin do not contain a streamwise pressure gradient term, so that there can be no upstream influence through the subsonic portion of the boundary layer. As a result, the equations behave in a strictly "parabolic" manner in the boundary-layer region. Because of this, Davis and Rubin (1980) refer to these equations as the parabolic Navier-Stokes equations instead of the "parabolized" Navier-Stokes equations. They use the latter name to refer to the sets of equations that do contain a streamwise pressure gradient term.

The PNS equations derived by Rudman and Rubin have been used to solve leading edge flows about both 2-D and 3-D geometries including flat plates, rectangular corners, cones, and wing tips (see Lin and Rubin, 1973b, for references). The 3-D equations are derived in a manner similar to the 2-D equations. The coordinates x, y, z are first nondimensionalized using L, δ_y, and δ_z, respectively. The velocities u, v, w are nondimensionalized using V_∞, $V_\infty \delta_y^*$, and $V_\infty \delta_z^*$, respectively, where $\delta_y^* = \delta_y/L$ and $\delta_z^* = \delta_z/L$. Terms of order $(\delta_z^*)^2$, $(\delta_y^*)^2$, $\delta_y^* \delta_z^*$, etc., are assumed small. After substituting the series expansions into the Navier-Stokes equations and neglecting higher-order terms, the 3-D zeroth-order equations become

continuity:

$$\frac{\partial \rho u}{\partial x} + \frac{\partial \rho v}{\partial y} + \frac{\partial \rho w}{\partial z} = 0 \tag{8.24}$$

x momentum:

$$\rho u \frac{\partial u}{\partial x} + \rho v \frac{\partial u}{\partial y} + \rho w \frac{\partial u}{\partial z} = \frac{\partial}{\partial y}\left(\mu \frac{\partial u}{\partial y}\right) + \frac{\partial}{\partial z}\left(\mu \frac{\partial u}{\partial z}\right) \tag{8.25}$$

y momentum:

$$\begin{aligned} \rho u \frac{\partial v}{\partial x} + \rho v \frac{\partial v}{\partial y} + \rho w \frac{\partial v}{\partial z} &= -\frac{\partial p}{\partial y} + \frac{4}{3}\frac{\partial}{\partial y}\left(\mu \frac{\partial v}{\partial y}\right) + \frac{\partial}{\partial z}\left(\mu \frac{\partial v}{\partial z}\right) + \frac{\partial}{\partial x}\left(\mu \frac{\partial u}{\partial y}\right) \\ &\quad - \frac{2}{3}\frac{\partial}{\partial y}\left(\mu \frac{\partial u}{\partial x} + \mu \frac{\partial w}{\partial z}\right) + \frac{\partial}{\partial z}\left(\mu \frac{\partial w}{\partial y}\right) \end{aligned} \tag{8.26}$$

z momentum:

$$\rho u\frac{\partial w}{\partial x} + \rho v\frac{\partial w}{\partial y} + \rho w\frac{\partial w}{\partial z}$$
$$= -\frac{\partial p}{\partial z} + \frac{4}{3}\frac{\partial}{\partial z}\left(\mu\frac{\partial w}{\partial z}\right) + \frac{\partial}{\partial y}\left(\mu\frac{\partial w}{\partial y}\right) + \frac{\partial}{\partial x}\left(\mu\frac{\partial u}{\partial z}\right)$$
$$-\frac{2}{3}\frac{\partial}{\partial z}\left(\mu\frac{\partial v}{\partial y} + \mu\frac{\partial u}{\partial x}\right) + \frac{\partial}{\partial y}\left(\mu\frac{\partial v}{\partial z}\right) \tag{8.27}$$

energy:

$$\rho u c_v\frac{\partial T}{\partial x} + \rho v c_v\frac{\partial T}{\partial y} + \rho w c_v\frac{\partial T}{\partial z}$$
$$= -p\left(\frac{\partial u}{\partial x} + \frac{\partial v}{\partial y} + \frac{\partial w}{\partial z}\right) + \frac{\partial}{\partial y}\left(k\frac{\partial T}{\partial y}\right)$$
$$+\frac{\partial}{\partial z}\left(k\frac{\partial T}{\partial z}\right) + \mu\left[\left(\frac{\partial u}{\partial y}\right)^2 + \left(\frac{\partial u}{\partial z}\right)^2 + \left(\frac{\partial w}{\partial y} + \frac{\partial v}{\partial z}\right)^2\right]$$
$$+\frac{4}{3}\mu\left[\left(\frac{\partial v}{\partial y}\right)^2 + \left(\frac{\partial w}{\partial z}\right)^2 - \frac{\partial v}{\partial y}\frac{\partial w}{\partial z}\right] \tag{8.28}$$

A set of PNS equations very similar to those of Rudman and Rubin's were derived independently by Cheng et al. (1970). Cheng et al. included a streamwise pressure gradient term in their equations.

The most common form of the PNS equations (Lubard and Helliwell, 1973, 1974) and the one that will be used for the rest of this chapter is obtained by assuming that the streamwise viscous derivative terms (including heat flux terms) are negligible compared to the normal and transverse viscous derivative terms. In other words, the streamwise viscous derivative terms are assumed to be of $O(1)$, while the normal and transverse viscous derivative terms are of $O(\mathrm{Re}_L^{1/2})$. Hence these PNS equations are derived by simply dropping all viscous terms containing partial derivatives with respect to the streamwise direction from the steady Navier-Stokes equations. The resulting set of equations for a Cartesian coordinate system (x is the streamwise direction) is given by

continuity:

$$\frac{\partial \rho u}{\partial x} + \frac{\partial \rho v}{\partial y} + \frac{\partial \rho w}{\partial z} = 0 \tag{8.29}$$

x momentum:

$$\rho u\frac{\partial u}{\partial x} + \rho v\frac{\partial u}{\partial y} + \rho w\frac{\partial u}{\partial z} = -\frac{\partial p}{\partial x} + \frac{\partial}{\partial y}\left(\mu\frac{\partial u}{\partial y}\right) + \frac{\partial}{\partial z}\left(\mu\frac{\partial u}{\partial z}\right) \tag{8.30}$$

y momentum:

$$\rho u\frac{\partial v}{\partial x} + \rho v\frac{\partial v}{\partial y} + \rho w\frac{\partial v}{\partial z} = -\frac{\partial p}{\partial y} + \frac{4}{3}\frac{\partial}{\partial y}\left(\mu\frac{\partial v}{\partial y}\right) + \frac{\partial}{\partial z}\left(\mu\frac{\partial v}{\partial z}\right) + \frac{\partial}{\partial z}\left(\mu\frac{\partial w}{\partial y}\right) - \frac{2}{3}\frac{\partial}{\partial y}\left(\mu\frac{\partial w}{\partial z}\right) \tag{8.31}$$

z momentum:

$$\rho u\frac{\partial w}{\partial x} + \rho v\frac{\partial w}{\partial y} + \rho w\frac{\partial w}{\partial z} = -\frac{\partial p}{\partial z} + \frac{4}{3}\frac{\partial}{\partial z}\left(\mu\frac{\partial w}{\partial z}\right) + \frac{\partial}{\partial y}\left(\mu\frac{\partial w}{\partial y}\right) + \frac{\partial}{\partial y}\left(\mu\frac{\partial v}{\partial z}\right) - \frac{2}{3}\frac{\partial}{\partial z}\left(\mu\frac{\partial v}{\partial y}\right) \tag{8.32}$$

energy

$$\begin{aligned}\rho u c_v\frac{\partial T}{\partial x} + \rho v c_v\frac{\partial T}{\partial y} + \rho w c_v\frac{\partial T}{\partial z} &= -p\left(\frac{\partial u}{\partial x} + \frac{\partial v}{\partial y} + \frac{\partial w}{\partial z}\right) + \frac{\partial}{\partial y}\left(k\frac{\partial T}{\partial y}\right) \\ &\quad + \frac{\partial}{\partial z}\left(k\frac{\partial T}{\partial z}\right) + \mu\left[\left(\frac{\partial u}{\partial y}\right)^2 + \left(\frac{\partial u}{\partial z}\right)^2 + \left(\frac{\partial w}{\partial y} + \frac{\partial v}{\partial z}\right)^2\right] \\ &\quad + \frac{4}{3}\mu\left[\left(\frac{\partial v}{\partial y}\right)^2 + \left(\frac{\partial w}{\partial z}\right)^2 - \frac{\partial v}{\partial y}\frac{\partial w}{\partial z}\right]\end{aligned} \tag{8.33}$$

It is interesting to compare this set of PNS equations with the equations of Rudman and Rubin [Eqs. (8.24) – (8.28)]. We note that the continuity and energy equations are identical but the momentum equations are different. In particular, the present x momentum equation contains the streamwise pressure gradient term as discussed previously.

We now wish to express the PNS equations in terms of a generalized coordinate system. For the generalized transformation described in Section 5.6.2, the complete Navier-Stokes equations can be written as

$$\begin{aligned}&\frac{\partial}{\partial t}\left(\frac{\mathbf{U}}{J}\right) + \frac{\partial}{\partial \xi}\left\{\frac{1}{J}\left[\xi_x(\mathbf{E}_i - \mathbf{E}_v) + \xi_y(\mathbf{F}_i - \mathbf{F}_v) + \xi_z(\mathbf{G}_i - \mathbf{G}_v)\right]\right\} \\ &\quad + \frac{\partial}{\partial \eta}\left\{\frac{1}{J}\left[\eta_x(\mathbf{E}_i - \mathbf{E}_v) + \eta_y(\mathbf{F}_i - \mathbf{F}_v) + \eta_z(\mathbf{G}_i - \mathbf{G}_v)\right]\right\} \\ &\quad + \frac{\partial}{\partial \zeta}\left\{\frac{1}{J}\left[\zeta_x(\mathbf{E}_i - \mathbf{E}_v) + \zeta_y(\mathbf{F}_i - \mathbf{F}_v) + \zeta_z(\mathbf{G}_i - \mathbf{G}_v)\right]\right\} = 0\end{aligned} \tag{8.34}$$

where

$$\mathbf{U} = \begin{bmatrix} \rho \\ \rho u \\ \rho v \\ \rho w \\ E_t \end{bmatrix}$$

$$\mathbf{E}_i = \begin{bmatrix} \rho u \\ \rho u^2 + p \\ \rho uv \\ \rho uw \\ (E_t + p)u \end{bmatrix} \qquad \mathbf{E}_v = \begin{bmatrix} 0 \\ \tau_{xx} \\ \tau_{xy} \\ \tau_{xz} \\ u\tau_{xx} + v\tau_{xy} + w\tau_{xz} - q_x \end{bmatrix}$$

$$\mathbf{F}_i = \begin{bmatrix} \rho v \\ \rho uv \\ \rho v^2 + p \\ \rho vw \\ (E_t + p)v \end{bmatrix} \qquad \mathbf{F}_v = \begin{bmatrix} 0 \\ \tau_{xy} \\ \tau_{yy} \\ \tau_{yz} \\ u\tau_{xy} + v\tau_{yy} + w\tau_{yz} - q_y \end{bmatrix} \tag{8.35}$$

$$\mathbf{G}_i = \begin{bmatrix} \rho w \\ \rho uw \\ \rho vw \\ \rho w^2 + p \\ (E_t + p)w \end{bmatrix} \qquad \mathbf{G}_v = \begin{bmatrix} 0 \\ \tau_{xz} \\ \tau_{yz} \\ \tau_{zz} \\ u\tau_{xz} + v\tau_{yz} + w\tau_{zz} - q_z \end{bmatrix}$$

and

$$E_t = \rho\left(e + \frac{u^2 + v^2 + w^2}{2}\right)$$

$$\begin{aligned}
\tau_{xx} &= \tfrac{2}{3}\mu\big[2(\xi_x u_\xi + \eta_x u_\eta + \zeta_x u_\zeta) - (\xi_y v_\xi + \eta_y v_\eta + \zeta_y v_\zeta) \\
&\qquad - (\xi_z w_\xi + \eta_z w_\eta + \zeta_z w_\zeta)\big] \\
\tau_{yy} &= \tfrac{2}{3}\mu\big[2(\xi_y v_\xi + \eta_y v_\eta + \zeta_y v_\zeta) - (\xi_x u_\xi + \eta_x u_\eta + \zeta_x u_\zeta) \\
&\qquad - (\xi_z w_\xi + \eta_z w_\eta + \zeta_z w_\zeta)\big] \\
\tau_{zz} &= \tfrac{2}{3}\mu\big[2(\xi_z w_\xi + \eta_z w_\eta + \zeta_z w_\zeta) - (\xi_x u_\xi + \eta_x u_\eta + \zeta_x u_\zeta) \\
&\qquad - (\xi_y v_\xi + \eta_y v_\eta + \zeta_y v_\zeta)\big] \\
\tau_{xy} &= \mu(\xi_y u_\xi + \eta_y u_\eta + \zeta_y u_\zeta + \xi_x v_\xi + \eta_x v_\eta + \zeta_x v_\zeta) \\
\tau_{xz} &= \mu(\xi_z u_\xi + \eta_z u_\eta + \zeta_z u_\zeta + \xi_x w_\xi + \eta_x w_\eta + \zeta_x w_\zeta) \\
\tau_{yz} &= \mu(\xi_z v_\xi + \eta_z v_\eta + \zeta_z v_\zeta + \xi_y w_\xi + \eta_y w_\eta + \zeta_y w_\zeta)
\end{aligned} \tag{8.36}$$

$$q_x = -k(\xi_x T_\xi + \eta_x T_\eta + \zeta_x T_\zeta)$$
$$q_y = -k(\xi_y T_\xi + \eta_y T_\eta + \zeta_y T_\zeta)$$
$$q_z = -k(\xi_z T_\xi + \eta_z T_\eta + \zeta_z T_\zeta)$$

Note that the usual **E**, **F**, and **G** vectors have been split into an inviscid part (subscript i) and a viscous part (subscript v). The reason for doing this will become evident in Section 8.3.3, when we describe numerical procedures for solving the PNS equations. The PNS equations in generalized coordinates can now be obtained by simply dropping the unsteady terms and the viscous terms containing partial derivatives with respect to the streamwise direction ξ. The resulting equations become

$$\frac{\partial \mathbf{E}_3}{\partial \xi} + \frac{\partial \mathbf{F}_3}{\partial \eta} + \frac{\partial \mathbf{G}_3}{\partial \zeta} = 0 \tag{8.37}$$

where

$$\mathbf{E}_3 = \frac{1}{J}(\xi_x \mathbf{E}_i + \xi_y \mathbf{F}_i + \xi_z \mathbf{G}_i)$$
$$\mathbf{F}_3 = \frac{1}{J}\left[\eta_x(\mathbf{E}_i - \mathbf{E}'_v) + \eta_y(\mathbf{F}_i - \mathbf{F}'_v) + \eta_z(\mathbf{G}_i - \mathbf{G}'_v)\right] \tag{8.38}$$
$$\mathbf{G}_3 = \frac{1}{J}\left[\zeta_x(\mathbf{E}_i - \mathbf{E}'_v) + \zeta_y(\mathbf{F}_i - \mathbf{F}'_v) + \zeta_z(\mathbf{G}_i - \mathbf{G}'_v)\right]$$

and the prime is used to indicate that terms containing partial derivatives with respect to ξ have been omitted. Likewise, the shear stress and heat flux terms in Eqs. (8.36) reduce to

$$\tau'_{xx} = \tfrac{2}{3}\mu\left[2(\eta_x u_\eta + \zeta_x u_\zeta) - (\eta_y v_\eta + \zeta_y v_\zeta) - (\eta_z w_\eta + \zeta_z w_\zeta)\right]$$
$$\tau'_{yy} = \tfrac{2}{3}\mu\left[2(\eta_y v_\eta + \zeta_y v_\zeta) - (\eta_x u_\eta + \zeta_x u_\zeta) - (\eta_z w_\eta + \zeta_z w_\zeta)\right]$$
$$\tau'_{zz} = \tfrac{2}{3}\mu\left[2(\eta_z w_\eta + \zeta_z w_\zeta) - (\eta_x u_\eta + \zeta_x u_\zeta) - (\eta_y v_\eta + \zeta_y v_\zeta)\right]$$
$$\tau'_{xy} = \mu(\eta_y u_\eta + \zeta_y u_\zeta + \eta_x v_\eta + \zeta_x v_\zeta)$$
$$\tau'_{xz} = \mu(\eta_z u_\eta + \zeta_z u_\zeta + \eta_x w_\eta + \zeta_x w_\zeta) \tag{8.39}$$
$$\tau'_{yz} = \mu(\eta_z v_\eta + \zeta_z v_\zeta + \eta_y w_\eta + \zeta_y w_\zeta)$$
$$q'_x = -k(\eta_x T_\eta + \zeta_x T_\zeta)$$
$$q'_y = -k(\eta_y T_\eta + \zeta_y T_\zeta)$$
$$q'_z = -k(\eta_z T_\eta + \zeta_z T_\zeta)$$

For many applications (Schiff and Steger, 1979), the thin-layer approximation can also be applied to the PNS equations. With this additional assumption, the resulting equations are simply the steady form of the TLNS equations. For the generalized transformation described previously, these equations can be written

as

$$\frac{\partial \mathbf{E}_2}{\partial \xi} + \frac{\partial \mathbf{F}_2}{\partial \eta} + \frac{\partial \mathbf{G}_2}{\partial \zeta} = \frac{\partial \mathbf{S}_2}{\partial \eta} \tag{8.40}$$

where $\mathbf{E}_2$, $\mathbf{F}_2$, $\mathbf{G}_2$, and $\mathbf{S}_2$ are defined by Eqs. (8.10) and (8.11).

8.3.2 STREAMWISE PRESSURE GRADIENT

The presence of the streamwise pressure gradient term in the streamwise momentum equation permits information to be propagated upstream through subsonic portions of the flow field such as a boundary layer. As a consequence, a single-pass space-marching method of solution is not well posed, and in many cases, exponentially growing solutions (departure solutions) are encountered. These departure solutions are characterized by either a separation-like increase in wall pressure or an expansion-like decrease in wall pressure. A similar behavior (Lighthill, 1953) is observed for the boundary-layer equations when the streamwise pressure gradient is not prescribed. The one difference, however, is that in the case of the PNS equations the normal momentum equation allows a

$$\mathbf{F}_v = \mu \begin{bmatrix} 0 \\ u_y \\ \frac{4}{3} v_y \\ u u_y + \frac{4}{3} v v_y + \frac{k}{\mu} T_y \end{bmatrix}$$

Note that in these equations a parameter ω has been inserted in front of the streamwise pressure gradient term in the x momentum equation. Thus if ω is set equal to zero, the streamwise pressure gradient term is omitted. On the other hand, if ω is set equal to 1, the term is retained completely.

If we first consider the inviscid limit ($\mu \to 0$), Eq. (8.41) reduces to the Euler equation

$$\frac{\partial \mathbf{E}}{\partial x} + \frac{\partial \mathbf{F}}{\partial y} = 0 \tag{8.43}$$

which is equivalent to

$$[A_1]\mathbf{Q}_x + [B_1]\mathbf{Q}_y = 0 \tag{8.44}$$

where

$$[A_1] = \begin{bmatrix} u & \rho & 0 & 0 \\ 0 & \rho u & 0 & \omega \\ 0 & 0 & \rho u & 0 \\ 0 & \rho u^2 + \dfrac{\gamma p}{\gamma - 1} & \rho u v & \dfrac{\gamma u}{\gamma - 1} \end{bmatrix} \qquad \mathbf{Q} = \begin{bmatrix} \rho \\ u \\ v \\ p \end{bmatrix} \tag{8.45}$$

$$[B_1] = \begin{bmatrix} v & 0 & \rho & 0 \\ 0 & \rho v & 0 & 0 \\ 0 & 0 & \rho v & 1 \\ 0 & \rho u v & \rho v^2 + \dfrac{\gamma p}{\gamma - 1} & \dfrac{\gamma v}{\gamma - 1} \end{bmatrix}$$

These equations are hyperbolic in x, provided that the eigenvalues of $[A_1]^{-1}[B_1]$ are real (see Section 2.5). The eigenvalues are

$$\lambda_{1,2} = \frac{v}{u}$$
$$\lambda_{3,4} = \frac{-b \pm \sqrt{b^2 - 4\bar{a}c}}{2\bar{a}} \tag{8.46}$$

where

$$\bar{a} = [\gamma - \omega(\gamma - 1)]u^2 - \omega a^2$$
$$b = -uv[1 + \gamma - \omega(\gamma - 1)]$$
$$c = v^2 - a^2$$

and a is the speed of sound. If the streamwise pressure gradient is retained completely (i.e., $\omega = 1$), it is easy to show that the eigenvalues are all real, provided that

$$u^2 + v^2 \geqslant a^2$$

or

$$M \geqslant 1$$

This is the usual requirement that must be satisfied if the Euler equations are to be integrated using a space-marching technique. However, if only a fraction of the streamwise pressure gradient is retained (i.e., $0 \leqslant \omega \leqslant 1$), the eigenvalues will remain real even in subsonic regions, provided that

$$\omega \leqslant \frac{\gamma M_x^2}{1 + (\gamma - 1)M_x^2} \tag{8.47}$$

where $M_x = u/a$. This condition on the streamwise pressure gradient is derived by assuming that the normal component of velocity (v) is much smaller than the streamwise component (u).

We next consider the viscous limit by ignoring terms in Eq. (8.41) containing first derivatives with respect to y. The resulting equations can be written as

$$[A_2]\mathbf{Q}_x = [B_2]\mathbf{Q}_{yy} \tag{8.48}$$

where

$$[A_2] = \begin{bmatrix} u & \rho & 0 & 0 \\ u^2 & 2\rho u & 0 & \omega \\ uv & \rho v & \rho u & 0 \\ \dfrac{u(u^2+v^2)}{2} & \dfrac{\gamma p}{\gamma - 1} + \dfrac{\rho(3u^2+v^2)}{2} & \rho uv & \dfrac{\gamma u}{\gamma - 1} \end{bmatrix} \tag{8.49}$$

$$[B_2] = \mu \begin{bmatrix} 0 & 0 & 0 & 0 \\ 0 & 1 & 0 & 0 \\ 0 & 0 & \dfrac{4}{3} & 0 \\ \dfrac{-\gamma p}{(\gamma - 1)\rho^2 \,\mathrm{Pr}} & u & \dfrac{4}{3}v & \dfrac{\gamma}{(\gamma - 1)\rho \,\mathrm{Pr}} \end{bmatrix}$$

These equations are parabolic in the positive x direction if the eigenvalues of $[A_2]^{-1}[B_2]$ are real and positive (see Section 2.5). The eigenvalues must be positive in order for a positive viscosity to produce damping in the streamwise direction. The eigenvalues can be found from the following polynomial (assuming $u \neq 0$):

$$\lambda\left(\frac{\rho u}{\mu}\lambda - \frac{4}{3}\right)\left[\left(\frac{\rho u}{\mu}\lambda\right)^2 \{M_x^2[\gamma - \omega(\gamma - 1)] - \omega\} + \left(\frac{\rho u}{\mu}\lambda\right)\left\{\left[\omega(\gamma - 1) - \gamma\left(\frac{1 + \mathrm{Pr}}{\mathrm{Pr}}\right)\right]M_x^2 + \frac{\omega}{\mathrm{Pr}}\right\} + \frac{\gamma M_x^2}{\mathrm{Pr}}\right] = 0 \tag{8.50}$$

Vigneron et al. (1978a) have shown that the eigenvalues determined from this equation will be real and positive if

$$u > 0 \tag{8.51}$$

and

$$\omega < \frac{\gamma M_x^2}{1 + (\gamma - 1)M_x^2} \tag{8.52}$$

Equation (8.51) prohibits reverse flows, while Eq. (8.52) places a restriction on the streamwise pressure gradient term in an identical manner to that given previously by Eq. (8.47). From this, we can conclude that the instability caused by the presence of the streamwise pressure gradient term in the PNS equations is actually an inviscid phenomenon.

Note that the right-hand side of Eq. (8.52), denoted by $f(M_x)$, is a function of the local streamwise Mach number (M_x) and becomes equal to 1 when $M_x = 1$ and is greater than 1 when $M_x > 1$ (see Fig. 8.4). Hence the streamwise pressure gradient term can be included fully when $M_x > 1$. However, when $M_x < 1$, only a fraction of this term (i.e., $\omega\, \partial p/\partial x$) can be retained if the

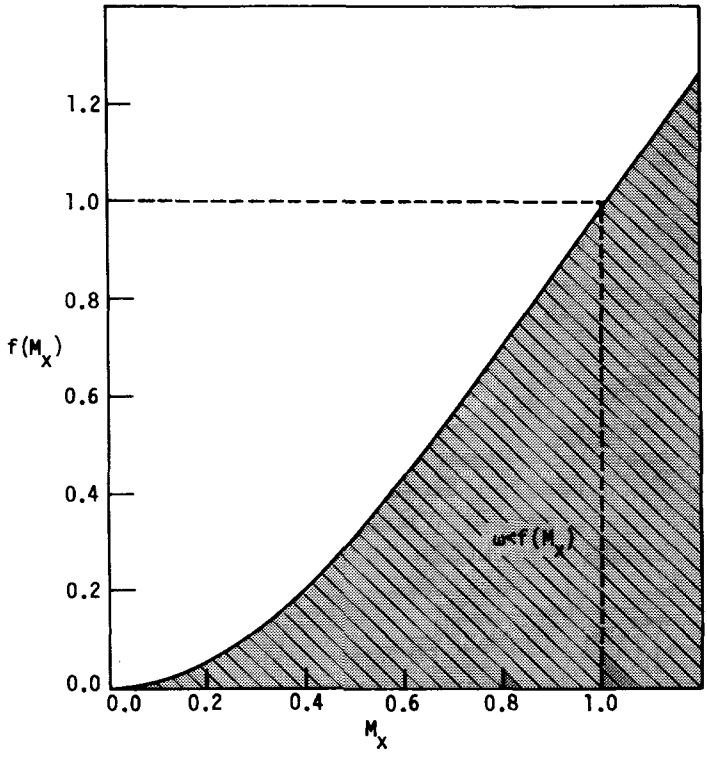

Figure 8.4 Constraint on streamwise pressure gradient term in subsonic regions.

eigenvalues are to remain real and positive. Note also that ω approaches zero close to a wall where $M_x = 0$. Thus we see that space-marched solutions of the PNS equations are subject to instabilities (departure solutions) when the streamwise pressure gradient term is retained fully in the subsonic portion of the boundary layer, since an "elliptic-like" behavior is introduced. A number of different techniques have been proposed to circumvent this difficulty, and they will now be discussed.

The obvious technique is to drop completely the streamwise pressure gradient term in subsonic regions. This will produce a stable marching scheme but will introduce errors in flow fields with large streamwise pressure gradients. It should be noted, however, that streamwise pressure variations will still exist in the numerical solution being evaluated through the y momentum equation and the energy equation. An alternative procedure is to specify the variation of the streamwise pressure gradient. Obviously, setting the pressure gradient equal to zero is just one of many ways that this can be done. If the streamwise pressure gradient is specified, we can remove this term from matrices $[A_1]$ and $[A_2]$ in Eqs. (8.44) and (8.48) and treat it as a source term in the eigenvalue analyses. As a consequence, the streamwise pressure gradient will not affect the mathematical character of the equations. For the solution of the boundary-layer equations, the streamwise pressure gradient is usually known either from the external inviscid flow or, for the case of internal flows, from the conservation-of-mass law. Unfortunately, for the flow fields normally computed with the PNS equations, the streamwise pressure gradient is not known a priori but must be computed as part of the solution.

In several studies the streamwise pressure gradient term has been retained in the subsonic viscous region by employing a backward-difference formula, which uses information from the previous marching step. For example, when the solution at the $i + 1$ station is computed, $\partial p/\partial x$ can be evaluated from

$$\frac{\partial p}{\partial x} \cong \frac{p_i - p_{i-1}}{\Delta x} \tag{8.53}$$

which is a first-order backward-difference expression. Lubard and Helliwell (1973) studied the stability (departure behavior) of using a backward-difference formula for the streamwise pressure gradient term in both the momentum and energy equations. They applied a simple implicit differencing scheme to the PNS equations and used a Fourier stability analysis to show that an instability will occur if

$$\Delta x < (\Delta x)_{\min} \tag{8.54}$$

This stability condition is highly unusual, since we normally find from a Fourier stability analysis that an instability occurs when Δx is greater than some $(\Delta x)_{\max}$. When this analysis is applied to the 2-D PNS equations given by Eqs.

(8.48)–(8.49), $(\Delta x)_{\min}$ is given by

$$(\Delta x)_{\min} = \frac{\frac{1}{4}(\rho u/\mu)\left[(1/M_x^2) - 1\right](\Delta y)^2}{\gamma \sin^2(\beta/2)} \tag{8.55}$$

where β is the wave number $(k_m \Delta y)$. Lubard and Helliwell have also shown that if the streamwise pressure gradient term is differenced implicitly, like the rest of the terms in the PNS equations when simple implicit differencing is applied, the minimum allowable step size $(\Delta x)_{\min}$ is doubled. In order to explain these unusual stability conditions, Rubin (1981) has observed that $(\Delta x)_{\min}$ appears to represent the extent of the upstream elliptic interaction. If $(\Delta x) > (\Delta x)_{\min}$, the interaction is overstepped, and a forward marching procedure is stable. On the other hand, if $(\Delta x) < (\Delta x)_{\min}$, the numerical solution attempts to represent the elliptic interaction, and this leads to departure solutions, since upstream effects are not permitted by a forward-marched solution. Rubin and Lin (1980) have shown that the extent of the elliptic interaction region is of the order of the thickness of the subsonic region. Thus, if the subsonic region is relatively large, the minimum allowable Δx may be too large to permit accurate (or stable) calculations.

Another method that has been used to treat the streamwise pressure gradient term is called the "*sublayer approximation*" technique. This method was originally proposed by Rubin and Lin (1971) and later applied to the PNS equations by Schiff and Steger (1979). In the sublayer approximation technique, the pressure gradient term in the subsonic viscous region is calculated at a supersonic point outside of the sublayer region. This approximation is based on the fact that for a thin subsonic viscous layer, $\partial p/\partial y$ is negligible. Since the pressure gradient is specified in the subsonic region, it would appear that this technique would lead to stable space-marched solutions. However, it has been observed by Schiff and Steger that departure solutions still exist for some cases. This may be due to the pressure interaction between the supersonic and subsonic regions, which is permitted by the normal momentum equation and the energy equation.

A novel technique for handling the streamwise pressure gradient term was proposed by Vigneron et al. (1978a). In this approach, a fraction of the pressure gradient term $\omega(\partial p/\partial x)$ in the streamwise momentum equation is retained in the subsonic viscous region, and the remainder $(1 - \omega)(\partial p/\partial x)$ is usually omitted or is evaluated explicitly using a backward-difference formula or the "sublayer approximation" technique. For the Vigneron approach, Eq. (8.41) is rewritten as

$$\frac{\partial \mathbf{E}}{\partial x} + \frac{\partial \mathbf{P}}{\partial x} + \frac{\partial \mathbf{F}}{\partial y} = \frac{\partial \mathbf{F}_v}{\partial y} \tag{8.56}$$

where

$$\mathbf{P} = \begin{bmatrix} 0 \\ (1 - \omega)p \\ 0 \\ 0 \end{bmatrix} \tag{8.57}$$

and $\mathbf{E}$, $\mathbf{F}$, and $\mathbf{F}_v$ are defined in Eqs. (8.42). The parameter ω is computed using Eq. (8.47) with a safety factor σ applied:

$$\omega = \frac{\sigma\gamma M_x^2}{1 + (\gamma - 1)M_x^2} \tag{8.58}$$

Vigneron et al. (1978b) have used a Fourier stability analysis to study the "departure behavior" of this technique. They applied the simple implicit (Euler implicit) scheme to Eq. (8.56), with $\partial\mathbf{F}/\partial y$ omitted, and used a backward difference for $\partial\mathbf{P}/\partial x$. As expected, they found that if the "elliptic" pressure gradient term $\partial\mathbf{P}/\partial x$ is omitted, this technique will always lead to a stable space-marched solution, since the equations remain hyperbolic-parabolic. However, if this term is retained, an instability results if Δx is less than some $(\Delta x)_{\min}$. For $\omega = 0$, it was found that $(\Delta x)_{\min}$ is given by Eq. (8.55), which confirms the previous findings of Lubard and Helliwell. Thus it is obvious that in order to completely eliminate departure solutions, it is necessary to drop the term $(1 - \omega)(\partial p/\partial x)$ in subsonic regions when solving the PNS equations with a single marching sweep of the flow field. Other techniques for treating the streamwise pressure gradient term include those proposed by Lin and Rubin (1979), Buggeln et al. (1980), Yanenko et al. (1980), and Bhutta and Lewis (1985a).

For many flow problems the upstream elliptic effects are relatively small and the techniques described above will successfully prevent departure solutions while permitting an accurate solution to be computed with a single marching sweep through the flow field. For other problems where the upstream influence is significant (due to separation, wakes, shocks, etc.), the above techniques may prove to be inadequate. Either a departure solution results or the inconsistency introduced into the PNS equations to prevent the departure solution will lead to large errors. For these cases, a *global pressure relaxation procedure* (Rubin and Lin, 1980) can be used. In this procedure, an initial pressure distribution is used to determine the pressure gradient at each point in the elliptic region. The initial pressure distribution can be obtained by either setting the streamwise pressure gradient equal to zero, by using the "Vigneron" technique with $\partial\mathbf{P}/\partial x = 0$, or by taking a sufficiently large Δx. With the pressure gradient known, the PNS equations can be solved in a stable manner using a space-marching technique, provided that the pressure gradient term is differenced in an appropriate manner. The resulting solution will contain a new pressure distribution that can be used to determine the pressure gradient for the next sweep of the flow field. This iteration procedure is continued until the solution converges. In order for the elliptic character of the flow field to be properly modeled, the pressure gradient term must introduce downstream contributions. This can be accomplished by applying appropriate "upwind" differences to the "elliptic" and "hyperbolic" components of the pressure gradient term:

$$\frac{\partial p}{\partial x} = \underbrace{\omega\frac{\partial p}{\partial x}}_{\text{hyperbolic}} + \underbrace{(1 - \omega)\frac{\partial p}{\partial x}}_{\text{elliptic}} \tag{8.59}$$

For example, when the solution at the $i + 1$ station is computed, the streamwise pressure gradient term can be differenced on an equally spaced grid (Rakich, 1983) as

$$\left(\frac{\partial p}{\partial x}\right) \cong \omega\left(\frac{p_{i+1}^{n+1} - p_i^{n+1}}{\Delta x}\right) + (1 - \omega)\left(\frac{p_{i+2}^{n} - p_{i+1}^{n+1}}{\Delta x}\right)$$

where the superscript $n + 1$ indicates the current iteration level. This type of differencing is only possible when the global pressure relaxation procedure is used, since p_{i+2}^{n} is normally unknown.

The global pressure relaxation procedure can be used for problems where the upstream influence is significant. Although this procedure requires more computer time than a standard PNS calculation that employes one sweep of the flow field, it still offers advantages over the complete Navier-Stokes equations. One of the primary advantages is that only the pressure must be stored (if $u > 0$) during each sweep of the flow field. The global pressure relaxation procedure has been used by several investigators, including Rubin and Lin (1980), Rakich (1983), Barnett and Davis (1986), Khosla and Rubin (1987), Barnett and Power (1988), Power and Barber (1988), Power (1990), Rubin and Khosla (1990), and Miller et al. (1997).

The concept of splitting the streamwise pressure gradient term into its "elliptic" and "hyperbolic" components has led to the introduction of a new set of equations called the reduced Navier-Stokes (RNS) equations (Rubin, 1984). The RNS equations are derived from the complete unsteady Navier-Stokes equations by dropping the streamwise viscous terms, omitting the viscous terms in the normal momentum equation, and splitting the streamwise pressure gradient using Eq. (8.59). In most applications, the time-derivative terms are also omitted. For supersonic flows with embedded "elliptic" regions, the global pressure relaxation procedure (just described) can be used to solve the RNS equations. For subsonic flows the RNS equations are solved using the techniques described in Section 8.4.3 for the PPNS equations.

8.3.3 Numerical Solution of PNS Equations

As discussed previously, the PNS equations are a mixed set of hyperbolic-parabolic equations in the streamwise direction, provided that the following conditions are satisfied.

1. Inviscid flow is supersonic.
2. Streamwise velocity component is everywhere greater than zero.
3. Streamwise pressure gradient term in streamwise momentum equation is either omitted or the "departure behavior" is suppressed using one of the techniques described in the last section.

If these conditions are met, the PNS equations can be solved using methods similar to those employed for the parabolic boundary-layer equations. Thus the

solution can be marched downstream in a stable manner from an initial data surface to the desired final station.

Early schemes. Some of the earliest solutions of the PNS equations were obtained using explicit finite-difference techniques (Rudman and Rubin, 1968; Boynton and Thomson, 1969; Rubin et al., 1969; Cresci et al., 1969; Cheng et al., 1970). Explicit schemes were used more for convenience than efficiency, since we have demonstrated in Chapter 7 that implicit methods are much more efficient for equations of this type. In later studies, the PNS equations have been primarily solved using implicit algorithms. Cheng et al. (1970) used the simple implicit scheme, Nardo and Cresci (1971) employed the Peaceman-Rachford alternating direction implicit (ADI) scheme, while Rubin and Lin (1972) and Lubard and Helliwell (1973) used similar iterative-implicit schemes. Rubin and Lin's predictor-corrector multiple iteration scheme is described in Section 4.5.10, where it is applied to the 3-D linear Burgers equation

$$u_x + cu_y + du_z = \mu(u_{yy} + u_{zz}) \tag{8.60}$$

The 3-D linear Burgers equation is a useful model equation for the PNS equations, but of course, it does not represent the nonlinear character of these equations. Thus, when the predictor-corrector multiple-iteration method is applied to the PNS equations, nonlinear terms such as $(u^{m+1}_{i+1,j,k})^2$ appear, where m is the iteration level, $x = i\,\Delta x$, $y = j\,\Delta y$, and $z = k\,\Delta z$. These nonlinear terms are linearized using a Newton-Raphson procedure (see Section 7.3.3). That is, if $f = f(x_1, x_2, \ldots, x_l)$ is a nonlinear term, then

$$f^{m+1} = f^m + \sum_{k=1}^{l} \left(\frac{\partial f}{\partial x_k}\right)^m (x_k^{m+1} - x_k^m) \tag{8.61}$$

where x_k denotes the dependent variables. Applying this formula to the nonlinear term $(u^{m+1}_{i+1,j,k})^2$ gives

$$\left(u^{m+1}_{i+1,j,k}\right)^2 = 2u^{m+1}_{i+1,j,k}u^m_{i+1,j,k} - (u^m_{i+1,j,k})^2 \tag{8.62}$$

After all the nonlinear terms are linearized in this manner, the resulting set of algebraic equations (at iteration level $m + 1$) can be solved using an efficient block tridiagonal solver. The iteration is continued until the solution converges at the $i + 1$ station. This method is implicit in the y direction, where the gradients are largest, but is explicit in the z direction (see Section 4.5.10), which leads to the following stability condition when applied to the 3-D PNS equations:

$$\Delta x \leqslant \Delta z \left|\frac{w}{u}\right| \tag{8.63}$$

Beam-Warming scheme. Until the latter part of the 1970s, the PNS equations were mainly solved using iterative, implicit finite-difference schemes like the ones described above. Vigneron et al. (1978a) were the first to employ a more efficient noniterative implicit approximate-factorization finite-difference scheme to solve the PNS equations. Their algorithm was adapted from the class of ADI schemes developed by Lindemuth and Killeen (1973), McDonald and Briley

(1975), and Beam and Warming (1978) to solve time-dependent equations such as the Navier-Stokes equations. Working independently of Vigneron et al. (1978a), Schiff and Steger (1979) developed a nearly identical algorithm except that the pressure gradient in the subsonic viscous layer was calculated at a supersonic point outside the layer using the "sublayer approximation" technique. In addition, a different linearization procedure was employed by Schiff and Steger.

In order to explain the Vigneron et al. algorithm, let us apply it to the 3-D PNS equations written in Cartesian coordinates (x is the streamwise direction) for a perfect gas. In this case, the generalized coordinates become

$$\begin{aligned} \xi &= x \\ \eta &= y \\ \zeta &= z \end{aligned} \tag{8.64}$$

and Eqs. (8.37)–(8.38) reduce to

$$\frac{\partial \mathbf{E}}{\partial x} + \frac{\partial \mathbf{F}}{\partial y} + \frac{\partial \mathbf{G}}{\partial z} = 0 \tag{8.65}$$

where

$$\begin{aligned} \mathbf{E} &= \mathbf{E}_i \\ \mathbf{F} &= \mathbf{F}_i - \mathbf{F}_v \\ \mathbf{G} &= \mathbf{G}_i - \mathbf{G}_v \end{aligned} \tag{8.66}$$

The vectors $\mathbf{E}_i$, $\mathbf{F}_i$, $\mathbf{G}_i$, $\mathbf{F}_v$, and $\mathbf{G}_v$ are given by Eqs. (8.35) and contain the following "parabolized" shear stress and heat flux terms:

$$\begin{aligned} \tau_{xx} &= \tfrac{2}{3}\mu(-v_y - w_z) \\ \tau_{yy} &= \tfrac{2}{3}\mu(2v_y - w_z) \\ \tau_{zz} &= \tfrac{2}{3}\mu(2w_z - v_y) \\ \tau_{xy} &= \mu u_y \\ \tau_{xz} &= \mu u_z \\ \tau_{yz} &= \mu(v_z + w_y) \\ q_x &= 0 \\ q_y &= -kT_y \\ q_z &= -kT_z \end{aligned} \tag{8.67}$$

In order to use the "Vigneron" technique for handling the streamwise pressure gradient, $\mathbf{E}$ can be replaced by $\mathbf{E}' + \mathbf{P}$, so that, Eq. (8.65) becomes

$$\frac{\partial \mathbf{E}'}{\partial x} + \frac{\partial \mathbf{P}}{\partial x} + \frac{\partial \mathbf{F}}{\partial y} + \frac{\partial \mathbf{G}}{\partial z} = 0 \tag{8.68}$$

where $\mathbf{E}'$ and $\mathbf{P}$ are given by

$$\mathbf{E}' = \begin{bmatrix} \rho u \\ \rho u^2 + \omega p \\ \rho uv \\ \rho uw \\ (E_t + p)u \end{bmatrix} \qquad \mathbf{P} = \begin{bmatrix} 0 \\ (1 - \omega)p \\ 0 \\ 0 \\ 0 \end{bmatrix} \tag{8.69}$$

The solution of Eq. (8.65) is marched in x using the following difference formula suggested by Beam and Warming (1978):

$$\Delta^i \mathbf{E} = \frac{\theta_1 \Delta x}{1 + \theta_2} \frac{\partial}{\partial x}(\Delta^i \mathbf{E}) + \frac{\Delta x}{1 + \theta_2} \frac{\partial}{\partial x}(\mathbf{E}^i) + \frac{\theta_2}{1 + \theta_2} \Delta^{i-1} \mathbf{E} + O\left[\left(\theta_1 - \frac{1}{2} - \theta_2\right)(\Delta x)^2 + (\Delta x)^3\right] \tag{8.70}$$

where

$$\Delta^i \mathbf{E} = \mathbf{E}^{i+1} - \mathbf{E}^i \tag{8.71}$$

and $x = i\,\Delta x$. This general difference formula, with the appropriate choice of the parameters θ_1 and θ_2, reproduces many of the standard difference schemes as seen in Table 8.1. For the PNS equations, either the first-order Euler implicit scheme ($\theta_1 = 1, \theta_2 = 0$) or the second-order, three-point backward scheme ($\theta_1 = 1, \theta_2 = \frac{1}{2}$) are normally used. As shown by Beam and Warming, the second-order trapezoidal differencing scheme ($\theta_1 = \frac{1}{2}, \theta_2 = 0$) will lead to unstable calculations when applied to parabolic equations. Note that the truncation error (T.E.) in Table 8.1 is for $\Delta^i \mathbf{E}$. When $\partial \mathbf{E}/\partial x$ is replaced by $\Delta^i \mathbf{E}/\Delta x$ in the numerical scheme, the T.E. is divided by Δx.

Substituting Eq. (8.65) into Eq. (8.70) yields

$$\Delta^i \mathbf{E} = -\frac{\theta_1 \Delta x}{1 + \theta_2}\left[\frac{\partial}{\partial y}(\Delta^i \mathbf{F}) + \frac{\partial}{\partial z}(\Delta^i \mathbf{G})\right] - \frac{\Delta x}{1 + \theta_2}\left[\frac{\partial}{\partial y}(\mathbf{F}^i) + \frac{\partial}{\partial z}(\mathbf{G}^i)\right] + \frac{\theta_2}{1 + \theta_2} \Delta^{i-1} \mathbf{E} \tag{8.72}$$

with the T.E. term omitted. The difference formula is in the so-called "delta" form as discussed in Section 4.4.7. The delta terms $\Delta^i \mathbf{E}$, $\Delta^i \mathbf{F}$, and $\Delta^i \mathbf{G}$, which can

Table 8.1 Finite-difference schemes contained in Eq. (8.70)

θ_1	θ_2	Scheme	Truncation error in Eq. (8.70)
0	0	Euler explicit	$O[(\Delta x)^2]$
0	$-\frac{1}{2}$	Leap frog (explicit)	$O[(\Delta x)^3]$
$\frac{1}{2}$	0	Trapezoidal (implicit)	$O[(\Delta x)^3]$
1	0	Euler implicit	$O[(\Delta x)^2]$
1	$\frac{1}{2}$	Three-point backward (implicit)	$O[(\Delta x)^3]$

be written as

$$\begin{aligned}\Delta^i\mathbf{E} &= \Delta^i\mathbf{E}' + \Delta^i\mathbf{P}\\ \Delta^i\mathbf{F} &= \Delta^i\mathbf{F}_i - \Delta^i\mathbf{F}_v\\ \Delta^i\mathbf{G} &= \Delta^i\mathbf{G}_i - \Delta^i\mathbf{G}_v\end{aligned} \tag{8.73}$$

are linearized using truncated Taylor-series expansions. In order to linearize the inviscid delta terms $\Delta^i\mathbf{E}'$, $\Delta^i\mathbf{F}_i$, and $\Delta^i\mathbf{G}_i$, we make use of the fact that $\mathbf{E}'$, $\mathbf{F}_i$, and $\mathbf{G}_i$ are functions only of the $\mathbf{U}$ vector,

$$\mathbf{U} = \begin{bmatrix}\rho\\ \rho u\\ \rho v\\ \rho w\\ E_t\end{bmatrix} = \begin{bmatrix}U_1\\ U_2\\ U_3\\ U_4\\ U_5\end{bmatrix} \tag{8.74}$$

For example, $\mathbf{F}_i$ can be expressed as

$$\mathbf{F}_i = \begin{bmatrix} U_3 \\ \dfrac{U_2U_3}{U_1} \\ \dfrac{U_3^2}{U_1} + (\gamma-1)\left(U_5 - \dfrac{U_2^2+U_3^2+U_4^2}{2U_1}\right) \\ \dfrac{U_3U_4}{U_1} \\ \left[U_5 + (\gamma-1)\left(U_5 - \dfrac{U_2^2+U_3^2+U_4^2}{2U_1}\right)\right]\dfrac{U_3}{U_1} \end{bmatrix} \tag{8.75}$$

As a consequence, we can readily expand $\mathbf{E}'$, $\mathbf{F}_i$, and $\mathbf{G}_i$ as

$$\begin{aligned}(\mathbf{E}')^{i+1} &= (\mathbf{E}')^i + \left(\frac{\partial\mathbf{E}'}{\partial\mathbf{U}}\right)^i \Delta^i\mathbf{U} + O[(\Delta x)^2]\\ (\mathbf{F}_i)^{i+1} &= (\mathbf{F}_i)^i + \left(\frac{\partial\mathbf{F}_i}{\partial\mathbf{U}}\right)^i \Delta^i\mathbf{U} + O[(\Delta x)^2]\\ (\mathbf{G}_i)^{i+1} &= (\mathbf{G}_i)^i + \left(\frac{\partial\mathbf{G}_i}{\partial\mathbf{U}}\right)^i \Delta^i\mathbf{U} + O[(\Delta x)^2]\end{aligned} \tag{8.76}$$

or

$$\begin{aligned}\Delta^i\mathbf{E}' &= [Q]^i\,\Delta^i\mathbf{U} + O[(\Delta x)^2]\\ \Delta^i\mathbf{F}_i &= [R]^i\,\Delta^i\mathbf{U} + O[(\Delta x)^2]\\ \Delta^i\mathbf{G}_i &= [S]^i\,\Delta^i\mathbf{U} + O[(\Delta x)^2]\end{aligned} \tag{8.77}$$

where $[Q]$, $[R]$, and $[S]$ are the Jacobian matrices $\partial\mathbf{E}'/\partial\mathbf{U}$, $\partial\mathbf{F}_i/\partial\mathbf{U}$, and $\partial\mathbf{G}_i/\partial\mathbf{U}$ given by

$$\frac{\partial \mathbf{E}'}{\partial \mathbf{U}} = \begin{bmatrix} 0 & 1 & 0 & 0 & 0 \\ \dfrac{\omega(\gamma-1)-2}{2}u^2 + \dfrac{\omega(\gamma-1)}{2}(v^2+w^2) & [2-\omega(\gamma-1)]u & -\omega(\gamma-1)v & -\omega(\gamma-1)w & \omega(\gamma-1) \\ -uv & v & u & 0 & 0 \\ -uw & w & 0 & u & 0 \\ \left[-\dfrac{\gamma E_t}{\rho} + (\gamma-1)(u^2+v^2+w^2)\right]u & \dfrac{\gamma E_t}{\rho} - (\gamma-1)\dfrac{3u^2+v^2+w^2}{2} & -(\gamma-1)uv & -(\gamma-1)uw & \gamma u \end{bmatrix} \tag{8.78}$$

$$\frac{\partial \mathbf{F}_i}{\partial \mathbf{U}} = \begin{bmatrix} 0 & 0 & 1 & 0 & 0 \\ -uv & v & u & 0 & 0 \\ \dfrac{\gamma-1}{2}(u^2+w^2) + \dfrac{\gamma-3}{2}v^2 & -(\gamma-1)u & (3-\gamma)v & -(\gamma-1)w & \gamma-1 \\ -vw & 0 & w & v & 0 \\ \left[-\dfrac{\gamma E_t}{\rho} + (\gamma-1)(u^2+v^2+w^2)\right]v & -(\gamma-1)uv & \dfrac{\gamma E_t}{\rho} - \dfrac{\gamma-1}{2}(u^2+3v^2+w^2) & -(\gamma-1)vw & \gamma v \end{bmatrix} \tag{8.79}$$

$$\frac{\partial \mathbf{G}_i}{\partial \mathbf{U}} = \begin{bmatrix} 0 & 0 & 0 & 1 & 0 \\ -uw & w & 0 & u & 0 \\ -vw & 0 & w & v & 0 \\ \dfrac{\gamma-1}{2}(u^2+v^2) + \dfrac{\gamma-3}{2}w^2 & -(\gamma-1)u & -(\gamma-1)v & (3-\gamma)w & \gamma-1 \\ \left[-\dfrac{\gamma E_t}{\rho} + (\gamma-1)(u^2+v^2+w^2)\right]w & -(\gamma-1)uw & -(\gamma-1)vw & \dfrac{\gamma E_t}{\rho} - \dfrac{\gamma-1}{2}(u^2+v^2+3w^2) & \gamma w \end{bmatrix} \tag{8.80}$$

The expression for the Jacobian $\partial \mathbf{E}'/\partial \mathbf{U}$ is derived by assuming ω to be locally independent of $\mathbf{U}$.

The viscous delta terms can be linearized using a method suggested by Steger (1977). In order to apply this linearization method, the coefficients of viscosity (μ) and the thermal conductivity (k) are assumed to be locally independent of $\mathbf{U}$ and the cross-derivative viscous terms are neglected. As a result of these assumptions, elements of $\mathbf{F}_v$ and $\mathbf{G}_v$ have the general form

$$\begin{aligned} f_k &= \alpha_k \frac{\partial}{\partial y}(\beta_k) \\ g_k &= \alpha_k \frac{\partial}{\partial z}(\beta_k) \end{aligned} \tag{8.81}$$

where α_k is independent of $\mathbf{U}$ and β_k is a function of $\mathbf{U}$. These elements are linearized in the following manner:

$$\begin{aligned} f^{i+1} &= f^i + \alpha_k^i \frac{\partial}{\partial y}\left[\sum_{l=1}^{5}\left(\frac{\partial \beta_k}{\partial U_l}\right)^i \Delta^i U_l\right] + O[(\Delta x)^2] \\ g^{i+1} &= g^i + \alpha_k^i \frac{\partial}{\partial z}\left[\sum_{l=1}^{5}\left(\frac{\partial \beta_k}{\partial U_l}\right)^i \Delta^i U_l\right] + O[(\Delta x)^2] \end{aligned} \tag{8.82}$$

so that we can write

$$\begin{aligned} \Delta^i \mathbf{F}_v &= [V]^i \Delta^i \mathbf{U} + O[(\Delta x)^2] \\ \Delta^i \mathbf{G}_v &= [W]^i \Delta^i \mathbf{U} + O[(\Delta x)^2] \end{aligned} \tag{8.83}$$

where $[V]$ and $[W]$ are the Jacobian matrices $\partial \mathbf{F}_v/\partial \mathbf{U}$ and $\partial \mathbf{G}_v/\partial \mathbf{U}$ given by

$$\frac{\partial \mathbf{F}_v}{\partial \mathbf{U}} = \mu \begin{bmatrix} 0 & 0 & 0 & 0 & 0 \\ -\partial_y\left(\frac{u}{\rho}\right) & \partial_y\left(\frac{1}{\rho}\right) & 0 & 0 & 0 \\ -\frac{4}{3}\partial_y\left(\frac{v}{\rho}\right) & 0 & \frac{4}{3}\partial_y\left(\frac{1}{\rho}\right) & 0 & 0 \\ -\partial_y\left(\frac{w}{\rho}\right) & 0 & 0 & \partial_y\left(\frac{1}{\rho}\right) & 0 \\ -\partial_y\left(\frac{u^2}{\rho}\right) - \frac{4}{3}\partial_y\left(\frac{v^2}{\rho}\right) - \partial_y\left(\frac{w^2}{\rho}\right) & \left(1-\frac{\gamma}{\mathrm{Pr}}\right)\partial_y\left(\frac{u}{\rho}\right) & \left(\frac{4}{3}-\frac{\gamma}{\mathrm{Pr}}\right)\partial_y\left(\frac{v}{\rho}\right) & \left(1-\frac{\gamma}{\mathrm{Pr}}\right)\partial_y\left(\frac{w}{\rho}\right) & \frac{\gamma}{\mathrm{Pr}}\partial_y\left(\frac{1}{\rho}\right) \\ -\frac{\gamma}{\mathrm{Pr}}\partial_y\left[\frac{p}{(\gamma-1)\rho^2} - \frac{u^2+v^2+w^2}{2\rho}\right] & & & & \end{bmatrix} \tag{8.84}$$

$$\frac{\partial \mathbf{G}_v}{\partial \mathbf{U}} = \mu \begin{bmatrix} 0 & 0 & 0 & 0 & 0 \\ -\partial_z\left(\frac{u}{\rho}\right) & \partial_z\left(\frac{1}{\rho}\right) & 0 & 0 & 0 \\ -\partial_z\left(\frac{v}{\rho}\right) & 0 & \partial_z\left(\frac{1}{\rho}\right) & 0 & 0 \\ -\frac{4}{3}\partial_z\left(\frac{w}{\rho}\right) & 0 & 0 & \frac{4}{3}\partial_z\left(\frac{1}{\rho}\right) & 0 \\ -\partial_z\left(\frac{u^2}{\rho}\right) - \partial_z\left(\frac{v^2}{\rho}\right) - \frac{4}{3}\partial_z\left(\frac{w^2}{\rho}\right) & \left(1-\frac{\gamma}{\mathrm{Pr}}\right)\partial_z\left(\frac{u}{\rho}\right) & \left(1-\frac{\gamma}{\mathrm{Pr}}\right)\partial_z\left(\frac{v}{\rho}\right) & \left(\frac{4}{3}-\frac{\gamma}{\mathrm{Pr}}\right)\partial_z\left(\frac{w}{\rho}\right) & \frac{\gamma}{\mathrm{Pr}}\partial_z\left(\frac{1}{\rho}\right) \\ -\frac{\gamma}{\mathrm{Pr}}\partial_z\left[\frac{p}{(\gamma-1)\rho^2} - \frac{u^2+v^2+w^2}{2\rho}\right] & & & & \end{bmatrix} \tag{8.85}$$

In these Jacobian matrices, ∂_y and ∂_z represent the partial derivatives $\partial/\partial y$ and $\partial/\partial z$.

We now substitute Eqs. (8.73), (8.77), and (8.83) into Eq. (8.72) to obtain

$$\left\{\left(\frac{\partial \mathbf{E}'}{\partial \mathbf{U}}\right)^i + \frac{\theta_1 \Delta x}{1+\theta_2}\left[\frac{\partial}{\partial y}\left(\frac{\partial \mathbf{F}_i}{\partial \mathbf{U}} - \frac{\partial \mathbf{F}_v}{\partial \mathbf{U}}\right) + \frac{\partial}{\partial z}\left(\frac{\partial \mathbf{G}_i}{\partial \mathbf{U}} - \frac{\partial \mathbf{G}_v}{\partial \mathbf{U}}\right)\right]^i\right\} \Delta^i \mathbf{U}$$

$$= -\frac{\Delta x}{1+\theta_2}\left[\frac{\partial}{\partial y}(\mathbf{F}^i) + \frac{\partial}{\partial z}(\mathbf{G}^i)\right] + \frac{\theta_2}{1+\theta_2}\Delta^{i-1}\mathbf{E} - \Delta^i \mathbf{P} \qquad (8.86)$$

where the expression

$$\left[\frac{\partial}{\partial y}\left(\frac{\partial \mathbf{F}_i}{\partial \mathbf{U}} - \frac{\partial \mathbf{F}_v}{\partial \mathbf{U}}\right)\right] \Delta^i \mathbf{U}$$

implies

$$\frac{\partial}{\partial y}\left[\left(\frac{\partial \mathbf{F}_i}{\partial \mathbf{U}} - \frac{\partial \mathbf{F}_v}{\partial \mathbf{U}}\right) \Delta^i \mathbf{U}\right]$$

and the partial derivatives appearing in $\partial \mathbf{F}_v/\partial \mathbf{U}$ and $\partial \mathbf{G}_v/\partial \mathbf{U}$ are to be applied to all terms on their right, including $\Delta^i \mathbf{U}$. Note that in Eq. (8.86), all the implicit terms have been placed on the left-hand side of the equation, while all the explicit terms appear on the right-hand side. Included in the right-hand side of the equation is the pressure gradient term $\Delta^i \mathbf{P}$, which must be dropped in subsonic regions to avoid departure solutions when marching the solution with a single sweep of the flow field.

The left-hand side of Eq. (8.86) is approximately factored in the following manner:

$$\left\{\left[\left(\frac{\partial \mathbf{E}'}{\partial \mathbf{U}}\right)^i + \frac{\theta_1 \Delta x}{1+\theta_2}\frac{\partial}{\partial z}\left(\frac{\partial \mathbf{G}_i}{\partial \mathbf{U}} - \frac{\partial \mathbf{G}_v}{\partial \mathbf{U}}\right)^i\right]\left[\left(\frac{\partial \mathbf{E}'}{\partial \mathbf{U}}\right)^i\right]^{-1}\right.$$

$$\left.\times\left[\left(\frac{\partial \mathbf{E}'}{\partial \mathbf{U}}\right)^i + \frac{\theta_1 \Delta x}{1+\theta_2}\frac{\partial}{\partial y}\left(\frac{\partial \mathbf{F}_i}{\partial \mathbf{U}} - \frac{\partial \mathbf{F}_v}{\partial \mathbf{U}}\right)^i\right]\right\} \Delta^i \mathbf{U} = \text{RHS of Eq. (8.86)} \quad (8.87)$$

The order of accuracy of this factored expression can be determined by multiplying out the factored terms and comparing the result with the left-hand side of Eq. (8.86). Upon doing this, we obtain

$$\left\{\left(\frac{\partial \mathbf{E}'}{\partial \mathbf{U}}\right)^i + \frac{\theta_1 \Delta x}{1+\theta_2}\left[\frac{\partial}{\partial y}\left(\frac{\partial \mathbf{F}_i}{\partial \mathbf{U}} - \frac{\partial \mathbf{F}_v}{\partial \mathbf{U}}\right) + \frac{\partial}{\partial z}\left(\frac{\partial \mathbf{G}_i}{\partial \mathbf{U}} - \frac{\partial \mathbf{G}_v}{\partial \mathbf{U}}\right)\right]^i\right.$$

$$\left. + \left(\frac{\theta_1 \Delta x}{1+\theta_2}\right)^2 \frac{\partial}{\partial z}\left(\frac{\partial \mathbf{G}_i}{\partial \mathbf{U}} - \frac{\partial \mathbf{G}_v}{\partial \mathbf{U}}\right)^i\left[\left(\frac{\partial \mathbf{E}'}{\partial \mathbf{U}}\right)^i\right]^{-1} \frac{\partial}{\partial y}\left(\frac{\partial \mathbf{F}_i}{\partial \mathbf{U}} - \frac{\partial \mathbf{F}_v}{\partial \mathbf{U}}\right)^i\right\} \Delta^i \mathbf{U}$$

$$= \text{RHS of Eq. (8.86)} \qquad (8.88)$$

so that

$$\text{LHS of Eq. (8.87)} = \text{LHS of Eq. (8.86)} + O[(\Delta x)^2] \tag{8.89}$$

As a consequence, the formal accuracy of the numerical algorithm is not affected by the approximate factorization. However, it has been observed that approximate factorization may lead to sizable errors in certain computations.

The partial derivatives $\partial/\partial y$ and $\partial/\partial z$ in Eq. (8.87) are approximated with second-order accurate central differences. For example, the inviscid term

$$\frac{\partial}{\partial y}\left(\frac{\partial \mathbf{F}_i}{\partial \mathbf{U}}\right)^i \Delta^i \mathbf{U}$$

is differenced as

$$\frac{\left[(\partial \mathbf{F}_i/\partial \mathbf{U})^i \, \Delta^i \mathbf{U}\right]_{j+1} - \left[(\partial \mathbf{F}_i/\partial \mathbf{U})^i \, \Delta^i \mathbf{U}\right]_{j-1}}{2\,\Delta y} \tag{8.90}$$

and each element of the viscous term,

$$\frac{\partial}{\partial y}\left(\frac{\partial \mathbf{F}_v}{\partial \mathbf{U}}\right)^i \Delta^i \mathbf{U}$$

which has the general form

$$\frac{\partial}{\partial y}\left[\alpha \frac{\partial}{\partial y}(\beta \, \Delta^i U_l)\right]$$

is differenced as

$$\begin{aligned}
&\frac{\{\alpha[\partial(\beta\,\Delta^i U_l)/\partial y]\}_{j+1/2} - \{\alpha[\partial(\beta\,\Delta^i U_l)/\partial y]\}_{j-1/2}}{\Delta y} \\
&\quad \cong \frac{\alpha_{j+1/2}[(\beta\,\Delta^i U_l)_{j+1} - (\beta\,\Delta^i U_l)_j] - \alpha_{j-1/2}[(\beta\,\Delta^i U_l)_j - (\beta\,\Delta^i U_l)_{j-1}]}{(\Delta y)^2} \\
&\quad \cong \frac{(\alpha_j + \alpha_{j+1})[(\beta\,\Delta^i U_l)_{j+1} - (\beta\,\Delta^i U_l)_j] - (\alpha_j + \alpha_{j-1})[(\beta\,\Delta^i U_l)_j - (\beta\,\Delta^i U_l)_{j-1}]}{2(\Delta y)^2}
\end{aligned} \tag{8.91}$$

The algorithm given by Eq. (8.87) is implemented in the following manner:

Step 1:

$$\left[\left(\frac{\partial \mathbf{E}'}{\partial \mathbf{U}}\right)^i + \frac{\theta_1 \, \Delta x}{1 + \theta_2} \frac{\partial}{\partial z}\left(\frac{\partial \mathbf{G}_i}{\partial \mathbf{U}} - \frac{\partial \mathbf{G}_v}{\partial \mathbf{U}}\right)^i\right] \Delta^i \mathbf{U}_1 = \text{RHS of Eq. (8.86)} \tag{8.92}$$

Step 2:
$$\Delta^i \mathbf{U}_2 = \left(\frac{\partial \mathbf{E}'}{\partial \mathbf{U}}\right)^i \Delta^i \mathbf{U}_1 \tag{8.93}$$

Step 3:
$$\left[\left(\frac{\partial \mathbf{E}'}{\partial \mathbf{U}}\right)^i + \frac{\theta_1 \Delta x}{1+\theta_2}\frac{\partial}{\partial y}\left(\frac{\partial \mathbf{F}_i}{\partial \mathbf{U}} - \frac{\partial \mathbf{F}_v}{\partial \mathbf{U}}\right)^i\right]\Delta^i \mathbf{U} = \Delta^i \mathbf{U}_2 \tag{8.94}$$

Step 4:
$$\mathbf{U}^{i+1} = \mathbf{U}^i + \Delta^i \mathbf{U} \tag{8.95}$$

In Step 1, $\Delta^i \mathbf{U}_1$ represents the vector quantity

$$\left[\left(\frac{\partial \mathbf{E}'}{\partial \mathbf{U}}\right)^i\right]^{-1}\left[\left(\frac{\partial \mathbf{E}'}{\partial \mathbf{U}}\right)^i + \frac{\theta_1 \Delta x}{1+\theta_2}\frac{\partial}{\partial y}\left(\frac{\partial \mathbf{F}_i}{\partial \mathbf{U}} - \frac{\partial \mathbf{F}_v}{\partial \mathbf{U}}\right)^i\right]\Delta^i \mathbf{U}$$

which is determined by solving the system of equations given by Eq. (8.92). This system of equations has the following block tridiagonal structure:

$$\begin{bmatrix} [B_1] & [C_1] & & & 0 \\ [A_2] & [B_2] & [C_2] & & \\ & [A_3] & [B_3] & [C_3] & \\ & & \ddots & \ddots & \ddots \\ & & & [A_{K-1}] & [B_{K-1}] & [C_{K-1}] \\ 0 & & & & [A_K] & [B_K] \end{bmatrix} \begin{bmatrix} [\Delta^i U_1]_1 \\ [\Delta^i U_1]_2 \\ [\Delta^i U_1]_3 \\ \vdots \\ [\Delta^i U_1]_{K-1} \\ [\Delta^i U_1]_K \end{bmatrix} = \begin{bmatrix} [\mathrm{RHS}]_1 \\ [\mathrm{RHS}]_2 \\ [\mathrm{RHS}]_3 \\ \vdots \\ [\mathrm{RHS}]_{K-1} \\ [\mathrm{RHS}]_K \end{bmatrix} \tag{8.96}$$

where $[A]$, $[B]$, and $[C]$ are 5×5 matrices and $[\Delta^i \mathbf{U}_1]$ and [RHS] are column matrices whose elements are the components of the vectors $\Delta^i \mathbf{U}_1$ and the RHS

of Eq. (8.86). This system of equations can be solved using the block tridiagonal solver given in Appendix B. Once $\Delta^i \mathbf{U}_1$ is determined, it is multiplied by $(\partial \mathbf{E}'/\partial \mathbf{U})^i$ in Step 2. As a result of this multiplication, the inverse matrix $[(\partial \mathbf{E}'/\partial \mathbf{U})^i]^{-1}$ does not have to be determined in the solution process. In Step 3, the block tridiagonal system of equations in the y direction is solved. Finally, in Step 4, the vector of unknowns at station $i + 1$ (i.e., $\mathbf{U}^{i+1}$) is determined by simply adding $\Delta^i \mathbf{U}$ to the vector of unknowns at station i. The primitive variables can then be obtained from $\mathbf{U}^{i+1}$ in the following manner:

$$\begin{aligned}
\rho^{i+1} &= U_1^{i+1} \\
u^{i+1} &= \frac{U_2^{i+1}}{U_1^{i+1}} \\
v^{i+1} &= \frac{U_3^{i+1}}{U_1^{i+1}} \\
w^{i+1} &= \frac{U_4^{i+1}}{U_1^{i+1}} \\
e^{i+1} &= \frac{U_5^{i+1}}{U_1^{i+1}} - \frac{(u^{i+1})^2 + (v^{i+1})^2 + (w^{i+1})^2}{2}
\end{aligned} \tag{8.97}$$

For centrally differenced algorithms like the present one, it is often necessary to add smoothing (artificial viscosity) in order to suppress high-frequency oscillations. This can easily be accomplished by adding a fourth-order explicit dissipation term of the form

$$-\epsilon_e \left[(\Delta y)^4 \frac{\partial^4}{\partial y^4}(\mathbf{U}^i) + (\Delta z)^4 \frac{\partial^4}{\partial z^4}(\mathbf{U}^i) \right] \tag{8.98}$$

to the right-hand side of Eq. (8.86). Since this is a fourth-order term, it does not affect the formal accuracy of the algorithm. The negative sign is required in front of the fourth derivatives in order to produce positive damping [see Eq. (4.21)]. The smoothing coefficient ϵ_e should be less than approximately $\frac{1}{16}$ for stability. The fourth-derivative terms can be evaluated using the following finite-difference approximations:

$$\begin{aligned}
(\Delta y)^4 \frac{\partial^4}{\partial y^4}(\mathbf{U}^i) &\cong \mathbf{U}^i_{j+2,k} - 4\mathbf{U}^i_{j+1,k} + 6\mathbf{U}^i_{j,k} - 4\mathbf{U}^i_{j-1,k} + \mathbf{U}^i_{j-2,k} \\
(\Delta z)^4 \frac{\partial^4}{\partial z^4}(\mathbf{U}^i) &\cong \mathbf{U}^i_{j,k+2} - 4\mathbf{U}^i_{j,k+1} + 6\mathbf{U}^i_{j,k} - 4\mathbf{U}^i_{j,k-1} + \mathbf{U}^i_{j,k-2}
\end{aligned} \tag{8.99}$$

In the Schiff and Steger (1979) algorithm as well as that developed by Vigneron et al. (1978a), the solution is advanced using computational planes (i.e., solution surfaces) normal to the body axis. Most body shapes can be treated in this manner. However, for bodies with large surface slopes, the axial component of velocity in the inviscid part of the flow field may become subsonic, which prevents the computation from proceeding further. To alleviate this

difficulty, Tannehill et al. (1982) have applied the numerical scheme (described previously) to the PNS equations written in general nonorthogonal coordinates, Eqs. (8.37)–(8.39). As a result, the orientation of each solution surface ($\xi =$ const) is left arbitrary, so that the most appropriate orientation can be selected for a given problem. In general, the optimum orientation occurs when the solution surface is nearly perpendicular to the local flow direction. In a similar manner, Helliwell et al. (1980) have incorporated a nonorthogonal coordinate system into the Lubard-Helliwell method to permit a more optimum orientation of the computational planes.

The PNS code developed by Schiff and Steger (1979) was further refined (Chaussee et al., 1981) and became the basis for the widely used AFWAL (Air Force Wright Aeronautical Laboratories) PNS code (Shanks et al., 1982; Stalnaker et al., 1986). Other implicit algorithms for solving the PNS equations have been developed by McDonald and Briley (1975) and Briley and McDonald (1980), who utilize a consistently split linearized block implicit (LBI) scheme, and by Li (1981a), who uses an iterative factored implicit scheme. The LBI scheme of McDonald and Briley has a linearized block implicit structure that is identical to the structure of the "delta" form of the Beam-Warming scheme.

The explicit-implicit scheme of MacCormack (1981) was applied to the solution of the PNS equations by Lawrence et al. (1984). This scheme requires the inversion of block bidiagonal systems rather than the block tridiagonal systems of the previous factored algorithms. The advent of high-speed vector-processing computers led Gielda and McRae (1986) to use the original explicit MacCormack (1969) scheme to solve the PNS equations. Since this scheme can be almost completely vectorized, it becomes competitive for certain classes of problems. In this algorithm the conservative streamwise flux vector $\mathbf{E}$ is solved at each ξ station, instead of the usual $\mathbf{U}$ vector. In another approach, Bhutta and Lewis (1985a) employed an implicit algorithm in conjunction with a pseudo-unsteady technique to solve the PNS equations.

Roe scheme. Nearly all of the previously described algorithms employ central differences for the derivatives in the crossflow (η, ζ) plane. A major difficulty for algorithms of this type is that the central differencing of fluxes across flow field discontinuities tends to introduce errors into the solution in the form of local flow property oscillations. In order to control these oscillations, some type of artificial dissipation is required. The correct magnitude of this added "smoothing" must be determined through a trial-and-error process. This has led to frustration on the part of many users of central-difference PNS codes. To alleviate this difficulty, Lawrence et al. (1986, 1987) developed an upwind implicit approximately factored finite-volume scheme based on Roe's approximate Riemann problem solver (Roe, 1981). With this upwind scheme, no user-specified smoothing coefficients are required when capturing discontinuities such as shock waves. The resulting upwind PNS code has been named UPS.

The development of the finite-volume scheme of Lawrence et al. begins with

the integral form of the steady Navier-Stokes equations (Eq. 5.263):

$$\oiint_S \bar{\mathbf{H}} \cdot d\mathbf{S} = 0 \tag{8.100}$$

The tensor $\bar{\mathbf{H}}$ can be expressed in terms of the Cartesian fluxes,

$$\bar{\mathbf{H}} = (\mathbf{E}_i - \mathbf{E}_v)\mathbf{i} + (\mathbf{F}_i - \mathbf{F}_v)\mathbf{j} + (\mathbf{G}_i - \mathbf{G}_v)\mathbf{k} \tag{8.101}$$

where the inviscid (subscript i) and viscous (subscript v) flux vectors are given by Eq. (8.35). The flow field is discretized using small but finite hexahedrons like the one shown in Fig. 8.5. Since the numerical solution is marched in the ξ direction, the flow field is discretized by successively adding slabs of thickness $\Delta\xi$ as the solution proceeds. The nth slab (n is the index for the ξ coordinate) is bounded by the two (η, ζ) systems of grid points at n and $n + 1$. Vinokur (1986) refers to these grid points as the primary grids. The vertices of each cell are located at mesh points of the primary grids and are connected by straight-line segments. The η and ζ coordinates are indexed using k and l, respectively. The present scheme is applied to area-averaged flow properties, which are assigned to the secondary grid points. The secondary grid points (see Fig. 8.5) are defined by averaging coordinates of the primary grids that define the constant ξ cell faces.

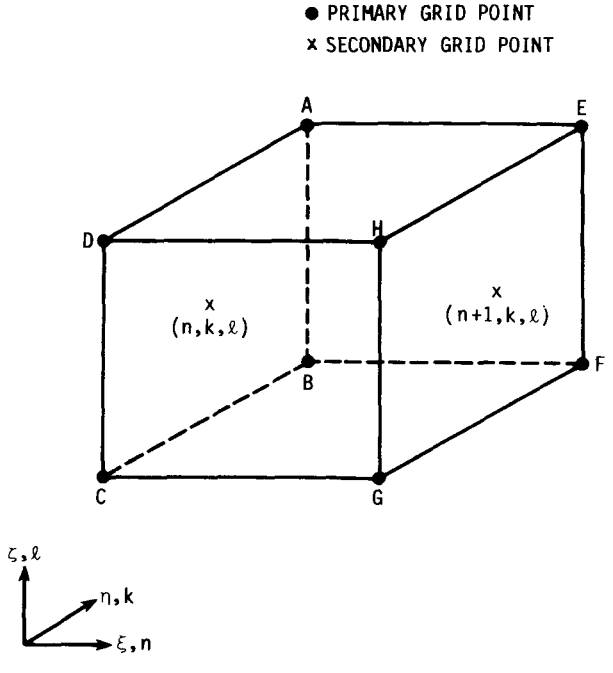

Figure 8.5 Finite-volume geometry.

After applying Eq. (8.100) to the structured-grid volume shown in Fig. 8.5, with constant properties on each cell face, the discretization becomes

$$\overline{\mathbf{H}}_{k,l}^{n+1} \cdot \mathbf{S}_{k,l}^{n+1} + \overline{\mathbf{H}}_{k+\frac{1}{2},l}^{n+\frac{1}{2}} \cdot \mathbf{S}_{k+\frac{1}{2},l}^{n+\frac{1}{2}} + \overline{\mathbf{H}}_{k,l+\frac{1}{2}}^{n+\frac{1}{2}} \cdot \mathbf{S}_{k,l+\frac{1}{2}}^{n+\frac{1}{2}} - \overline{\mathbf{H}}_{k,l}^{n} \cdot \mathbf{S}_{k,l}^{n} - \overline{\mathbf{H}}_{k-\frac{1}{2},l}^{n+\frac{1}{2}} \cdot \mathbf{S}_{k-\frac{1}{2},l}^{n+\frac{1}{2}} - \overline{\mathbf{H}}_{k,l-\frac{1}{2}}^{n+\frac{1}{2}} \cdot \mathbf{S}_{k,l-\frac{1}{2}}^{n+\frac{1}{2}} = 0 \tag{8.102}$$

with the cell-face-area vectors oriented in the positive coordinate directions. The cell-face-area vectors are indexed as follows:

$$\begin{aligned} \mathbf{S}_{\mathrm{ABCD}} &\Leftrightarrow \mathbf{S}_{k,l}^{n} & \mathbf{S}_{\mathrm{EHGF}} &\Leftrightarrow \mathbf{S}_{k,l}^{n+1} \\ \mathbf{S}_{\mathrm{DCGH}} &\Leftrightarrow \mathbf{S}_{k-\frac{1}{2},l}^{n+\frac{1}{2}} & \mathbf{S}_{\mathrm{AEFB}} &\Leftrightarrow \mathbf{S}_{k+\frac{1}{2},l}^{n+\frac{1}{2}} \\ \mathbf{S}_{\mathrm{BFGC}} &\Leftrightarrow \mathbf{S}_{k,l-\frac{1}{2}}^{n+\frac{1}{2}} & \mathbf{S}_{\mathrm{ADHE}} &\Leftrightarrow \mathbf{S}_{k,l+\frac{1}{2}}^{n+\frac{1}{2}} \end{aligned} \tag{8.103}$$

and can be expressed with respect to a Cartesian coordinate system as

$$\begin{aligned} \mathbf{S}_{k,l}^{n+1} &= \left(\frac{\xi_x}{J}\right)_{k,l}^{n+1}\mathbf{i} + \left(\frac{\xi_y}{J}\right)_{k,l}^{n+1}\mathbf{j} + \left(\frac{\xi_z}{J}\right)_{k,l}^{n+1}\mathbf{k} \\ \mathbf{S}_{k+\frac{1}{2},l}^{n+\frac{1}{2}} &= \left(\frac{\eta_x}{J}\right)_{k+\frac{1}{2},l}^{n+\frac{1}{2}}\mathbf{i} + \left(\frac{\eta_y}{J}\right)_{k+\frac{1}{2},l}^{n+\frac{1}{2}}\mathbf{j} + \left(\frac{\eta_z}{J}\right)_{k+\frac{1}{2},l}^{n+\frac{1}{2}}\mathbf{k} \\ \mathbf{S}_{k,l+\frac{1}{2}}^{n+\frac{1}{2}} &= \left(\frac{\zeta_x}{J}\right)_{k,l+\frac{1}{2}}^{n+\frac{1}{2}}\mathbf{i} + \left(\frac{\zeta_y}{J}\right)_{k,l+\frac{1}{2}}^{n+\frac{1}{2}}\mathbf{j} + \left(\frac{\zeta_z}{J}\right)_{k,l+\frac{1}{2}}^{n+\frac{1}{2}}\mathbf{k} \\ \mathbf{S}_{k,l}^{n} &= -\left(\frac{\xi_x}{J}\right)_{k,l}^{n}\mathbf{i} - \left(\frac{\xi_y}{J}\right)_{k,l}^{n}\mathbf{j} - \left(\frac{\xi_z}{J}\right)_{k,l}^{n}\mathbf{k} \\ \mathbf{S}_{k-\frac{1}{2},l}^{n+\frac{1}{2}} &= -\left(\frac{\eta_x}{J}\right)_{k-\frac{1}{2},l}^{n+\frac{1}{2}}\mathbf{i} - \left(\frac{\eta_y}{J}\right)_{k-\frac{1}{2},l}^{n+\frac{1}{2}}\mathbf{j} - \left(\frac{\eta_z}{J}\right)_{k-\frac{1}{2},l}^{n+\frac{1}{2}}\mathbf{k} \\ \mathbf{S}_{k,l-\frac{1}{2}}^{n+\frac{1}{2}} &= -\left(\frac{\zeta_x}{J}\right)_{k,l-\frac{1}{2}}^{n+\frac{1}{2}}\mathbf{i} - \left(\frac{\zeta_y}{J}\right)_{k,l-\frac{1}{2}}^{n+\frac{1}{2}}\mathbf{j} - \left(\frac{\zeta_z}{J}\right)_{k,l-\frac{1}{2}}^{n+\frac{1}{2}}\mathbf{k} \end{aligned} \tag{8.104}$$

Equations (8.104) and (8.101) can then be inserted into Eq. (8.102) to yield

$$\left(\hat{\mathbf{E}}_i - \hat{\mathbf{E}}_v\right)_{k,l}^{n+1} + \left(\hat{\mathbf{F}}_i - \hat{\mathbf{F}}_v\right)_{k+\frac{1}{2},l}^{n+\frac{1}{2}} + \left(\hat{\mathbf{G}}_i - \hat{\mathbf{G}}_v\right)_{k,l+\frac{1}{2}}^{n+\frac{1}{2}} - \left(\hat{\mathbf{E}}_i - \hat{\mathbf{E}}_v\right)_{k,l}^{n} - \left(\hat{\mathbf{F}}_i - \hat{\mathbf{F}}_v\right)_{k-\frac{1}{2},l}^{n+\frac{1}{2}} - \left(\hat{\mathbf{G}}_i - \hat{\mathbf{G}}_v\right)_{k,l-\frac{1}{2}}^{n+\frac{1}{2}} = 0 \tag{8.105}$$

where

$$\left(\hat{\mathbf{E}}_i - \hat{\mathbf{E}}_v\right) = \left(\frac{\xi_x}{J}\right)(\mathbf{E}_i - \mathbf{E}_v) + \left(\frac{\xi_y}{J}\right)(\mathbf{F}_i - \mathbf{F}_v) + \left(\frac{\xi_z}{J}\right)(\mathbf{G}_i - \mathbf{G}_v)$$

$$\left(\hat{\mathbf{F}}_i - \hat{\mathbf{F}}_v\right) = \left(\frac{\eta_x}{J}\right)(\mathbf{E}_i - \mathbf{E}_v) + \left(\frac{\eta_y}{J}\right)(\mathbf{F}_i - \mathbf{F}_v) + \left(\frac{\eta_z}{J}\right)(\mathbf{G}_i - \mathbf{G}_v) \quad (8.106)$$

$$\left(\hat{\mathbf{G}}_i - \hat{\mathbf{G}}_v\right) = \left(\frac{\zeta_x}{J}\right)(\mathbf{E}_i - \mathbf{E}_v) + \left(\frac{\zeta_y}{J}\right)(\mathbf{F}_i - \mathbf{F}_v) + \left(\frac{\zeta_z}{J}\right)(\mathbf{G}_i - \mathbf{G}_v)$$

The metrics (i.e., components of the cell-face-area vectors) are evaluated using the formulas of Vinokur (1986), which were discussed in Section 5.7. For the three forward-facing sides of the finite volume shown in Fig. 8.5, these formulas yield

$$\left(\frac{\xi_x}{J}\right)_{k,l}^{n+1} = \frac{1}{2}[(y_D - y_B)(z_A - z_C) - (y_A - y_C)(z_D - z_B)]$$

$$\left(\frac{\xi_y}{J}\right)_{k,l}^{n+1} = -\frac{1}{2}[(x_D - x_B)(z_A - z_C) - (x_A - x_C)(z_D - z_B)]$$

$$\left(\frac{\xi_z}{J}\right)_{k,l}^{n+1} = \frac{1}{2}[(x_D - x_B)(y_A - y_C) - (x_A - x_C)(y_D - y_B)]$$

$$\left(\frac{\eta_x}{J}\right)_{k+\frac{1}{2},l}^{n+\frac{1}{2}} = \frac{1}{2}[(y_E - y_D)(z_H - z_A) - (y_H - y_A)(z_E - z_D)]$$

$$\left(\frac{\eta_y}{J}\right)_{k+\frac{1}{2},l}^{n+\frac{1}{2}} = -\frac{1}{2}[(x_E - x_D)(z_H - z_A) - (x_H - x_A)(z_E - z_D)] \quad (8.107)$$

$$\left(\frac{\eta_z}{J}\right)_{k+\frac{1}{2},l}^{n+\frac{1}{2}} = \frac{1}{2}[(x_E - x_D)(y_H - y_A) - (x_H - x_A)(y_E - y_D)]$$

$$\left(\frac{\zeta_x}{J}\right)_{k,l+\frac{1}{2}}^{n+\frac{1}{2}} = \frac{1}{2}[(y_F - y_A)(z_E - z_B) - (y_E - y_B)(z_F - z_A)]$$

$$\left(\frac{\zeta_y}{J}\right)_{k,l+\frac{1}{2}}^{n+\frac{1}{2}} = -\frac{1}{2}[(x_F - x_A)(z_E - z_B) - (x_E - x_B)(z_F - z_A)]$$

$$\left(\frac{\zeta_z}{J}\right)_{k,l+\frac{1}{2}}^{n+\frac{1}{2}} = \frac{1}{2}[(x_F - x_A)(y_E - y_B) - (x_E - x_B)(y_F - y_A)]$$

Metrics calculated using these formulas satisfy the geometric conservation law

$$\oiint_S d\mathbf{S} = 0 \quad (8.108)$$

which is obtained from Eq. (8.100) under uniform flow conditions. The description of the geometry is completed by determining the volume of the cell. The volume is only needed for evaluating the metrics in the viscous terms. Using the formula given in Section 5.7 by Vinokur (1986), the volume (i.e., Jacobian) is computed from

$$J = \tfrac{1}{3}\left(\mathbf{S}_{k,l}^{n} + \mathbf{S}_{k,l-\frac{1}{2}}^{n+\frac{1}{2}} + \mathbf{S}_{k+\frac{1}{2},l}^{n+\frac{1}{2}}\right) \cdot \left(\mathbf{r}_{k+\frac{1}{2},l-\frac{1}{2}}^{n} - \mathbf{r}_{k-\frac{1}{2},l+\frac{1}{2}}^{n+1}\right) \quad (8.109)$$

The parabolizing assumption is now applied to Eq. (8.105) dropping $\hat{\mathbf{E}}_v$ as well as derivatives with respect to ξ in $\hat{\mathbf{F}}_v$ and $\hat{\mathbf{G}}_v$. In addition, Vigneron's technique is used to suppress the ellipticity that is inherent in a space-marching procedure. This is accomplished by splitting the inviscid streamwise flux vector in the following manner:

$$\left(\hat{\mathbf{E}}_i\right)_{k,l}^{n} = \hat{\mathbf{E}}^*(\mathbf{S}_{k,l}^n, \mathbf{U}_{k,l}^n) + \hat{\mathbf{E}}^p(\mathbf{S}_{k,l}^n, \mathbf{U}_{k,l}^{n-1}) \tag{8.110}$$

where

$$\hat{\mathbf{E}}^* = \left[\rho\hat{U}, \rho u\hat{U} + \left(\frac{\xi_x}{J}\right)\omega p, \rho v\hat{U} + \left(\frac{\xi_y}{J}\right)\omega p, \rho w\hat{U} + \left(\frac{\xi_z}{J}\right)\omega p, (E_t + p)\hat{U}\right]^T$$

$$\hat{\mathbf{E}}^p = (1-\omega)p\left[0, \left(\frac{\xi_x}{J}\right), \left(\frac{\xi_y}{J}\right), \left(\frac{\xi_z}{J}\right), 0\right]^T$$

and

$$\mathbf{U} = [\rho, \rho u, \rho v, \rho w, E_t]^T$$

$$\hat{U} = \left(\frac{\xi_x}{J}\right)u + \left(\frac{\xi_y}{J}\right)v + \left(\frac{\xi_z}{J}\right)w$$

The notation $\hat{\mathbf{E}}^*(\mathbf{S}_{k,l}^n, \mathbf{U}_{k,l}^n)$ indicates that $\hat{\mathbf{E}}^*$ is evaluated using geometrical properties at cell face $\mathbf{S}_{k,l}^n$ and flow variables from $\mathbf{U}_{k,l}^n$.

A change of dependent variable from $\hat{\mathbf{E}}^*$ to $\mathbf{U}$ is now made to avoid the difficult of extracting the flow properties from $\hat{\mathbf{E}}^*$ and also to simplify the application of the implicit algorithm. This is accomplished through the following linearization, which makes use of the homogeneous property of $\hat{\mathbf{E}}^*$:

$$\hat{\mathbf{E}}^*(\mathbf{S}^n, \mathbf{U}^n) = [\hat{A}^*]^{n-1}\mathbf{U}^n \tag{8.111}$$

where

$$[\hat{A}^*]^{n-1} = \frac{\partial \hat{\mathbf{E}}^*(\mathbf{S}^n, \mathbf{U}^{n-1})}{\partial \mathbf{U}^{n-1}}$$

After substituting Eqs. (8.110) and (8.111) into Eq. (8.105), the discretized conservation law becomes

$$\begin{aligned}[\hat{A}^*]_{k,l}^n \Delta^n \mathbf{U}_{k,l} = &-\left([\hat{A}^*]_{k,l}^n - [\hat{A}^*]_{k,l}^{n-1}\right)\mathbf{U}_{k,l}^n - \left[\left(\hat{\mathbf{F}}_i - \hat{\mathbf{F}}_v\right)_{k+\frac{1}{2},l}^{n+\frac{1}{2}} - \left(\hat{\mathbf{F}}_i - \hat{\mathbf{F}}_v\right)_{k-\frac{1}{2},l}^{n+\frac{1}{2}}\right] \\ &- \left[\left(\hat{\mathbf{G}}_i - \hat{\mathbf{G}}_v\right)_{k,l+\frac{1}{2}}^{n+\frac{1}{2}} - \left(\hat{\mathbf{G}}_i - \hat{\mathbf{G}}_v\right)_{k,l-\frac{1}{2}}^{n+\frac{1}{2}}\right] \\ &- \left[\hat{\mathbf{E}}^p(\mathbf{S}_{k,l}^{n+1}, \mathbf{U}_{k,l}^n) - \hat{\mathbf{E}}^p(\mathbf{S}_{k,l}^n, \mathbf{U}_{k,l}^{n-1})\right]\end{aligned} \tag{8.112}$$

where

$$\Delta^n \mathbf{U} = \mathbf{U}^{n+1} - \mathbf{U}^n$$

At this point the algorithm differs from a conventional finite-difference PNS solver only in the fact that the metrics are evaluated at cell interfaces rather than at grid points. A central-difference scheme is obtained by simply averaging the adjacent grid-point flow properties to obtain the cell-face numerical fluxes. Of course, this will lead to undesirable shock-capturing characteristics. To avoid this problem, Lawrence et al. determine the fluxes at the cell interfaces using

Roe's (1981) scheme, which is modified to make it applicable to a space-marching calculation. With Roe's scheme, the inviscid portions of the numerical fluxes are defined according to solutions of steady approximate Riemann problems. The fluxes $\hat{\mathbf{F}}_i$ and $\hat{\mathbf{G}}_i$ are determined separately by splitting the 2-D Riemann problem associated with the 3-D PNS equations into two 1-D Riemann problems. These 1-D problems have the generic form

$$\frac{\partial \hat{\mathbf{E}}^*}{\partial \xi} + [D]_{m+\frac{1}{2}} \frac{\partial \hat{\mathbf{E}}^*}{\partial \kappa} = 0 \tag{8.113}$$

with initial conditions

$$\hat{\mathbf{E}}^{*n} = \begin{cases} \hat{\mathbf{E}}^*\left(\mathbf{S}^n_{m+\frac{1}{2}}, \mathbf{U}_m\right) & \kappa < \kappa_{m+\frac{1}{2}} \\ \hat{\mathbf{E}}^*\left(\mathbf{S}^n_{m+\frac{1}{2}}, \mathbf{U}_{m+1}\right) & \kappa > \kappa_{m+\frac{1}{2}} \end{cases}$$

The coefficient matrix $[D]_{m+\frac{1}{2}}$ is defined by

$$[D]_{m+\frac{1}{2}} = \left(\frac{\kappa_x}{J}\right)_{m+\frac{1}{2}} \left(\frac{\partial \mathbf{E}_i}{\partial \hat{\mathbf{E}}^*}\right)_{m+\frac{1}{2}} + \left(\frac{\kappa_y}{J}\right)_{m+\frac{1}{2}} \left(\frac{\partial \mathbf{F}_i}{\partial \hat{\mathbf{E}}^*}\right)_{m+\frac{1}{2}} + \left(\frac{\kappa_z}{J}\right)_{m+\frac{1}{2}} \left(\frac{\partial \mathbf{G}_i}{\partial \hat{\mathbf{E}}^*}\right)_{m+\frac{1}{2}} \tag{8.114}$$

Although Eq. (8.113) is in nonconservative form, the local shock-capturing capabilities of the algorithm can be retained if the flow properties in $[D]_{m+\frac{1}{2}}$ are averaged between the grid points m and $m+1$, so that the following relation is satisfied:

$$[D]_{m+\frac{1}{2}}\left[\hat{\mathbf{E}}^*\left(\mathbf{S}^n_{m+\frac{1}{2}}, \mathbf{U}_{m+1}\right) - \hat{\mathbf{E}}^*\left(\mathbf{S}^n_{m+\frac{1}{2}}, \mathbf{U}_m\right)\right] = \left(\frac{\kappa_x}{J}\right)_{m+\frac{1}{2}} \Delta \mathbf{E}_i + \left(\frac{\kappa_y}{J}\right)_{m+\frac{1}{2}} \Delta \mathbf{F}_i + \left(\frac{\kappa_z}{J}\right)_{m+\frac{1}{2}} \Delta \mathbf{G}_i \tag{8.115}$$

When the flow is supersonic, Roe's averaging (see Section 6.5.1) of the flow variables yields flow properties that satisfy Eq. (8.115).

The solution to the preceding approximate Riemann problem consists of four constant property regions separated by three surfaces of discontinuity (see Fig. 8.6) emanating from the cell edge $(\xi^n, \kappa_{m+\frac{1}{2}})$ and having slopes given by the eigenvalues of $[D]_{m+\frac{1}{2}}$. The resulting first-order accurate inviscid flux across the $m+\frac{1}{2}$ cell interface is given by

$$\begin{aligned} \mathbf{H}_{m+\frac{1}{2}} = {} & \left(\frac{\kappa_x}{J}\right)_{m+\frac{1}{2}} \frac{1}{2}[(\mathbf{E}_i)_m + (\mathbf{E}_i)_{m+1}] + \left(\frac{\kappa_y}{J}\right)_{m+\frac{1}{2}} \frac{1}{2}[(\mathbf{F}_i)_m + (\mathbf{F}_i)_{m+1}] \\ & + \left(\frac{\kappa_z}{J}\right)_{m+\frac{1}{2}} \frac{1}{2}[(\mathbf{G}_i)_m + (\mathbf{G}_i)_{m+1}] \\ & - \frac{1}{2}[\operatorname{sgn} D]_{m+\frac{1}{2}}\left[\left(\frac{\kappa_x}{J}\right)_{m+\frac{1}{2}} \Delta \mathbf{E}_i + \left(\frac{\kappa_y}{J}\right)_{m+\frac{1}{2}} \Delta \mathbf{F}_i + \left(\frac{\kappa_z}{J}\right)_{m+\frac{1}{2}} \Delta \mathbf{G}_i\right] \end{aligned} \tag{8.116}$$

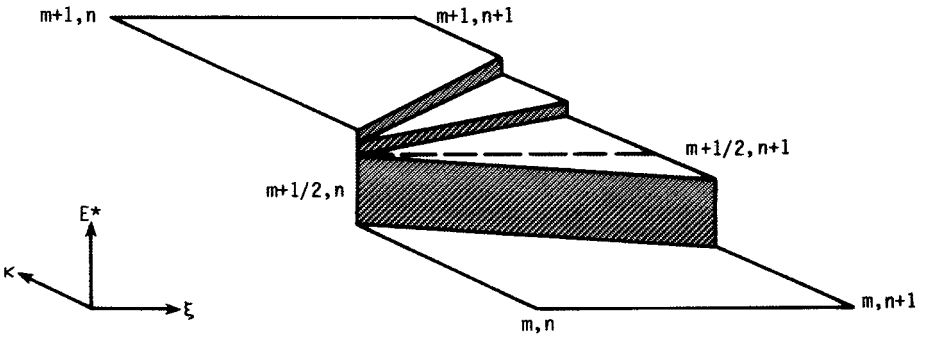

Figure 8.6 Approximate Riemann problem.

In this equation the matrix, [sgn D], is defined as

$$[\text{sgn } D] = [R][\text{sgn } \Lambda][R]^{-1}$$

where $[R]$ is the matrix of right eigenvectors of $[D]$ and [sgn Λ] is the diagonal matrix, which has elements related to the eigenvalues of $[D]$ by

$$\text{sgn } \lambda^i = \frac{\lambda^i}{|\lambda^i|}$$

First-order inviscid numerical fluxes in the η and ζ directions are then given by

$$\left(\hat{\mathbf{F}}_i\right)_{k+\frac{1}{2},l} = \mathbf{H}_{k+\frac{1}{2},l}$$

$$\left(\hat{\mathbf{G}}_i\right)_{k,l+\frac{1}{2}} = \mathbf{H}_{k,l+\frac{1}{2}}$$

In the definition of the flux in the η direction, $\mathbf{H}_{k+\frac{1}{2},l}$ is obtained by inserting η for κ and $k+\frac{1}{2},l$ for $m+\frac{1}{2}$. Likewise, for the flux in the ζ direction, $\mathbf{H}_{k,l+\frac{1}{2}}$ is obtained by replacing κ with ζ and $m+\frac{1}{2}$ with $k,l+\frac{1}{2}$. Lawrence et al. have extended the algorithm to second-order accuracy in the crossflow directions by adapting the approach of Chakravarthy and Szema (1985) to the PNS equations. Details on the second-order fluxes can be found in the work by Lawrence (1987). Viscous stresses and heat transfer fluxes are evaluated in both crossflow directions using standard central differences.

The algorithm is made implicit by evaluating the first-order numerical flux at the $n+1$ marching station. The second-order flux terms are evaluated at the n marching station. The first-order flux is linearized using

$$(\mathbf{H})^{n+1}_{m+\frac{1}{2}} = (\mathbf{H})^{n}_{m+\frac{1}{2}} + \left(\frac{\partial(\mathbf{H})_{m+\frac{1}{2}}}{\partial \mathbf{U}_{m+1}}\right)^n \Delta^n \mathbf{U}_{m+1} + \left(\frac{\partial(\mathbf{H})_{m+\frac{1}{2}}}{\partial \mathbf{U}_{m}}\right)^n \Delta^u \mathbf{U}_{m} \quad (8.117)$$

The [sgn D] matrix that appears in $\mathbf{H}$ is assumed locally constant for the evaluation of the Jacobians. The viscous fluxes at $n+1$ are linearized in a

similar manner using

$$\begin{aligned}
\left(\hat{\mathbf{F}}_v\right)^{n+1}_{k+\frac{1}{2},l} &= \left(\hat{\mathbf{F}}_v\right)^{n}_{k+\frac{1}{2},l} + \left(\frac{\partial\left(\hat{\mathbf{F}}_v\right)_{k+\frac{1}{2},l}}{\partial \mathbf{U}_{k+1,l}}\right)^n \Delta^n \mathbf{U}_{k+1,l} \\
&\quad + \left(\frac{\partial\left(\hat{\mathbf{F}}_v\right)_{k+\frac{1}{2},l}}{\partial \mathbf{U}_{k,l}}\right)^n \Delta^n \mathbf{U}_{k,l} \\
\left(\hat{\mathbf{G}}_v\right)^{n+1}_{k,l+\frac{1}{2}} &= \left(\hat{\mathbf{G}}_v\right)^{n}_{k,l+\frac{1}{2}} + \left(\frac{\partial\left(\hat{\mathbf{G}}_v\right)_{k,l+\frac{1}{2}}}{\partial \mathbf{U}_{k,l+1}}\right)^n \Delta^n \mathbf{U}_{k,l+1} \\
&\quad + \left(\frac{\partial\left(\hat{\mathbf{G}}_v\right)_{k,l+\frac{1}{2}}}{\partial \mathbf{U}_{k,l}}\right)^n \Delta^n \mathbf{U}_{k,l}
\end{aligned} \tag{8.118}$$

After substituting these linearized expressions into Eq. (8.112), the resulting block system of algebraic equations is approximately factored into two block tridiagonal systems. The algorithm can then be written as

$$\begin{aligned}
&\left[[\hat{A}^*]_{k,l} + \frac{\partial\left(\delta_\eta\left\{\hat{\mathbf{F}}_i - \hat{\mathbf{F}}_v\right\}\right)}{\partial \mathbf{U}_{k,l}} + \bar{\delta}_\eta\left(\frac{\partial\left\{\hat{\mathbf{F}}_i - \hat{\mathbf{F}}_v\right\}}{\partial \mathbf{U}}\right)\right]^n \left[[\hat{A}^*]^{-1}_{k,l}\right]^n \\
&\times\left[[\hat{A}^*]_{k,l} + \frac{\partial\left(\delta_\zeta\left\{\hat{\mathbf{G}}_i - \hat{\mathbf{G}}_v\right\}\right)}{\partial \mathbf{U}_{k,l}} + \bar{\delta}_\zeta\left(\frac{\partial\left\{\hat{\mathbf{G}}_i - \hat{\mathbf{G}}_v\right\}}{\partial \mathbf{U}}\right)\right]^n \Delta^n \mathbf{U}_{k,l} = (\mathbf{RHS})^n
\end{aligned} \tag{8.119}$$

where

$$\begin{aligned}
(\mathbf{RHS})^n = &-\left([\hat{A}^*]^n_{k,l} - [\hat{A}^*]^{n-1}_{k,l}\right)\mathbf{U}^n_{k,1} - \delta_\eta\left(\hat{\mathbf{F}}_i - \hat{\mathbf{F}}_v\right)^n - \delta_\zeta\left(\hat{\mathbf{G}}_i - \hat{\mathbf{G}}_v\right)^n \\
&-\left[\hat{\mathbf{E}}^p(\mathbf{S}^{n+1}_{k,l}, \mathbf{U}^n_{k,l}) - \hat{\mathbf{E}}^p(\mathbf{S}^n_{k,l}, \mathbf{U}^{n-1}_{k,l})\right]
\end{aligned} \tag{8.120}$$

and the difference operators are defined by

$$\begin{aligned}
\delta_\kappa \Phi &= \Phi_{m+\frac{1}{2}} - \Phi_{m-\frac{1}{2}} \\
\bar{\delta}_\kappa\left(\frac{\partial \Psi}{\partial \mathbf{U}}\Phi\right) &= \frac{\partial \Psi_{m+\frac{1}{2}}}{\partial \mathbf{U}_{m+1}}\Phi_{m+1} - \frac{\partial \Psi_{m-\frac{1}{2}}}{\partial \mathbf{U}_{m-1}}\Phi_{m-1}
\end{aligned}$$

The system of equations can be solved using the same procedure as employed in the Beam-Warming scheme described previously. Further details of the algorithm can be found in the works by Lawrence et al. (1986, 1987) and Lawrence (1987, 1992).

Other schemes. The PNS equations have been solved using other upwind algorithms including the explicit finite-volume scheme of Korte and McRae (1988), which is based on Roe's approximate Riemann solver; the explicit finite-volume scheme of Gerbsch and Agarwal (1990), which is based on Osher's upwind method (Osher and Chakravarthy, 1983); and the scheme of Sturmayr et al. (1993), which is based on the ENO (essentially nonoscillatory) scheme of Yang (1991).

In addition, several upwind PNS algorithms have been developed that are derivatives of upwind time-dependent Navier-Stokes or TLNS solvers. These solvers are modified for space-marching using local time iterations at each streamwise step. Included in this group are the space-marched conservative supra-characteristic methods (CSCM-S) of Lombard et al. (1984) and Stookesberry and Tannehill (1987). The CSCM-S method is based on the CSCM for eigenvalue-based differencing developed by Lombard. Also included in this group is the algorithm of Newsome et al. (1987), which is based on the upwind Navier-Stokes scheme of Thomas and Walters (1987), and the algorithms of Ota et al. (1988), Thompson and Matus (1989), Molvik and Merkle (1989), and Matus and Bender (1990). An advantage of the time-iterative approach is that errors due to linearization and factorization can be reduced to negligible levels by iteration. An obvious disadvantage is that multiple iterations are required at each streamwise marching step.

8.3.4 Applications of PNS Equations

The PNS equations have been used to successfully compute the 3-D supersonic/hypersonic viscous flow over a variety of body shapes. For pointed bodies the initial starting solution is frequently obtained using the conical Navier-Stokes approximation (see Section 8.6). For blunt-nosed bodies, the initial starting solution is normally obtained using either a Navier-Stokes code or a viscous shock-layer (VSL) code.

Early studies involved the computation of flows over simple body shapes such as flat plates (Rudman and Rubin, 1968; Rubin et al., 1969; Cheng et al., 1970; Nardo and Cresci, 1971), corners (Cresci et al., 1969; Rubin and Lin, 1972), pointed cones (Rubin et al., 1969; Lin and Rubin, 1973; Lubard and Helliwell, 1974; Vigneron et al., 1978a, 1978b), and spinning cones (Lin and Rubin, 1974; Agarwal and Rakich, 1978).

Later, flows were computed over more complicated body shapes such as sphere-cones (Lubard and Rakich, 1975; Waskiewicz and Lewis, 1978; Rizk et al., 1981; Bhutta and Lewis, 1985a), hemisphere-cylinders (Schiff and Steger, 1979), ogive-cylinders (Rakich et al., 1979; Degani and Schiff, 1983), ogive-cylinder-boattails (Schiff and Sturek, 1980; Gielda and McRae, 1986), blunt biconics (Mayne, 1977; Helliwell et al., 1980, Chaussee et al., 1981; Kim and Lewis, 1982; Gnoffo, 1983; Neumann and Patterson, 1988), hyperboloids (Bhutta

and Lewis, 1985b), sharp leading edge delta wings (Vigneron et al., 1978a, 1978b), blunt leading edge delta wings (Tannehill et al., 1982), and finned missiles (Rai et al., 1983).

More recently, flows have been computed over airplane-like vehicles such as the X-24C (Chaussee et al., 1981), Space Shuttle Orbiter (Li, 1981b; Rakich et al., 1984; Chaussee et al., 1984; Prabhu and Tannehill, 1984), generic fighter (Chaussee et al., 1985), hypersonic vehicles (Lawrence et al., 1987; Korte and McRae 1989; Bhutta and Lewis, 1989; Walker and Oberkampf, 1991), and generic versions of the National Aero-Space Plane (Buelow et al., 1990; Wadawadigi et al., 1994). See Fig. 8.7.

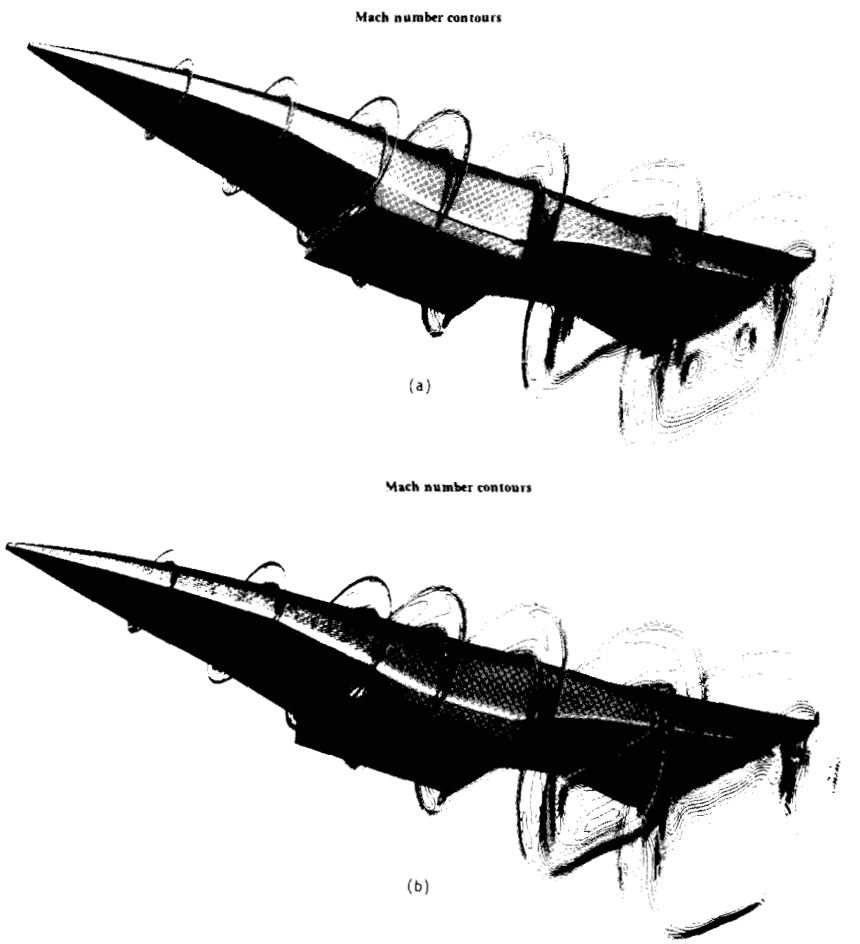

Figure 8.7 Comparison of Mach contours in various crossflow planes along the length of the Test Technology Demonstrator (TTD) configuration (Wadawadigi et al., 1994). (a) Scramjet engine off. (b) Scramjet engine on.

In addition to the computation of external flows, the PNS equations have been used to compute the supersonic/hypersonic flow in jets/plumes/wakes (Edelman and Weilerstein, 1969; Boynton and Thomson, 1969; Tannehill and Anderson, 1971; Dash and Wolf, 1984a, 1984b; Dash, 1985, 1989; Gielda and Agarwal, 1989; Sinha et al., 1990), ducts (Edelman and Weilerstein, 1969; Rubin et al., 1977; Sinha and Dash, 1986; Sinha et al., 1987, 1990), nozzles (Sinha and Dash, 1986; Chitsomboon and Northam, 1988; Gielda and Agarwal, 1989; Dang et al., 1989; Sinha et al., 1990), and inlets (Buggeln et al., 1980; Lawrence et al., 1986; Krawczyk and Harris, 1987; Gielda and Agarwal, 1989; Krawczyk et al., 1989).

The renewed interest in hypersonic aerothermodynamics has led to the development of several PNS codes that account for real-gas effects. PNS codes that include equilibrium chemistry have been written by Li (1981b), Gnoffo (1983), Prabhu and Tannehill (1984), Bhutta et al. (1985a), Banken et al. (1985), Molvik (1985), Stalnaker et al. (1986), Krawczyk and Harris (1987), Ota et al. (1988), Liou (1989), Tannehill et al. (1989), and Gerbsch and Agarwal (1991). For codes that utilize an upwind algorithm, it is also necessary to modify the numerical scheme to account for the equilibrium chemistry. Tannehill et al. (1989) have used both the approximate procedure of Grossman and Walters (1987) and the nearly exact procedure of Vinokur and Liu (1988) to modify the upwind implicit total variation diminishing (TVD) scheme in the UPS code to account for equilibrium chemistry.

For nonequilibrium (chemically reacting) flows, the species continuity equations must be solved in addition to the usual gas-dynamic equations. The gas-dynamic equations remain the same except for the additional diffusion term in the energy equation. The species continuity equations are parabolized by dropping the streamwise diffusion terms. The resulting nonequilibrium PNS equations have been solved using both fully coupled and loosely coupled approaches. In the fully coupled approach the gas-dynamic and species continuity equations are solved simultaneously using the same implicit algorithm. A drawback to this approach is that as the number of species increases, the size of the block matrices that must be inverted also increases. In the loosely coupled approach, the gas-dynamic and species continuity equations are solved separately, and the coupling between the two sets of equations is obtained through some type of iterative coupling. Nonequilibruim (finite-rate chemically reacting) PNS codes have been written by Bhutta et al. (1985b) Sinha and Dash (1986), Prabhu et al. (1987a, 1987b), Sinha et al. (1987), Tannehill et al. (1988) Gielda et al. (1988), Chitsomboon and Northam (1988), Gielda and Agarwal (1989), Molvik and Merkle (1989), Buelow et al. (1990), Kamath et al. (1991), Hugues and Vérant (1991), Wadawadigi et al. (1992), Ebrahimi and Gilbertson (1992), and White et al. (1993). A PNS code for both vibrational and chemical nonequilibrium flows has been developed by Miller et al. (1995). Other PNS codes have included the effects of ablation (Muramoto, 1993) and finite-catalytic walls (Miller et al., 1994).

8.4 PARABOLIZED AND PARTIALLY PARABOLIZED NAVIER-STOKES PROCEDURES FOR SUBSONIC FLOWS

Previous sections in this chapter dealt with flows that are predominantly supersonic. In this section we will discuss two computational strategies that are particularly useful for subsonic flows. These schemes can be categorized as either "once through" (fully parabolized) or multiple space-marching (partially parabolized). For both, the starting point is a form of the PNS equations. The approaches differ in the way that the pressure is treated.

8.4.1 Fully Parabolic Procedures

The fully parabolic procedure approach is applicable to a 3-D flow in which a predominant flow direction can be identified. The velocity component in this primary flow direction must generally be greater than zero, although some schemes may permit the existence of small regions of reversed flow by using the FLARE approximation in the primary flow direction. No restrictions are placed on the velocity components in the crossflow direction. As with all forms of the PNS equations, diffusion in the streamwise direction is neglected.

Unless further steps are taken, the PNS equations will permit transmission of influences in the streamwise direction through the pressure field for subsonic flows, as discussed in Section 8.3.2. In the present approach this elliptic behavior is suppressed in the streamwise direction by utilizing an approximation first suggested by Gosman and Spalding (1971). This approximation consists of representing the pressure gradient in the streamwise direction as an average over the flow cross section. A condition for using this approximation is that some method must exist for evaluating this pressure gradient. Possibilities include steady internal flows for which the pressure gradient can be determined with the aid of the global mass flow constraint and certain external flows for which the average pressure gradient can be taken as zero. Such external 3-D flows include flow in a corner and the subsonic jet discharging from a noncircular orifice into an ambient at rest or a co-flowing stream.

The computational strategy will be illustrated by considering flow through a straight rectangular channel. This permits use of the conservation equations in the Cartesian coordinate system. The same concepts are applicable to curved channels of constant cross-sectional area, but a different coordinate system must be used. The 3-D parabolic model has been extended to more general geometries by Briley and McDonald (1979).

The channel axis is in the x direction. Thus the y and z coordinates span planes perpendicular to the primary flow direction. The equations will be written in a form applicable to either laminar or turbulent flow. The variables are understood to represent time-mean quantities. This is the same convention as employed in Chapter 7. In developing the parabolized form of the Reynolds equations, diffusion in the streamwise direction by both molecular and turbulent mechanisms will be neglected. Furthermore, since only subsonic applications are to be considered, it will be assumed that $\overline{\rho' u'}/\bar{\rho}\bar{u}$, $\overline{\rho' v'}/\bar{\rho}\bar{v}$, and $\overline{\rho' w'}/\bar{\rho}\bar{w}$ are

small, so that the difference between conventional and mass-weighted variables can be neglected. Terms involving pressure fluctuations in the energy equation will also be neglected. The symbol τ will denote the effective stress due to both molecular and turbulent mechanisms. Similarly, the symbol q will denote heat flux quantities from both molecular and turbulent mechanisms. Apart from the pressure gradient terms, which will be discussed below, the equations for the 3-D parabolic procedure follow from Eqs. (5.68), (5.73), and (5.84) after the simplifying assumptions given above are invoked:

continuity:

$$\frac{\partial \rho u}{\partial x} + \frac{\partial \rho v}{\partial y} + \frac{\partial \rho w}{\partial z} = 0 \tag{8.121a}$$

$$\int_A \rho u \, dA = \text{const} \qquad \text{(global)} \tag{8.121b}$$

x momentum:

$$\rho u \frac{\partial u}{\partial x} + \rho v \frac{\partial u}{\partial y} + \rho w \frac{\partial u}{\partial z} = -\frac{d\hat{p}}{dx} + \frac{\partial \tau_{xy}}{\partial y} + \frac{\partial \tau_{xz}}{\partial z} \tag{8.122}$$

y momentum:

$$\rho u \frac{\partial v}{\partial x} + \rho v \frac{\partial v}{\partial y} + \rho w \frac{\partial v}{\partial z} = -\frac{\partial p}{\partial y} + \frac{\partial \tau_{yy}}{\partial y} + \frac{\partial \tau_{yz}}{\partial z} \tag{8.123}$$

z momentum:

$$\rho u \frac{\partial w}{\partial x} + \rho v \frac{\partial w}{\partial y} + \rho w \frac{\partial w}{\partial z} = -\frac{\partial p}{\partial z} + \frac{\partial \tau_{zy}}{\partial y} + \frac{\partial \tau_{zz}}{\partial z} \tag{8.124}$$

energy:

$$\rho u c_p \frac{\partial T}{\partial x} + \rho v c_p \frac{\partial T}{\partial y} + \rho w c_p \frac{\partial T}{\partial z}$$

$$= \frac{\partial}{\partial y}(-q_y) + \frac{\partial}{\partial z}(-q_z) + \beta T u \frac{d\hat{p}}{dx} + \tau_{xy}\frac{\partial u}{\partial y} + \tau_{xz}\frac{\partial u}{\partial z} \tag{8.125}$$

state:

$$\rho = \rho(p, T) \tag{8.126}$$

In the pressure approximation of Gosman and Spalding (1971), a pressure $\hat{p}$ is defined for use in the x momentum equation which is assumed to vary *only in the x direction*. The pressure $\hat{p}$ will be determined with the aid of the global mass flow constraint much as for 2-D or axisymmetric channel flows computed through the thin-shear-layer equations. On the other hand, the p employed in the y and z momentum equations is permitted to vary across the channel cross section. The static pressure in the channel is assumed to be the sum of $\hat{p}$ and p.

The physical assumption in this decoupling procedure is that the pressure variations across the channel are so small that they would have a negligible effect if included in the streamwise momentum equation. Thus cross-plane

pressure variations have been neglected in the streamwise momentum equation. On the other hand, these small pressure variations are included in the momentum equations in the y and z directions, since they play an important role in the distribution of the generally small components of velocity in the directions normal to the channel walls. The determination of $\hat{p}$ requires no information from downstream; $\hat{p}$ is a function of x only and can be uniquely determined at each cross section by employing the global mass flow constraint in combination with the momentum equations. This permits a "once through" calculation of the flow in a parabolic manner. On the other hand, since p varies with both y and z, the equations are elliptic (for subsonic flow) in the y-z plane. In fact, a Poisson equation can be developed for $p(y, z)$ in the cross plane from the y and z momentum equations. The overall calculation scheme then requires the use of procedures for elliptic equations in each cross plane, but the solution can be advanced in the x direction in a parabolic manner.

Using the Boussinesq approximation, the stresses (using summation notation) in the above equations can be evaluated from

$$\tau_{ij} = (\mu + \mu_T)\left(\frac{\partial u_i}{\partial x_j} + \frac{\partial u_j}{\partial x_i} - \frac{2}{3}\delta_{ij}\frac{\partial u_k}{\partial x_k}\right) - \frac{2}{3}\rho\bar{k}\delta_{ij} \tag{8.127}$$

With similar modeling assumptions, the heat flux quantities are normally represented by

$$q_y = -\left(k + \frac{\mu_T c_p}{\mathrm{Pr}_T}\right)\frac{\partial T}{\partial y}$$

$$q_z = -\left(k + \frac{\mu_T c_p}{\mathrm{Pr}_T}\right)\frac{\partial T}{\partial z}$$

Further simplifications to Eq. (8.127) are often found in specific applications, including the fully incompressible representation given by $\tau_{ij} = (\mu + \mu_T)\partial u_i/\partial x_j$. Suitable turbulence modeling for μ_T and Pr_T must be employed to close the system of equations. The usual boundary conditions for channel flow apply.

As was the case for the boundary-layer equations, the solution can proceed in either a coupled or sequential mode. The earliest and most widely used procedure followed the sequential strategy that will be outlined briefly here. We note that for a specified pressure field the momentum and energy equations would be entirely parabolic, and the solution could be marched in the primary flow direction using the x momentum equation to obtain u, the y momentum equation to obtain v, and the z momentum equation to obtain w. The energy equation provides T, and the density is obtained from the equation of state. However, for all but exactly the correct cross-plane pressure distribution, the velocity components will not satisfy the continuity equation. This, of course, is the crux of the problem—the momentum, energy, and state equations are a natural combination to use to advance the solution for the velocity components and density. The way in which the continuity and momentum equations can be used to determine the correct pressure distribution is less obvious. Workable

procedures have been devised for correcting the pressure field, and these will be discussed next.

The computational strategy of solving the momentum equations in an uncoupled manner for the velocity components using a prescribed provisional pressure distribution and then using the continuity and momentum equations to correct the pressure field is known as the *pressure correction* or *segregated approach.*

The earliest solutions reported in the literature for the fully parabolic 3-D procedure followed the algebraic strategy outlined by Patankar and Spalding (1972) as the semi-implicit method for pressure-linked equations (SIMPLE) procedure. Some notable improvements in some of the solution steps have been suggested, and these are mentioned below. The Patankar and Spalding (1972) approach, in turn, draws heavily upon the earlier work of Harlow and Welch (1965), Amsden and Harlow (1970), and Chorin (1968). The segregated strategy proceeds as follows. The superscript $n + 1$ refers to the streamwise station being computed.

1. Employing suitable linearization for coefficients in Eq. (8.122), the pressure $\hat{p}^{n+1}$ can be determined in the same manner as for 2-D and axisymmetric channel flows solved by means of the boundary-layer equations (see Section 7.5), by making use of the global conservation-of-mass constraint. Then $u_{j,k}^{n+1}$ can be determined from the finite-difference solution of Eq. (8.122). The energy equation can be solved for $T_{j,k}^{n+1}$, and the equation of state used to determine $\rho_{j,k}^{n+1}$. An alternating direction implicit (ADI) scheme works very well for solving the momentum and energy equations.
2. Using an assumed pressure distribution in Eqs. (8.123) and (8.124), provisional values of v and w can be determined from a marching solution (an ADI scheme is recommended here too) to these momentum equations just as for the x momentum equations.
3. These provisional solutions for v and w in the cross plane will not generally satisfy the difference form of the continuity equation. By applying the continuity equation to the provisional solutions for the velocity components, mass sources (or sinks) can be computed at each grid point. We now seek a means for adjusting the pressure field in the cross plane so as to eliminate the mass sources. It is in the computation of the velocity and pressure corrections that the 3-D parabolic methods differ the most. Several investigators, including Briley (1974), Ghia et al. (1977b), and Ghia and Sokhey (1977) have followed the suggestion of Chorin (1968) and assumed that the corrective flow in the cross plane is irrotational, being driven by a pressure-like potential in such a manner as to annihilate the mass source. A Poisson equation can be developed for this potential from the continuity equation. Using p subscripts to denote provisional velocities and c subscripts to denote corrective quantities, we demand that

$$\frac{\partial \rho u}{\partial x} + \frac{\partial}{\partial y}\left[\rho(v_p + v_c)\right] + \frac{\partial}{\partial z}\left[\rho(w_p + w_c)\right] = 0 \qquad (8.128)$$

The streamwise derivative term and derivatives of the provisional velocities are known at the time the corrections are sought and can be incorporated into a single source term S_{ϕ}. Thus we can define a potential function $\hat{\phi}$ by $\rho v_c = \partial\hat{\phi}/\partial y$, $\rho w_c = \partial\hat{\phi}/\partial z$, and write Eq. (8.128) as

$$\frac{\partial^2\hat{\phi}}{\partial y^2} + \frac{\partial^2\hat{\phi}}{\partial z^2} = S_{\phi} \tag{8.129}$$

The required velocity corrections can then be computed from the $\hat{\phi}$ distribution resulting from the numerical solution of the Poisson equation in the cross plane. This approach preserves the vorticity of the original v_p and w_p velocity fields.

The original Patankar and Spalding proposal assumed that the velocity corrections were driven by pressure corrections in accordance with a very approximate form of the momentum equations in which the streamwise convective terms were equated to the pressure terms. This can be indicated symbolically by

$$\rho u\frac{\partial v_c}{\partial x} = -\frac{\partial p'}{\partial y} \tag{8.130}$$

$$\rho u\frac{\partial w_c}{\partial x} = -\frac{\partial p'}{\partial z} \tag{8.131}$$

In the above, p' can be viewed merely as a potential function (much like $\hat{\phi}$) used to generate velocity corrections that satisfy the continuity equation. In some schemes [as in the original Patankar and Spalding (1972) proposal], p' is viewed as an actual correction to be added to the provisional values of pressure. Since the velocity corrections can be assumed to be zero at the previous streamwise station, Eqs. (8.130) and (8.131) can be interpreted as

$$v_c = -A\frac{\partial p'}{\partial y} \tag{8.132}$$

$$w_c = -B\frac{\partial p'}{\partial z} \tag{8.133}$$

where A and B are coefficients that involve ρ, u, and Δx. The derivatives of p' are, of course, eventually to be represented on the finite-difference grid. The similarity between Eqs. (8.132) and (8.133) and the representation given earlier for the velocity corrections in terms of the potential $\hat{\phi}$ should be noted. Equations (8.132) and (8.133) can now be used in the continuity equation to develop a Poisson equation of the form

$$\frac{\partial^2 p'}{\partial y^2} + \frac{\partial^2 p'}{\partial z^2} = S_{p'} \tag{8.134}$$

The required velocity corrections can then be computed from the numerical solution of Eq. (8.134) using Eqs. (8.132) and (8.133). This approach is known

as the p' procedure for obtaining velocity corrections. Improvements on this procedure have been suggested that attempt to employ a more complete form of the momentum equation in relating velocity corrections to p'. The paper by Raithby and Schneider (1979) describes several variations of the p' approach.

4. The next step is the pressure update. The velocity corrections just obtained have not been required to satisfy a complete momentum equation. It is now necessary to take steps to develop the improved pressure field in the cross plane that, when used in the complete momentum equations, will produce velocities that satisfy the continuity equation. Several procedures have been used. The corrected velocities can be employed in the difference form of the momentum equations to provide expressions for the pressure gradients that would be consistent with new velocities. We denote these symbolically by

$$\frac{\partial p}{\partial y} = F_1 \tag{8.135}$$

$$\frac{\partial p}{\partial z} = F_2 \tag{8.136}$$

One estimate of the "best" revised pressure field can be obtained by solving the Poisson equation that is developed from Eqs. (8.135) and (8.136):

$$\frac{\partial^2 p}{\partial y^2} + \frac{\partial^2 p}{\partial z^2} = \frac{\partial F_1}{\partial y} + \frac{\partial F_2}{\partial z} = S_p \tag{8.137}$$

The right-hand side of Eq. (8.137) is evaluated from the difference form of the momentum equations using the corrected velocities and is treated as a source term. Patankar (1980) has suggested a slightly different formulation, which also results in a Poisson equation to be solved for the updated pressure (the SIMPLER algorithm). SIMPLER stands for SIMPLE Revised. In all of these solutions of the Poisson equation, care must be taken in establishing the numerical representation of the boundary conditions. The differencing and solution strategy must ensure that the Gauss divergence theorem (see Section 3.3.7) is satisfied. A more detailed example of the boundary treatment for the Poisson equation for pressure is given in Section 8.4.3.

Raithby and Schneider (1979) have proposed a scheme for updating the pressure that does not require the solution of a second Poisson equation. They refer to this as the procedure for pressure update from multiple path integration (PUMPIN). The idea is that the pressure change from grid point to grid point can be computed from integrating Eqs. (8.135) and (8.136) again using the corrected velocities in the momentum equations to evaluate F_1 and F_2. For exactly the correct velocities v and w, the pressure change computed by this procedure between any two points within the cross plane would be independent of path. If the velocities v and w are not exactly correct (they will only be correct as convergence is achieved), then each different path between two points will lead to a different result. We can fix one point as a

reference and compute pressures at other points in the cross plane by averaging the pressures obtained by integrating over several different paths between the reference point and the grid point of interest. Raithby and Schneider (1979) reported good success at averaging pressures over only two paths, namely, from the reference point to the point of interest along constant y and then constant z, and also along constant z and then constant y.

The pressure can also be updated very simply by accepting the p' obtained in the velocity correction procedure of Patankar and Spalding (1972) [see Eq. (8.134)] as the correction to be added to the pressure.

5. Because the momentum and continuity equations have not been satisfied simultaneously in the procedures just described, steps 2–4 are normally repeated iteratively in sequence at each cross plane before the solution is advanced to the next marching station. Underrelaxation is commonly used for both the velocity and pressure corrections. That is, in moving from step 3 to 4, only a fraction of the computed velocity corrections may be added to the provisional v and w velocities. The fraction will vary from method to method. Likewise, it is common to only adjust the pressure by a fraction of the computed pressure correction before moving to step 2. Time-dependent forms of the governing equations are sometimes used to carry out this iterative process. Because steps 2–4 are to be repeated iteratively, it is common practice to terminate the intermediate Poisson equation solutions for velocity and pressure corrections (especially the latter) short of full convergence in early iterative passes through steps 2–4. The objective is to obtain an *improvement* in the pressure field with each iterative pass through steps 2–4. Until overall convergence is approached, there is little point in obtaining the best possible pressure field based on the wrong velocity distribution. The iterative sweeps through steps 2–4 are terminated when a pressure field has been established that will yield solutions to the momentum equations that satisfy the continuity equation within a specified tolerance; i.e., velocity corrections are no longer required.
6. After convergence to the specified degree is achieved, steps 1–5 are repeated for the next streamwise station.

Raithby and Schneider (1979) have reported on a comparative study of several of the methods described above for achieving the velocity and pressure corrections. The number of iterations through steps 2–5 above, required for convergence, was taken as the primary measure of merit. The computation time required for the various algorithms would be of interest but was not reported. Fixing the method for the pressure update, Raithby and Schneider observed that all of the methods given above for achieving the velocity corrections worked satisfactorily. There was very little difference between them in terms of the required number of iterations.

When the method for obtaining velocity corrections was fixed and several different methods for obtaining the pressure update were compared, the p'

method of Patankar and Spalding (1972) was observed to require notably more iterations for convergence than the other methods evaluated. The methods utilizing a Poisson equation and the PUMPIN procedure required only about half as many iterations as the p' method. The PUMPIN method required the fewest iterations by a slim margin. Use of the p' (Patankar and Spalding, 1972) method would not be recommended on the basis of the Raithby and Schneider (1979) study. This conclusion is confirmed by Patankar's (1980) recommendation that his SIMPLER algorithm that employs the Poisson equation formulation be used instead of the older p' method for updating the pressure. It is possible that the p' method may appear more competitive with the other methods when computation time rather than number of iterations is taken as the measure of merit.

Several investigators have reported calculations based on the 3-D parabolic model. These include the work of Patankar and Spalding (1972), Caretto et al. (1972), Briley (1974), Ghia et al. (1977b), Ghia and Sokhey (1977), and Patankar et al. (1974). For flows through channels of varying cross-sectional area, suggestions have been made to include an inviscid flow pressure (determined a priori) in the analysis to partially account for elliptic influences in the primary flow direction. Both regular and staggered grids have been used. The concepts of the mathematical model appear well established. The essential feature of the model is the replacement of the pressure in the streamwise momentum equation with an average pressure that can be determined in some manner (such as through application of global mass flow considerations) without consideration of the details of the downstream flow. Note that this pressure treatment is consistent with observations about solution methods for the PNS equations discussed earlier in this chapter for high-speed flows with embedded subsonic regions. The pressure decoupling discussed in this section is essential in order to avoid departure behavior when the solution is advanced in the streamwise direction. Aspects of this model, particularly the solution for the velocities and pressure in the cross plane, can be accomplished in a variety of ways, including through the use of a fully coupled procedure.

8.4.2 Parabolic Procedures for 3-D Free-Shear and Other Flows

As was mentioned above, the 3-D parabolic procedure is not restricted entirely to confined flows. The essential feature of the model was the decoupling of the pressure gradient terms in the primary flow and cross-flow directions. For confined flows the pressure gradient in the primary flow direction was determined with the aid of the global conservation-of-mass constraint. The main elements of the procedure can be used for other types of 3-D flows if the pressure gradient in the primary flow direction can be neglected or prescribed in advance. One such application occurs in the discharge of a subsonic free jet from a rectangular-shaped nozzle into a coflowing or quiescent ambient. The shape of such a jet gradually changes in the streamwise direction, eventually becoming round in cross section. For such flows, it is reasonable to neglect the streamwise pressure

gradient. Small pressure variations in the cross plane must still be considered, as for 3-D confined flows. McGuirk and Rodi (1977) and Hwang and Pletcher (1978) have computed such flows by the 3-D parabolic procedure by setting $d\hat{p}/dx = 0$. An example of the 3-D parabolic procedure applied to free surface flows is given by Raithby and Schneider (1980).

8.4.3 Partially Parabolized (Multiple Space-Marching) Model

If the PNS equations are solved for a subsonic flow without making simplifying approximations regarding the pressure, the equations are only *partially* parabolized, leading to the terminology PPNS. The system remains elliptic overall because of the influence of the pressure field. The elliptic system can be solved by a direct method, although the memory requirements to do so are substantial for most applications. If the system of equations is solved in a marching mode, multiple streamwise sweeps are needed to resolve the elliptic effects transmitted by the pressure field. Thus, in developing the PPNS model from the Navier-Stokes equations, only certain diffusion processes are neglected, and no assumptions are made about the pressure. The neglected processes always include diffusion in the streamwise direction, but some schemes employed in two dimensions (Rubin and Reddy, 1983; Liu and Pletcher, 1986) may go a step further and neglect all diffusion terms in the normal momentum equation. The PPNS model has also been referred to as the semi-elliptic or reduced Navier-Stokes (RNS) formulation in the literature. The equations for the partially parabolized model are as given in Eqs. (8.121)–(8.126) with $d\hat{p}/dx$ replaced by $\partial p/\partial x$. The primary flow direction is assumed to be aligned with the x coordinate axis.

The solution strategies employed for the PPNS model can be distinguished as either pressure-correction (segregated) schemes or coupled approaches. Multiple streamwise sweeps are required in both approaches. The earliest procedures were of the pressure-correction type, and these will be discussed first.

Pressure-correction PPNS schemes. The PPNS model was first suggested by Pratap and Spalding (1976). Other partially parabolized procedures of the pressure-correction type have been proposed by Dodge (1977), Moore and Moore (1979), and Chilukuri and Pletcher (1980). The PPNS scheme was originally thought to be restricted to flows in which flow reversal in the primary direction does not occur. For these flows, 3-D storage is only required for the pressure (and the source term in the Poisson equation for pressure if the Poisson equation formulation is used) and not for the velocity components. This is the main computational advantage of the PPNS procedure compared to procedures for the full Navier-Stokes equations. Madavan and Pletcher (1982) have demonstrated that the PPNS model can be extended to 2-D applications in which reversal occurs in the component of velocity in the primary direction. This

procedure requires that computer storage also be used for velocity components in and near the regions of primary flow reversal.

We will briefly describe how the PPNS strategy of Chilukuri and Pletcher (1980) can be applied to a steady incompressible 2-D laminar flow. The improvements suggested by Madavan and Pletcher (1982) will be included. For such a flow, the PPNS equations can be written

continuity:

$$\frac{\partial u}{\partial x} + \frac{\partial v}{\partial y} = 0 \tag{8.138}$$

x momentum:

$$u\frac{\partial u}{\partial x} + v\frac{\partial u}{\partial y} = -\frac{1}{\rho}\frac{\partial p}{\partial x} + \nu\frac{\partial^2 u}{\partial y^2} \tag{8.139}$$

y momentum:

$$u\frac{\partial v}{\partial x} + v\frac{\partial v}{\partial y} = -\frac{1}{\rho}\frac{\partial p}{\partial y} + \nu\frac{\partial^2 v}{\partial y^2} \tag{8.140}$$

A staggered grid (Harlow and Welch, 1965) is often used with pressure-correction schemes, and we will use it in the present 2-D example of the PPNS procedure. The idea is to define a different grid for each velocity component. This is illustrated in Fig. 8.8. To avoid confusion, only the grid location for the scalar variables (pressure and the velocity-correction potential $\hat{\phi}$, in this example)

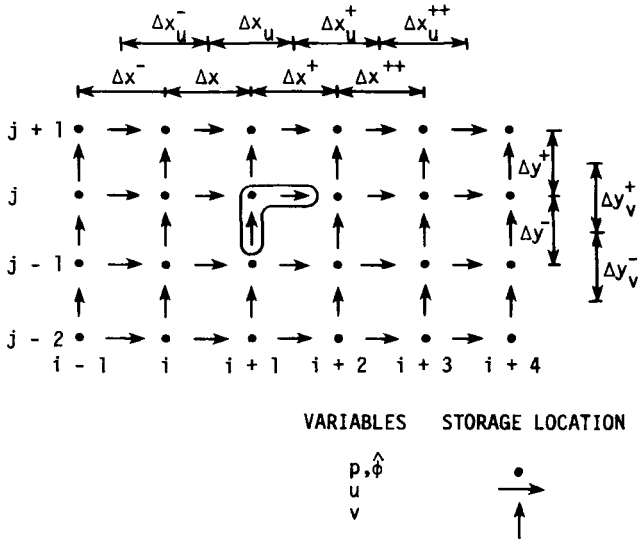

Figure 8.8 Grid spacing definitions and spatial location of variables on a staggered grid.

are denoted by solid symbols in the figure. Velocity components are calculated for "points" or locations on the faces of a control volume that could be drawn around the pressure points. The velocity components are located midway between pressure points, which means that for an unequally spaced grid, the pressure points are not necessarily in the geometric center of such a control volume. The locations of the velocity components are indicated by arrows in Fig. 8.8. Vertical arrows denote locations for v, and horizontal arrows indicate the locations for u. It is convenient to refer to the variables with a single set of grid indices, despite the fact that the variables are actually defined at different locations. Thus the designation $(i + 1, j)$ identifies a cluster of three distinct spatial locations as indicated by the boomerang-shaped enclosure in Fig. 8.8. In the staggered grid, $v_{i+1,j}^{n+1}$ is below $p_{i+1,j}$, and $u_{i+1,j}$ is to the right of $p_{i+1,j}$.

The staggered grid permits the divergence of the velocity field to be represented with second-order accuracy (for equally spaced grid points) at the solid grid points using velocity components at adjacent locations. Such a configuration ensures that the difference representation for this divergence has the conservative property. Also, the pressure difference between adjacent grid points becomes the natural driving force for velocity components located midway between the points. That is, a simple forward-difference representation for pressure derivatives is "central" relative to the location of velocity components. This permits the development of a Poisson equation for pressure that automatically satisfies the Gauss divergence theorem so long as care is taken in the treatment of the boundary conditions. Such boundary conditions are also more easily handled on the staggered grid. Patankar (1980) provides an excellent and more detailed discussion of the advantages of using a staggered grid for problems such as the present one.

The computational boundaries are most conveniently located along grid lines where components of velocity normal to the boundaries are located. This is illustrated in Fig. 8.9 for a lower boundary. Fictitious points are located outside of the physical boundary as necessary for imposing suitable boundary conditions. As an example, we will suppose that it is desired to impose no-slip boundary conditions at the lower boundary illustrated in Fig. 8.9. The v component of velocity is located at the physical boundary, and it is easy to simply specify $v_{i+1,1} = 0$. The treatment for the u component is not so obvious, since no u grid points are located on this boundary. Numerous possibilities exist. The main requirement is that the boundary formulation used must imply that the tangential component of velocity is zero at the location of the physical boundary. This can be achieved by developing a special difference form of the conservation equations for the control volume at the boundary, or by constraining the solution near the boundary such that an extrapolation to the boundary would satisfy the no-slip condition. A third and often used procedure is to employ a fictitious velocity point below the boundary with the constraint that $(u_{i+1,1} + u_{i+1,2})/2 = 0$. This is similar to the reflection technique for enforcing boundary conditions for inviscid flow, which was discussed in Chapter 6. The velocity at the fictitious point would then be used as required in the momentum equations in the

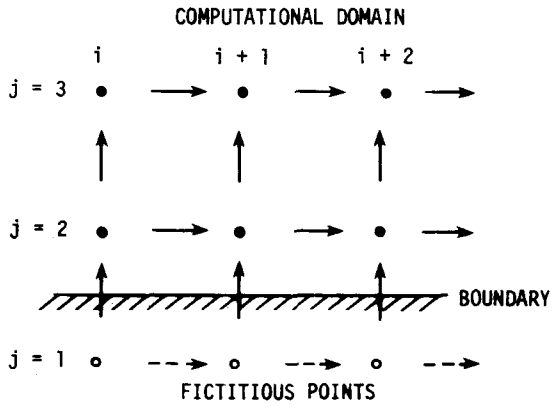

Figure 8.9 The staggered finite-difference grid near a boundary.

interior. Values of the potential function used to correct the velocities are also often obtained from points outside the physical boundaries. Values of pressure are not needed from such points for boundaries on which velocity boundary conditions are specified in the formulation described below. More details on the treatment of boundary conditions on a staggered grid can be found in the work of Amsden and Harlow (1970).

Several choices exist for the representation of the convective derivatives in the momentum equations. The scheme illustrated below makes use of three-point second-order accurate upwind representations for convective terms of the form $u\,\partial\phi/\partial x$. A hybrid scheme (see Section 7.3.3) will be used for terms of the form $v\,\partial\phi/\partial y$. These representations are linearized by extrapolating the coefficients based on values at the two adjacent upstream stations. When streamwise flow reversal is present, the direction of the "wind" changes, and this is taken into account in the representation used for the streamwise derivatives and in the extrapolation direction for the coefficients.

In the ensuing discussion, the following notation is adopted. The superscript $n + 1$ denotes the current marching sweep; the subscript $i + 1$ denotes the current streamwise step for which the solution is sought; and the subscript j denotes the grid points in the y direction. For the forward going flow, the following representation is used to obtain the extrapolated value of the coefficient $u_{i+1,j}^{n+1}$:

$$\hat{u}_{i+1,j}^{n+1} = \left(1 + \frac{\Delta x_u}{\Delta x_u^-}\right) u_{i,j}^{n+1} - \frac{\Delta x_u}{\Delta x_u^-} u_{i-1,j}^{n+1}$$

The circumflex indicates that $\hat{u}_{i+1,j}^{n+1}$ is a known quantity, determined by extrapolation. An extrapolation for $\hat{v}_{i+1,j}^{n+1}$ is obtained in a like manner using appropriate streamwise mesh increments. If $\hat{u}_{i+1,j}^{n+1}$ in the above expression becomes negative, the flow at $(i + 1, j)$ is assumed to be reversed. When this

occurs, the recommended procedure is to simply represent $\hat{u}^{n+1}_{i-1,j}$ by $u^n_{i-1,j}$ and $\hat{v}^{n+1}_{i+1,j}$ by $v^n_{i+1,j}$, making use of velocities from the previous iteration, which are stored for points in and near regions of reversed flow. As an alternative, extrapolation can also be used according to the expression

$$\hat{u}^{n+1}_{i+1,j} = \left(1 + \frac{\Delta x^+_u}{\Delta x^{++}_u}\right) u^n_{i+2,j} - \frac{\Delta x^+_u}{\Delta x^{++}_u} u^n_{i+3,j}$$

An expression for $\hat{v}^{n+1}_{i+1,j}$ can also be obtained by extrapolation in regions of reversed flow. The streamwise convective derivatives are then represented as follows. For the forward going flow,

$$\left(u\frac{\partial u}{\partial x}\right)^{n+1}_{i+1,j} \cong \hat{u}^{n+1}_{i+1,j}\left(\frac{\Delta x^-_u + 2\,\Delta x_u}{\Delta x_u(\Delta x^-_u + \Delta x_u)} u^{n+1}_{i+1,j} - \frac{\Delta x^-_u + \Delta x_u}{\Delta x^-_u\,\Delta x_u} u^{n+1}_{i,j} + \frac{\Delta x_u}{\Delta x^-_u(\Delta x^-_u + \Delta x_u)} u^{n+1}_{i-1,j}\right) \tag{8.141}$$

and for the reversed flow region,

$$\left(u\frac{\partial u}{\partial x}\right)^{n+1}_{i+1,j} \cong -\hat{u}^{n+1}_{i+1,j}\left(\frac{\Delta x^{++}_u + 2\,\Delta x^+_u}{\Delta x_u(\Delta x^{++}_u + \Delta x^+_u)} u^{n+1}_{i+1,j} + \frac{\Delta x^{++}_u + \Delta x^+_u}{\Delta x^{++}_u\,\Delta x^+_u} u^n_{i+2,j} - \frac{\Delta x^+_u}{\Delta x^{++}_u(\Delta x^{++}_u + \Delta x^+_u)} u^n_{i+3,j}\right) \tag{8.142}$$

The term $v\,\partial u/\partial y$ is represented by a hybrid scheme as follows:

$$\begin{aligned}\left(v\frac{\partial u}{\partial y}\right)^{n+1}_{i+1,j} \cong \Bigg[&\hat{v}^{n+1}_{i+1,j}\left(u^{n+1}_{i+1,j} - u^{n+1}_{i+1,j-1}\right)\frac{\Delta y^+}{\Delta y^+ + \Delta y^-} \\ &+ \hat{v}^{n+1}_{i+1,j+1}\,\frac{u^{n+1}_{i+1,j+1} - u^{n+1}_{i+1,j}}{\Delta y^+}\,\frac{\Delta y^-}{\Delta y^+ + \Delta y^-}\Bigg] W \\ &+ \hat{v}^{n+1}_{i+1,j}\,\frac{u^{n+1}_{i+1,j} - u^{n+1}_{i+1,j-1}}{\Delta y^-}(1 - W)A \\ &+ \hat{v}^{n+1}_{i+1,j+1}\,\frac{u^{n+1}_{i+1,j+1} - u^{n+1}_{i+1,j}}{\Delta y^+}(1 - W)B\end{aligned} \tag{8.143}$$

The magnitudes of W, A, and B are determined as follows. Defining

$$R^+_m = \frac{\hat{v}^{n+1}_{i+1,j+1}\,\Delta y^-}{\nu}$$

$$R^-_m = \frac{\hat{v}^{n+1}_{i+1,j}\,\Delta y^+}{\nu}$$

and R_c as the critical mesh Reynolds number, equal to 1.9 (see Section 7.3.3), then when $R_m^+ > R_c$,

$$W = \frac{R_c}{R_m^+} \qquad A = 1 \qquad B = 0$$

When $R_m^+ < -R_c$,

$$W = \frac{R_c}{R_m^-} \qquad A = 0 \qquad B = 1$$

When $R_m^- < R_c < R_m^+$,

$$W = 1 \qquad A = 0 \qquad B = 0$$

This scheme is thus a weighted average of central and upwind differences for larger mesh Reynolds numbers and degenerates to central differencing for small mesh Reynolds numbers.

The second derivative term is represented by

$$\left(\frac{\partial^2 u}{\partial y^2}\right)_{i+1,j}^{n+1} \cong \frac{2}{\Delta y^+ + \Delta y^-}\left(\frac{u_{i+1,j+1}^{n+1} - u_{i+1,j}^{n+1}}{\Delta y^+} - \frac{u_{i+1,j}^{n+1} - u_{i+1,j-1}^{n+1}}{\Delta y^-}\right) \tag{8.144}$$

The pressure derivative in the streamwise momentum equation is represented by

$$\left(\frac{\partial p}{\partial x}\right)_{i+1,j}^{n} \cong \frac{p_{i+2,j}^n - p_{i+1,j}^n}{\Delta x^+} \tag{8.145}$$

The differencing of the pressure gradient term ensures that $u_{i+1,j}^{n+1}$ is influenced by the pressure downstream.

The y momentum equation is differenced in a similar manner. Because of the staggered grid being used, $v_{i+1,j}^{n+1}$ is not located at the same point in the flow as $u_{i+1,j}^{n+1}$. The evaluation of the coefficients in the difference representation of the y momentum equation should reflect this. For example, in representing the term $u\,\partial v/\partial x$, the coefficient should be formed using the average of u at two j levels. The pressure derivative utilizes pressure values on both sides of $v_{i+1,j}^{n+1}$:

$$\left(\frac{\partial p}{\partial y}\right)_{i+1,j}^{n} \cong \frac{p_{i+1,j}^n - p_{i+1,j-1}^n}{\Delta y^-} \tag{8.146}$$

As the momentum equations are solved, the best current estimate of the pressure field is used. Additional details on how this pressure field is determined will be discussed below. With the pressure fixed, the momentum equations are parabolic and are solved in a segregated manner, the x momentum equation for $u_{i+1,j}^{n+1}$ and the y momentum equation for $v_{i+1,j}^{n+1}$. The system of algebraic equations for the unknowns at the $i + 1$ level is tridiagonal and can be solved by employing the Thomas algorithm. As was observed for the 3-D parabolic procedure, the solution for the velocities will not satisfy the continuity equation until the correct pressure field is determined. Thus the velocities obtained from

the solutions for the momentum equations are provisional. It is assumed that velocity corrections are driven by a potential $\hat{\phi}$ in such a manner that the continuity equation is satisfied by the corrected velocities. This requires that

$$\frac{\partial(u_p + u_c)}{\partial x} + \frac{\partial(v_p + v_c)}{\partial y} = 0 \tag{8.147}$$

where u_c and v_c are velocity corrections and u_p and v_p are the provisional velocities obtained from the solution to the momentum equations at marching level $i + 1$. Defining a potential function $\hat{\phi}$ by

$$u_c = \frac{\partial \hat{\phi}}{\partial x} \qquad v_c = \frac{\partial \hat{\phi}}{\partial y} \tag{8.148}$$

we obtain

$$\frac{\partial^2 \hat{\phi}}{\partial x^2} + \frac{\partial^2 \hat{\phi}}{\partial y^2} = -\frac{\partial u_p}{\partial x} - \frac{\partial v_p}{\partial y} = S_\phi \tag{8.149}$$

In difference form this becomes

$$\begin{aligned}
&\frac{1}{\Delta x_u}\left(\frac{\hat{\phi}_{i+2,j} - \hat{\phi}_{i+1,j}}{\Delta x^+} - \frac{\hat{\phi}_{i+1,j} - \hat{\phi}_{i,j}}{\Delta x}\right) \\
&\quad + \frac{1}{\Delta y_v^+}\left(\frac{\hat{\phi}_{i+1,j+1} - \hat{\phi}_{i+1,j}}{\Delta y^+} - \frac{\hat{\phi}_{i+1,j} - \hat{\phi}_{i+1,j-1}}{\Delta y^-}\right) \\
&\quad = -2\frac{(u_p)_{i+1,j} - (u_p)_{i,j}}{\Delta x + \Delta x^+} - 2\frac{(v_p)_{i+1,j+1} - (v_p)_{i+1,j}}{\Delta y^+ + \Delta y^-} = (S_\phi)_{i+1,j}
\end{aligned} \tag{8.150}$$

Such an algebraic equation can be written for each $\hat{\phi}$ grid point across the flow; $j = 2, 3, \ldots, NJ$, where $j = 2$ is the first $\hat{\phi}$ grid point above the lower boundary and $j = NJ$ denotes the $\hat{\phi}$ grid point just below the upper boundary. This results in a tridiagonal system of equations for the unknown $\hat{\phi}_{i+1,j}$ if $\hat{\phi}_{i,j}$ and $\hat{\phi}_{i+2,j}$ are known. The assumptions made to evaluate $\hat{\phi}_{i,j}$ and $\hat{\phi}_{i+2,j}$ are as follows.

Assumption 1: $$\hat{\phi}_{i,j} = \hat{\phi}_{i+1,j}$$

This implies that no corrective flow is present from the ith station where conservation of mass has already been established.

Assumption 2: $$\hat{\phi}_{i+2,j} = 0$$

This implies that $(v_c)_{i+2,j}$ is zero, which must be the case when convergence is achieved. Any other assumption regarding $\hat{\phi}_{i+2,j}$ would appear to be inconsistent with convergence. The boundary conditions used when solving the tridiagonal system of equations to determine $\hat{\phi}_{i+1,j}$ are chosen to be consistent with the

prescribed velocity boundary conditions. For example, if velocities are prescribed along the top and bottom boundaries, v_c would be zero along these boundaries and the conditions used would be $\hat{\phi}_{i+1,1} = \hat{\phi}_{i+1,2}$ and $\hat{\phi}_{i+1,NJ} = \hat{\phi}_{i+1,NJ+1}$.

After the $\hat{\phi}_{i+1,j}$ are determined, velocity corrections are evaluated from the finite-difference representation of Eq. (8.148), namely,

$$(u_c)_{i+1,j} = -\frac{\phi_{i+1,j}}{\Delta x^+}$$

and

$$(v_c)_{i+1,j} = \frac{\phi_{i+1,j} - \phi_{i+1,j-1}}{\Delta y^-}$$

The corrected velocities now satisfy continuity at each grid point at the $i + 1$ marching level, but unfortunately, until convergence, these velocities do not satisfy the momentum equations exactly.

The pressure is updated between marching sweeps by solving a Poisson equation for pressure using the method of SOR by points. The Poisson equation is formed from the difference representation of the momentum equations. That is, we can write

$$\frac{\partial p}{\partial x} = -\rho\left(u\frac{\partial u}{\partial x} + v\frac{\partial u}{\partial y} - \nu\frac{\partial^2 u}{\partial y^2}\right) = G1$$

$$\frac{\partial p}{\partial y} = -\rho\left(u\frac{\partial v}{\partial x} + v\frac{\partial v}{\partial y} - \nu\frac{\partial^2 v}{\partial y^2}\right) = G2$$

When the above equations are differenced, the G's are considered to be located midway between the pressure points used in representing the pressure derivatives on the left-hand side. Thus, $G1$ "points" are coincident with u locations, and $G2$ "points" are coincident with v locations. Then

$$\frac{\partial^2 p}{\partial x^2} + \frac{\partial^2 p}{\partial y^2} = \frac{\partial G1}{\partial x} + \frac{\partial G2}{\partial y} = S_p \tag{8.151}$$

where $G1$ and $G2$ are evaluated by using the *corrected* velocities that satisfy the continuity equation. The use of corrected velocities contributes to the development of a pressure field which will ultimately force the solutions to the momentum equations to conserve mass locally. The S_p terms are evaluated and stored as the marching integration sweep of the momentum equations proceeds. Normally, one successive overrelaxation (SOR) sweep of the pressure field is made during this marching procedure. It is easy to update the pressure by one line relaxation before advancing the velocity solution to the next i level. Several more SOR passes are made at the conclusion of the marching sweep. Overrelaxation factors of 1.7 have been successfully used, but the source term, S_p, is typically underrelaxed by a factor ranging from 0.2 to 0.65, the smaller factor being used for the earliest marching sweeps.

The boundary conditions for the Poisson equation for pressure are all Neumann conditions as derived from the momentum equations. The divergence theorem requires that

$$\iint S_p \, dx\, dy = \oint \frac{\partial p}{\partial n} \, dC$$

where C represents the boundary of the flow domain and $\partial p/\partial n$ is the magnitude of the Neumann boundary condition. The finite-difference equivalent of this constraint must be satisfied before the solution procedure for the Poisson equation will converge. With the staggered grid, this constraint can be satisfied by relating the boundary point pressures to the pressures in the interior through the specified derivative boundary conditions by an equation that is implicit with respect to iteration levels in the method of SOR by points. This step eliminates all dependence on the boundary pressures themselves (Miyakoda, 1962) when solving the Poisson equation for pressure. As long as the difference representation for S_p has the conservative property, the iterative procedure will converge. This boundary treatment is illustrated by writing Eq. (8.151) in difference form for a p point just inside the lower boundary

$$\begin{aligned}
&\frac{1}{\Delta x_u}\left(\frac{p^k_{i+2,2} - p^{k+1}_{i+1,2}}{\Delta x^+} - \frac{p^{k+1}_{i+1,2} - p^{k+1}_{i,2}}{\Delta x}\right) \\
&\quad + \frac{1}{\Delta y^+_v}\left(\frac{p^{k+1}_{i+1,3} - p^{k+1}_{i+1,2}}{\Delta y^+} - \frac{p^{k+1}_{i+1,2} - p^{k+1}_{i+1,1}}{\Delta y^-}\right) \\
&\quad = \frac{G1_{i+1,2} - G1_{i,2}}{\Delta x_u} + \frac{G2_{i,3} - G2_{i,2}}{\Delta y^+_v}
\end{aligned} \tag{8.152}$$

In the above, k refers to the iteration level in the SOR procedure for the Poisson equation, and $k + 1$ denotes the level currently being computed. The boundary condition on the Poisson equation at the lower boundary is taken as

$$\left(\frac{\partial p}{\partial y}\right)_{\text{bdy}} = G2$$

That is, the boundary pressure derivative is evaluated from the momentum equation. In difference form this becomes

$$\frac{p^{k+1}_{i+1,2} - p^{k+1}_{i+1,1}}{\Delta y^-} = G2_{i+1,2} \tag{8.153}$$

where the pressures have been written implicitly at the present iteration level. The pressure below the lower boundary, $p^{k+1}_{i+1,1}$, can now be eliminated from the Poisson equation by substituting Eq. (8.153) into Eq. (8.152). This gives

$$\begin{aligned}
&\frac{1}{\Delta x_u}\left(\frac{p^k_{i+2,2} - p^{k+1}_{i+1,2}}{\Delta x^+} - \frac{p^{k+1}_{i+1,2} - p^{k+1}_{i,2}}{\Delta x}\right) \\
&\quad + \frac{1}{\Delta y^+_v}\left(\frac{p^{k+1}_{i+1,3} - p^{k+1}_{i+1,2}}{\Delta y^+}\right) = \frac{G1_{i+1,2} - G1_{i,2}}{\Delta x_u} + \frac{G2_{i,3}}{\Delta y^+_v}
\end{aligned} \tag{8.154}$$

An examination of the representation for S_p substantiates that the constraint imposed by the divergence theorem is satisfied by this procedure. An evaluation of $\int\int S_p \, dx\, dy$ leaves only terms involving $G1$ and $G2$ along the boundaries owing to cancellation of all other G. These boundary $G1$ and $G2$ values are exactly equal to $\oint(\partial p/\partial n)\, dC$ when the boundary conditions are expressed in terms of G, as illustrated by Eqs. (8.153) and (8.154).

The steps in the PPNS solution procedure are summarized below.

1. The momentum equations are solved for tentative velocity profiles at the $i + 1$ station using an estimated pressure filed. For the first streamwise sweep, this pressure field can be obtained by (a) assuming that $\partial p/\partial x = -\rho u_e(du_e/dx)$ and $\partial p/\partial y = 0$ or (b) assuming that $\partial p/\partial y = 0$ and using a secant procedure (see Section 7.4.3) to determine the value of $\partial p/\partial x$ that will conserve mass globally across the flow, much as is done when solving internal flows with boundary-layer equations. For sweeps beyond the first, a block adjustment can be added (or subtracted) to the downstream pressure through use of the secant procedure at each i station to ensure that mass is conserved globally across the flow. This forces the algebraic sum of the mass sources across the flow to be zero and appears to speed convergence in some cases. A noniterative scheme (Chiu and Pletcher, 1986) has also been used successfully to determine the block adjustment of pressure required to satisfy the global mass flow constraint. For the first streamwise sweep only, the FLARE approximation (see Section 7.4.2) is used to advance the solution through any regions of reversed flow.
2. The velocities are corrected to satisfy continuity locally using the potential function $\hat{\phi}$ as indicated above.
3. The pressure at $i + 1$ is now updated by one SOR pass across the flow at the $i + 1$ level. This is optional at this point, as all pressures are further improved at the end of the marching sweep.
4. Steps 1–3 are repeated for all streamwise stations until the downstream boundary is reached.
5. At the conclusion of the marching sweep, the pressures throughout the flow are updated by several iterations using the Poisson equation. This completes one global iteration. The next marching sweep then starts at the inflow boundary using the revised pressure field. The process continues until the velocity corrections become negligible; i.e., the pressure field obtained permits solutions to the momentum equations that also satisfy the continuity equation.

Sample computational results from the PPNS procedure are shown in Figs. 8.10 and 8.11. Chilukuri and Pletcher (1980) found that solutions to the PPNS equations for 2-D laminar channel inlet flows agreed well with solutions to the full Navier-Stokes equations for channel Reynolds numbers as low as 10. Velocity profiles predicted by the PPNS procedure are compared with the Navier-Stokes solutions obtained by McDonald et al. (1972) for a channel Reynolds number ($\mathrm{Re} = u_\infty a/\nu$, where a is the channel half-width) equal to 75

in Fig. 8.10. For reference, solutions to the boundary-layer equations are also shown in the figure. The boundary-layer solutions fail to exhibit the velocity overshoots characteristic of solutions of the PPNS and Navier-Stokes equations. The PPNS scheme employed 32 grid points in the streamwise direction and 18 across the flow. The sum of the magnitudes of the mass sources at any streamwise station were reduced to less than 1% of the channel mass flow rate in seven streamwise marching sweeps.

PPNS results obtained by Madavan and Pletcher (1982) for a separated external flow are compared with numerical solutions to the Navier-Stokes equations obtained by Briley (1971) in Fig. 8.11. The flow separates under the influence of a linearly decelerating external stream. At a point downstream of separation, the external stream velocity becomes constant, causing the flow to reattach. Reversed flow exists over approximately one-third of the streamwise extent of the computational domain. In the PPNS calculation, 35 grid points were employed in the streamwise direction and 32 across the flow. Sixteen streamwise sweeps were required to reduce the sum of the magnitudes of the mass sources at any streamwise station to less than 1% of the mass flow rate. The computation was continued for a total of 43 streamwise sweeps, at which

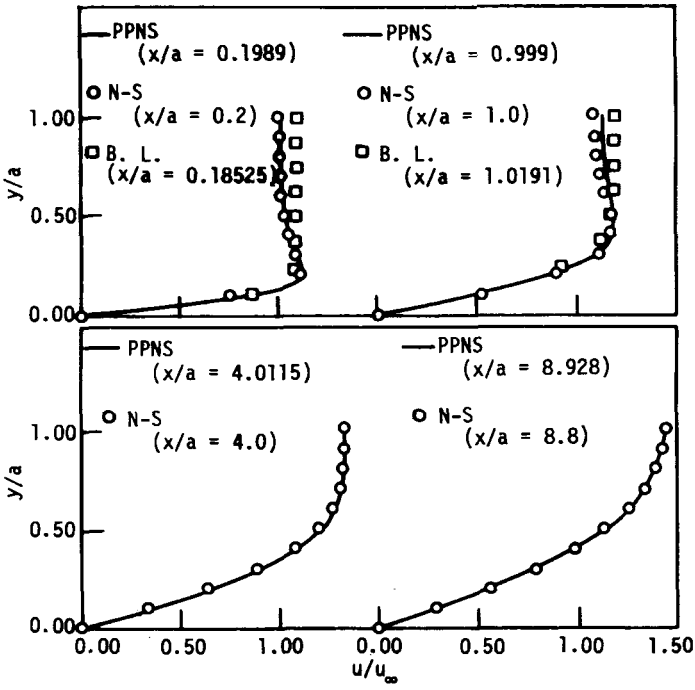

Figure 8.10 Comparison of velocity profiles predicted by the PPNS procedure (Chilukuri and Pletcher, 1980) with the Navier-Stokes (N-S) solutions of McDonald et al. (1972) and with boundary-layer (B.L.) solutions obtained using the method of Nelson and Pletcher (1974), Re = 75.

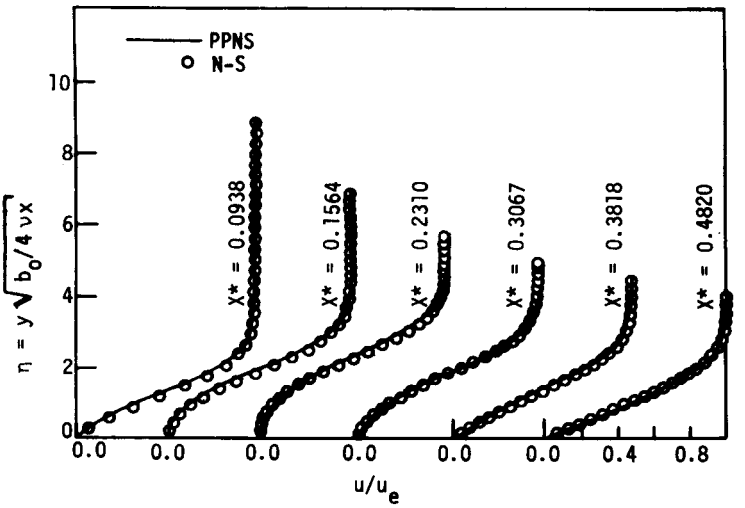

Figure 8.11 Comparison of velocity profiles predicted by the PPNS procedure (Madavan and Pletcher, 1982) with the Navier-Stokes (N-S) solutions of Briley (1971) for a laminar separating and reattaching flow; $x^* = b_1 x/b_0$, $b_0 = 30.48$ m/s, $b_1 = 300$ s^{-1}.

time the sum of the magnitudes of the mass sources at any streamwise station was less than 0.05%.

Coupled PPNS schemes. Although the multiple space-marching strategy for coupled systems does not require that the pressure be entirely fixed for each streamwise marching sweep, certain constraints do exist. Specifically, stability requires that the downstream value of pressure in the difference expression for the streamwise pressure gradient be fixed. To see this, we will consider solving the following 2-D system by a coupled space-marching scheme.

continuity:

$$\frac{\partial(\rho^* u^*)}{\partial x^*} + \frac{\partial(\rho^* v^*)}{\partial y^*} = 0 \tag{8.155}$$

x momentum:

$$\rho^* u^* \frac{\partial u^*}{\partial x^*} + \rho^* v^* \frac{\partial u^*}{\partial y^*} = -\frac{\partial p^*}{\partial x^*} + \frac{1}{\mathrm{Re}} \frac{\partial}{\partial y^*}\left(\mu \frac{\partial u^*}{\partial y^*}\right) \tag{8.156}$$

y momentum:

$$\rho^* u^* \frac{\partial v^*}{\partial x^*} + \rho^* v^* \frac{\partial v^*}{\partial y^*} = -\frac{\partial p^*}{\partial y^*} + \underbrace{\frac{1}{\mathrm{Re}} \frac{\partial}{\partial y^*}\left(\mu \frac{\partial v^*}{\partial y^*}\right)} \tag{8.157}$$

energy:

$$T^* + \tfrac{1}{2}(u^{*2} + v^{*2}) = H_0 \tag{8.158}$$

state:

$$p^* = \frac{\gamma - 1}{\gamma} \rho^* T^* \tag{8.159}$$

In the above equations, asterisks denote nondimensional variables. Length coordinates have been nondimensionalized by a characteristic length L, the velocities by a reference velocity u_∞, the density by ρ_∞, the pressure by $\rho_\infty u_\infty^2$, the temperature by u_∞^2/c_{p_∞} and the viscosity by μ_∞. Note that a simplified version of the energy equation, a statement of constant total enthalpy, is used here for convenience. The Reynolds number is given by $\mathrm{Re} = \rho_\infty u_\infty L/\mu_\infty$ and $\gamma = 1.4$. The term marked off by a brace in Eq. (8.157) is often omitted on the basis of order-of-magnitude arguments (Rubin, 1984). Without the viscous term in the y momentum equation, the system represents the composite of the traditional interacting boundary-layer flow model in which the boundary-layer equations are solved in viscous regions using a pressure gradient determined by a solution of the Euler equations. Most often, such a system has been called the RNS equations, although more general formulations (Ramakrishnan and Rubin, 1987) have also included the time term in the RNS system.

It is instructive to consider the conditions under which Eqs. (8.155)–(8.159) can be solved by a space-marching procedure. Following Liu and Pletcher (1986), we first use the equations of state and energy to rewrite the continuity equation in the form

$$\left(1 + \frac{u^{*2}}{T^*}\right)\frac{\partial u^*}{\partial x^*} + \frac{u^* v^*}{T^*}\frac{\partial v^*}{\partial x^*} + \frac{u^*}{p^*}\frac{\partial p^*}{\partial x^*} + \frac{u^* v^*}{T^*}\frac{\partial u^*}{\partial y^*} + \left(1 + \frac{v^{*2}}{T^*}\right)\frac{\partial v^*}{\partial y^*} + \frac{v^*}{p^*}\frac{\partial p^*}{\partial y^*} = 0 \tag{8.160}$$

We let $\mathbf{Z}$ be the vector of primitive variables u, v, p and write Eqs. (8.156), (8.157), and (8.160) in matrix-vector form as

$$[A]\frac{\partial \mathbf{Z}}{\partial x^*} + [B]\frac{\partial \mathbf{Z}}{\partial y^*} = [C]\frac{\partial}{\partial y^*}\left(\mu \frac{\partial \mathbf{Z}}{\partial y^*}\right) + \mathbf{d} \tag{8.161}$$

where

$$[A] = \begin{bmatrix} \rho^* u^* & 0 & 1 \\ 0 & \rho^* u^* & 0 \\ 1 + \dfrac{u^{*2}}{T^*} & \dfrac{u^* v^*}{T^*} & \dfrac{u^*}{p^*} \end{bmatrix} \qquad [B] = \begin{bmatrix} \rho^* v^* & 0 & 0 \\ 0 & \rho^* v^* & 1 \\ \dfrac{u^* v^*}{T^*} & 1 + \dfrac{v^{*2}}{T^*} & \dfrac{v^*}{p^*} \end{bmatrix}$$

$$[C] = \begin{bmatrix} \dfrac{1}{\mathrm{Re}} & 0 & 0 \\ \dfrac{1}{\mathrm{Re}} & 0 & 0 \\ 0 & 0 & 0 \end{bmatrix} \qquad \mathbf{d} = \begin{bmatrix} 0 \\ 0 \\ 0 \end{bmatrix} \tag{8.162}$$

As indicated in Chapter 2, a marching procedure in the x^* direction can be used to solve Eq. (8.161) if the eigenvalues of $[A]^{-1}[C]$ are nonnegative and real. Wang et al. (1981) have shown that the necessary condition is actually that the roots of the characteristic equation

$$\det |[C] - \lambda[A]| = 0 \tag{8.163}$$

be real and nonnegative. The roots (eigenvalues) of Eq. (8.163) and the eigenvalues of $[A]^{-1}[C]$ are identical as long as the inverse of $[A]$ exists. The three eigenvalues of $[A]^{-1}[C]$ are $\{0, 0, [(u^* + p^* v^*/\rho^*)/\mathrm{Re}\, p^*(M^2 - 1)]\}$. When all viscous terms are neglected in the y momentum equation, the expression simplifies to $\{0, 0, [u^*/\mathrm{Re}\, p^*(M^2 - 1)]\}$. In both cases, when the velocities are positive, the eigenvalues will be nonnegative only for supersonic flow. Thus for subsonic flow the system is not well posed for a marching solution in x^*.

To enable space-marching for subsonic flow, the system can be rearranged by treating the pressure gradient in the x momentum equation as a source term depending at most on the unknown pressure. That is, in the discretization of the pressure gradient, the pressure at one streamwise location must be fixed, for example, by using a value from the previous global sweep. Stability considerations as well as arguments based on characteristics dictate that it is the downstream pressure that should be fixed. This can be incorporated into the system by modifying $[A]$ and $\mathbf{d}$ in Eq. (8.162) as follows:

$$[A] = \begin{bmatrix} \rho^* u^* & 0 & 0 \\ 0 & \rho^* u^* & 0 \\ 1 + \dfrac{u^{*2}}{T^*} & \dfrac{u^* v^*}{T^*} & \dfrac{u^*}{p^*} \end{bmatrix} \qquad \mathbf{d} = \begin{bmatrix} -\dfrac{\partial p^{*+}}{\partial x^*} \\ 0 \\ 0 \end{bmatrix}$$

where it is understood that the pressure gradient in $\mathbf{d}$ is to be discretized such that the downstream value is fixed and the other pressure in the difference is treated as an unknown. The eigenvalues for the system so modified are $\{0, 0, [1/\mathrm{Re}\, \rho^* u^*)]\}$ with or without the viscous term included in the y momentum equation. Thus for $u^* > 0$, the system can be solved by marching in the positive x^* direction. In some applications of interest, local regions of flow reversal are embedded in a flow that is predominantly in the positive x^* direction. Under these conditions ($u^* < 0$, $M^2 < 1$), type-dependent differencing can be used for the streamwise convective terms in the momentum equations with the values at the upstream point in the difference being fixed using values from a previous global sweep. The FLARE approximation can be used for the very first global sweep. In the context of marching the solution in the positive x^* direction, this amounts to treating the streamwise convective term as a source term as was done for the pressure gradient in the streamwise momentum equation. The eigenvalues for the system treated as indicated above in embedded regions of reversed flow are $(0, 0, 0)$.

In the coupled-marching approach, values of u, v, and p (in 2-D) are computed at each global sweep. For flows that are fully attached ($u > 0$), as was

the case for the pressure-correction methods, the entire history of the flow from one global sweep to the next is recorded in the pressure field. Storage for the entire velocity field is not required. If flow reversal occurs, velocities in the reversed flow region must be stored for use in the type-dependent differencing of convective terms in the next global sweep.

Rubin and Lin (1981), Rubin and Reddy (1983), and Israeli and Lin (1985) were among the first to report coupled space-marching methods for reduced forms of the Navier-Stokes (RNS) equations for incompressible or subsonic flow. Other coupled approaches for reduced equations include those reported by Liu and Pletcher (1986) and TenPas (1990). A discussion of recent coupled approaches is included in the review article by Rubin and Tannehill (1992).

A variety of discretizations have been demonstrated for coupled space-marching schemes. Some have maintained the conservation-law form of the equations and have employed generalized coordinates. Implicit methods have been most often used. In two dimensions, a block tridiagonal elimination scheme has worked well. Three-dimensional applications have been demonstrated by Reddy and Rubin (1988). Ramakrishnan and Rubin (1987) describe a time-consistent version of the 2-D PPNS formulation (all viscous terms in the y momentum equation neglected).

Many aspects of the discretization for the coupled PPNS approaches are similar to procedures discussed previously for the boundary-layer equations, PNS equations, and pressure-correction PPNS procedures. Two key features of the approach will be discussed in some detail for clarity. The most unique feature of the coupled multiple space-marching procedure is the treatment of the pressure term in the streamwise momentum equation. In order to accurately accommodate a wide range of flow Mach numbers, it is desirable (Rubin, 1988) to split the representation of the pressure gradient in the streamwise momentum equation into positive and negative flux contributions (as described in Section 8.3.2). This representation is given by

$$\left.\frac{\partial p^*}{\partial x^*}\right|_{i+1} \cong \omega_{i+1/2}\,\frac{p^*_{i+1} - p^*_i}{\Delta x^*} + (1 - \omega_{i+3/2})\frac{p^*_{i+2} - p^*_{i+1}}{\Delta x^*}$$

where ω is the Vigneron parameter, $0 \leqslant \omega \leqslant \min(1, \omega_m)$ and $\omega_m = \gamma M_x^2/[1 + (\gamma - 1)M_x^2]$ except that $\omega = 0$ is used in regions of reversed flow. In the above, M_x is the local Mach number of the flow in the x direction. Rubin (1988) reports that splitting the streamwise pressure gradient appearing in the energy equation is optional. For incompressible flows, $\omega = 0$ is clearly appropriate. For subsonic compressible flows the optimum value of ω is problem dependent, but satisfactory results have been observed using $\omega = 0$ over a wide range of low-speed subsonic flows.

To further illustrate, a simple two-point difference will be used in the Cartesian coordinate system for an incompressible or very low speed flow ($\omega = 0$). The solution is being advanced from the i to the $i + 1$ marching station, as is always the case for global sweeps of a space-marching procedure.

Thus the pressure term can be represented as

$$\left.\frac{\partial p^*}{\partial x^*}\right|_{i+1} \cong \frac{p_{i+2}^{*k} - p_{i+1}^{*k+1}}{\Delta x^*}$$

where the superscript k indicates the global marching level. It is important to notice that the value of p^* at the $i + 2$ position is being specified using the solution from a previous sweep, while the pressure at location $i + 1$ is being treated as an unknown. Note that when splitting is employed for subsonic flows, it is still only the pressure at $i + 2$ that is fixed. Of course, when pressure splitting is employed and the local flow is supersonic, $\omega = 1$ and the influence of the downstream pressure vanishes. Rubin and Reddy (1983) point out that the best agreement with known solutions is observed if the pressure computed at $i + 1$ for incompressible flow is interpreted as the pressure at the upstream station (station i for $u^* > 0$).

The other, somewhat subtle, point is the representation of streamwise convective terms in embedded regions of reversed flow. The procedure normally used is to treat the downwind value in the difference stencil as the unknown and the upwind value as known. In our example we shall let the value being computed (downwind value) be located at the $i + 1$ station. Thus the upwind station would be at level i for $u^* > 0$ and at level $i + 2$ for $u^* < 0$. Due to the existence of a predominant flow direction, at each streamwise location some of the flow is moving in the positive x^* direction. In that region a convective derivative (choosing an incompressible flow for simplicity) might be represented as

$$\left.\frac{\partial u^*\phi^*}{\partial x^*}\right|_{i+1} \cong \frac{u_{i+1}^{*k}\overline{\phi_{i+1}^{*k+1}} - u_i^{*k+1}\phi_i^{*k+1} + \overline{u_{i+1}^{*k+1}}\phi_{i+1}^{*k} - u_{i+1}^{*k}\phi_{i+1}^{*k}}{\Delta x^*}$$

where the expression has been linearized by a Newton method expanding about the values obtained at the previous global sweep. The values treated as unknowns in the algebraic formulation are marked by overbars for emphasis. The symbol ϕ indicates a variable such as u^* or v^*. In the reversed flow portion of the flow at $i + 1$ the representation would be

$$\left.\frac{\partial u^*\phi^*}{\partial x^*}\right|_{i+1} \cong \frac{u_{i+2}^{*k}\phi_{i+2}^{*k} - \overline{u_{i+1}^{*k+1}}\phi_{i+1}^{*k} - u_{i+1}^{*k}\overline{\phi_{i+1}^{*k+1}} + u_{i+1}^{*k}\phi_{i+1}^{*k}}{\Delta x^*}$$

where the unknown being determined is again marked by overbars.

Boundary condition specification may vary somewhat depending on the specific discretization employed, problem being solved, and whether or not a diffusion term is used in the y momentum equation. Most frequently for incompressible or subsonic flows, velocities or one velocity and a streamwise velocity derivative and a thermal variable (when an energy equation is included) would be specified at the inflow boundary. The pressure at inflow is extrapolated from the interior but specified at the outflow boundary. No-slip conditions are specified at solid boundaries, and one velocity and the pressure or a pressure

derivative is specified at free stream boundaries. When the viscous term is included in the y momentum equation, one more variable, usually the normal component of velocity, must be specified at one of the boundaries. Liu and Pletcher (1986) describe a systematic way to couple the boundary conditions on both sides of a 2-D domain, which provides flexibility for choosing the variables to be specified.

A number of improvements to the basic multiple space-marching coupled procedure have been suggested for subsonic applications. These have been motivated largely by the observation that the influence of the downstream pressure propagates upstream only one grid point per global iteration. Thus to improve convergence, some investigators (TenPas, 1990; Bentson and Vradis, 1987) have employed a backsweep of an approximate Poisson equation between global marching sweeps to rapidly transmit pressure changes in the upstream direction and thereby accelerate the global convergence.

It will be pointed out in the next chapter that space-marching procedures can be employed to solve the steady flow version of the full Navier-Stokes equations. The only difference between the PPNS equations and the steady-flow Navier-Stokes equations is the omission of streamwise diffusion terms in the former. Such terms can be included in a multiple space-marching scheme if values from a previous global sweep are used at the $i + 2$ level in the representation of the streamwise diffusion terms. The effects of streamwise diffusion are usually only significant for flows at low Reynolds numbers. Figure 8.12, taken from TenPas (1990), shows the streamwise development of the axial component of velocity at the center of a 2-D channel for several Reynolds numbers. A uniform velocity distribution was specified at the inlet. Solutions to the full Navier-Stokes equations and the PPNS equations are shown, revealing that at the lowest Re, 0.5, the differences are significant. Differences can still be discerned at Re = 10 but become insignificant at Re = 75.

8.5 VISCOUS SHOCK-LAYER EQUATIONS

The viscous shock-layer (VSL) equations are a more approximate set of equations than the PNS equations. In terms of complexity, they fall between the PNS equations and the boundary-layer equations. The major advantage of the VSL equations is that they remain hyperbolic-parabolic in both the streamwise and crossflow directions. Thus the VSL equations can be solved using a marching procedure in both directions very similar to techniques employed for the 3-D boundary-layer equations. This is in contrast to the PNS equations, which must be solved simultaneously over the entire crossflow plane. As a consequence, the VSL equations can be solved (in most cases) with less computer time than the PNS equations. An additional advantage of the VSL equations is that they can be used to compute the viscous flow in the subsonic blunt-nose region, where the PNS equations are not applicable. Thus, for bodies with blunt noses, the VSL equations can be solved to provide a starting solution for a subsequent PNS

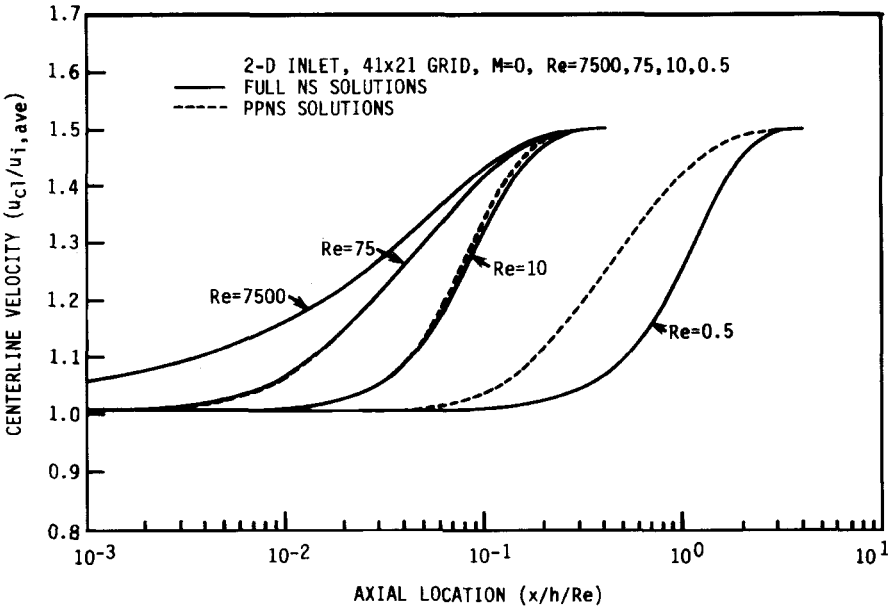

Figure 8.12 Comparison of Navier-Stokes (NS) and PPNS solutions for laminar developing two-dimensional flow in a channel (TenPas, 1990).

computation. The major disadvantage of the VSL equations is that they cannot be used to compute flow fields with crossflow separations. This is a direct result of the fact that the VSL equations are not elliptic in the crossflow plane.

The concept of using a set of equations such as the VSL equations to solve for the high Mach number flow past a blunt body had its origins in the work of Cheng (1963) and Davis and Flügge-Lotz (1964). As mentioned previously, the solution of a set of equations like the VSL equations avoids the need to explicitly determine the second-order boundary-layer effects of vorticity and displacement thickness. Furthermore, it eliminates the difficulty encountered in matching the viscous and inviscid solutions, when the boundary layer is significantly merged with the outer inviscid flow.

Of all the early studies involving the use of the VSL equations, the method of Davis (1970) was the most successful. He solved the axisymmetric VSL equations in order to determine the hypersonic laminar flow over a hyperboloid. The VSL equations used by Davis are derived by first nondimensionalizing the Navier-Stokes equations with variables that are of order 1 in the boundary layer for large Reynolds numbers. In a similar manner, another set of equations is formed by nondimensionalizing the Navier-Stokes equations with variables that are of order 1 in the inviscid region of the flow field. In both sets of equations,

terms up to second order in ϵ are retained:

$$\epsilon = \left(\frac{\mu_{\text{ref}}}{\rho_\infty V_\infty r_{\text{nose}}} \right)^{1/2} \tag{8.164}$$

where μ_{ref} is the coefficient of viscosity evaluated at the reference temperature.

$$T_{\text{ref}} = \frac{V_\infty^2}{c_{p_\infty}} \tag{8.165}$$

The two sets of equations are then compared and combined into a single set of equations, which is valid to second order from the body to the shock. For a 2-D ($m = 0$) or axisymmetric ($m = 1$) body intrinsic coordinate system (see Fig. 5.3), the VSL equations in nondimensional form become as follows:

continuity:

$$\frac{\partial}{\partial \xi^*}\left[(r^* + \eta^* \cos \phi)^m \rho^* u^*\right] + \frac{\partial}{\partial \eta^*}\left[(1 + K^*\eta^*)(r^* + \eta^* \cos \phi)^m \rho^* v^*\right] = 0 \tag{8.166}$$

ξ momentum:

$$\rho^*\left(\frac{u^*}{1 + K^*\eta^*} \frac{\partial u^*}{\partial \xi^*} + v^* \frac{\partial u^*}{\partial \eta^*} + \frac{K^* u^* v^*}{1 + K^*\eta^*} \right) + \frac{1}{1 + K^*\eta^*} \frac{\partial p^*}{\partial \xi^*}$$
$$= \frac{\epsilon^2}{(1 + K^*\eta^*)^2 (r^* + \eta^* \cos \phi)^m} \frac{\partial}{\partial \eta^*}\left[(1 + K^*\eta^*)^2 (r^* + \eta^* \cos \phi)^m \tau^*\right] \tag{8.167}$$

where

$$\tau^* = \mu^*\left(\frac{\partial u^*}{\partial \eta^*} - \frac{K^* u^*}{1 + K^*\eta^*} \right)$$

η momentum:

$$\rho^*\left(\frac{u^*}{1 + K^*\eta^*} \frac{\partial v^*}{\partial \xi^*} + v^* \frac{\partial v^*}{\partial \eta^*} - \frac{K^*(u^*)^2}{1 + K^*\eta^*} \right) + \frac{\partial p^*}{\partial \eta^*} = 0 \tag{8.168}$$

energy:

$$\rho^*\left(\frac{u^*}{1 + K^*\eta^*} \frac{\partial T^*}{\partial \xi^*} + v^* \frac{\partial T^*}{\partial \eta^*} \right) - \frac{u^*}{1 + K^*\eta^*} \frac{\partial p^*}{\partial \xi^*} - v^* \frac{\partial p^*}{\partial \eta^*}$$
$$= \frac{\epsilon^2 (\tau^*)^2}{\mu^*} + \frac{\epsilon^2}{(1 + K^*\eta^*)(r^* + \eta^* \cos \phi)^m}$$
$$\times \frac{\partial}{\partial \eta^*}\left[(1 + K^*\eta^*)(r^* + \eta^* \cos \phi)^m \frac{\mu^*}{\text{Pr}} \frac{\partial T^*}{\partial \eta^*} \right] \tag{8.169}$$

These equations have been nondimensionalized in the following manner:

$$\xi^* = \frac{\xi}{r_{\text{nose}}} \qquad \eta^* = \frac{\eta}{r_{\text{nose}}} \qquad r^* = \frac{r}{r_{\text{nose}}} \qquad K^* = \frac{K}{r_{\text{nose}}}$$

$$u^* = \frac{u}{V_\infty} \qquad v^* = \frac{v}{V_\infty} \qquad T^* = \frac{T}{T_{\text{ref}}} \tag{8.170}$$

$$p^* = \frac{p}{\rho_\infty V_\infty^2} \qquad \rho^* = \frac{\rho}{\rho_\infty} \qquad \mu^* = \frac{\mu}{\mu_{\text{ref}}}$$

By assuming a thin shock layer, the normal momentum equation reduces to

$$\frac{\partial p^*}{\partial \eta^*} = \frac{K^* \rho^* (u^*)^2}{1 + K^* \eta^*} \tag{8.171}$$

The above equations can be readily converted to a 2-D Cartesian coordinate system by setting

$$\begin{aligned} m &= 0 \\ K^* &= 0 \\ x^* &= \xi^* \\ y^* &= \eta^* \end{aligned} \tag{8.172}$$

The resulting VSL equations in Cartesian coordinates can then be compared directly with the PNS equations given previously by Eqs. (8.29)–(8.33). This comparison shows that the continuity and x momentum equations are the same but the y momentum and energy equations in the VSL set of equations are simpler than the corresponding PNS equations.

In the original solution technique of Davis, the VSL equations were normalized with variable values behind the shock. This was done to permit the same grid in the normal direction to be used over the entire body. An initial global solution was obtained by utilizing the thin shock-layer assumption. This assumption makes the VSL equations totally parabolic and permits the use of standard boundary-layer solution algorithms. Subsequent global iterations retained the complete normal momentum equation. Also, for the first global iteration the shock was assumed to be concentric with the body. This assumption was possible because only hyperboloid body shapes were considered because of the difficulties associated with curvature discontinuities in body shapes such as sphere-cones. The shock angles for the second iteration were determined from the shock-layer thicknesses computed during the first iteration.

The marching procedure was initiated from an approximate stagnation streamline solution. This stagnation streamline solution was obtained from the VSL equations, which reduce to ODEs along $\xi = 0$. The solution at each subsequent ξ station was obtained by solving the VSL equations individually in

the following order:

1. energy
2. ξ momentum
3. continuity
4. η momentum

The original method of Davis was not entirely satisfactory because of several limitations. First, the method was restricted to analytic body shapes such as hyperboloids. This difficulty was circumvented by Miner and Lewis (1975). who computed the flow around a sphere-cone body. They started with an initial shock shape from an inviscid blunt-body solution and used a transition function near the sphere-cone juncture in order to obtain a smooth distribution of curvature. Later, Srivastava et al. (1978) overcame this same difficulty by applying special difference formulas to the jump conditions across surface discontinuities.

Another difficulty associated with the original Davis method was the poor convergence of the shock shape when the shock layer became thick. This problem was resolved by Srivastava et al. (1978, 1979), who noted that the relaxation process associated with the shock shape was similar to the interaction between displacement thickness and the outer inviscid flow in supersonic interacting boundary-layer theory. As a result of this observation, they were able to solve the shock-shape divergence problem by adapting the ADI method of Werle and Vatsa (1974) for interacting boundary layers. Another problem with the original Davis method was that it was not able to solve the flow far downstream on slender bodies. This difficulty was traced to the fact that the VSL equations were being solved in an uncoupled manner. In particular, the two first-order equations (continuity and normal momentum) introduced instabilities that grew in the streamwise direction. By solving the continuity and normal momentum equations in a coupled fashion, Waskiewicz et al. (1978) were able to eliminate this stability problem. In a similar manner, Hosny et al. (1978) overcame the problem by completely coupling the VSL equations through a quasi-linearization technique. More recently, Gordon and Davis (1992) coupled the VSL equations with an additional equation for the shock standoff distance and have thereby eliminated the need for local iterations. They also developed a new global iteration procedure that uses Vigneron's technique (Vigneron et al., 1978a, 1978b) to split the differencing of the streamwise derivatives, $\partial p/\partial \xi$ and $\partial v/\partial \xi$, into forward and backward parts. In addition, Gupta et al. (1992) developed a solution procedure for the VSL equations in which global iterations are required only in the nose region of a blunt body.

The VSL equations have been successfully applied to a large number of different blunt-body flow fields. Murray and Lewis (1978) were the first to solve the flow around general 3-D body shapes at angle of attack. Since then, the VSL equations have been applied to a variety of body shapes, including sphere-cones (Murray and Lewis, 1978; Gogineni et al., 1980; Thompson et al., 1987),

ellipsoids (Szema and Lewis, 1981), sphere-cone-cylinder-flares (Kim and Lewis, 1982), space shuttle geometry (Szema and Lewis, 1981; Shinn et al., 1982; Kim et al., 1983; Thompson, 1987), and aeroassist orbital transfer vehicles (Shinn and Jones, 1983; Carlson and Gally, 1991). In addition, VSL codes have been enhanced to account for turbulence (Anderson et al., 1976; Szema and Lewis, 1980; Thareja et al., 1982; Gupta et al., 1990), equilibrium chemistry (Thareja et al., 1982; Swaminathan et al., 1982; Gupta, 1987), nonequilibrium chemistry (Moss, 1974; Miner and Lewis, 1975; Swaminathan et al., 1983; Shinn et al., 1982; Kim et al., 1983; Song and Lewis, 1986; Thompson, 1987; Gupta et al., 1987; Zoby et al., 1989; Bhutta and Lewis, 1991), ablation (Thompson et al., 1983; Song and Lewis, 1986; Bhutta et al., 1989; Gupta et al., 1990), slip effects (Swaminathan et al., 1984; Lee et al., 1990), and catalytic walls (Shinn et al., 1982; Kim et al., 1983; Thompson, 1987).

8.6 "CONICAL" NAVIER-STOKES EQUATIONS

The conical flow assumption for inviscid flows makes use of the fact that a significant length scale is missing in the conical direction for a flow field surrounded by conical boundaries. As a result, no variations in flow properties in the radial direction can occur, and a 3-D inviscid flow problem is reduced to a 2-D problem. This leads to a self-similar solution, which is the same for all constant radius surfaces but scales linearly with the radius. The concept of conical flow is strictly valid only for inviscid flows. However, the viscous portions of the same flow fields have been observed in experiments to be strongly dominated by the outer inviscid conical flow. For these flow fields, Anderson (1973) suggested that a quick estimate of the heat transfer and skin friction could be obtained by solving the unsteady Navier-Stokes equations in a time-dependent fashion on the unit sphere with all derivatives in the radial direction set equal to zero. Thus the Navier-Stokes equations are solved subject to a local conical approximation. We will refer to the equations solved in this manner as the "conical" Navier-Stokes (CNS) equations. The local Reynolds number is determined by the radial position where the solution is computed. As a result, the solution is not self-similar in the sense of inviscid conical flow, but is scaled through the local Reynolds number, which remains in the resulting set of equations.

The CNS equations were originally used by McRae (1976) to compute the laminar flow over a cone at high angle of attack. Since then, Vigneron et al. (1978a), Bluford (1978), McMillin et al. (1987), and Ruffin and Murman (1988) have computed the laminar flow over a delta wing, and Tannehill and Anderson (1980) have computed the flow in a 3-D axial corner. Also, McRae and Hussaini (1978) have employed an eddy viscosity model in conjunction with the CNS equations to compute the turbulent flow over a cone at high angle of attack. In all of the above cases (except one, where the inviscid flow was not completely

conical) the computed inviscid and viscous portions of the flow field agree surprisingly well with the available experimental data.

The CNS equations have also proved quite useful in computing starting solutions for PNS calculations of flows over conical (or pointed) body shapes. This is the primary use of the CNS equations today. Schiff and Steger (1979) and others have incorporated a marching step-back method in their PNS codes, which is equivalent to solving the CNS equations using the time-dependent approach described above. In these codes the flow variables are initially set equal to their free stream values, and the equations are marched from $x = x_0$ to $x = x_0 + \Delta x$ using the same implicit scheme as used to solve the PNS equations but with $\partial p/\partial x = 0$. After each marching step, the solution is scaled back to $x = x_0$. The computation is repeated until no change in flow variables occurs.

The CNS equations are derived from the complete Navier-Stokes equations,

$$\frac{\partial \mathbf{U}^*}{\partial t^*} + \frac{\partial \mathbf{E}^*}{\partial x^*} + \frac{\partial \mathbf{F}^*}{\partial y^*} + \frac{\partial \mathbf{G}^*}{\partial z^*} = 0 \tag{8.173}$$

where $\mathbf{U}^*$, $\mathbf{E}^*$, $\mathbf{F}^*$, and $\mathbf{G}^*$ are the nondimensional vectors defined by Eqs. (5.46). The following conical transformation

$$\begin{aligned} \alpha &= \left[(x^*)^2 + (y^*)^2 + (z^*)^2\right]^{1/2} \\ \beta &= \frac{y^*}{x^*} \\ \gamma &= \frac{z^*}{x^*} \\ \tau &= t^* \end{aligned} \tag{8.174}$$

is initially applied to these equations. The resulting transformed equations can be written in the following strong conservation-law form:

$$\frac{\partial}{\partial \tau}\left(\frac{\alpha^2}{\lambda^3}\mathbf{U}^*\right) + \frac{\partial}{\partial \alpha}\left[\frac{\alpha^2}{\lambda^4}(\mathbf{E}^* + \beta\mathbf{F}^* + \gamma\mathbf{G}^*)\right] + \frac{\partial}{\partial \beta}\left[\frac{\alpha}{\lambda^2}(-\beta\mathbf{E}^* + \mathbf{F}^*)\right] + \frac{\partial}{\partial \gamma}\left[\frac{\alpha}{\lambda^2}(-\gamma\mathbf{E}^* + \mathbf{G}^*)\right] = 0 \tag{8.175}$$

where

$$\lambda = (1 + \beta^2 + \gamma^2)^{1/2}$$

The assumption of local conical self-similarity requires that

$$\begin{aligned} \frac{\partial \mathbf{E}^*}{\partial \alpha} &= 0 \\ \frac{\partial \mathbf{F}^*}{\partial \alpha} &= 0 \\ \frac{\partial \mathbf{G}^*}{\partial \alpha} &= 0 \end{aligned} \tag{8.176}$$

which reduces Eq. (8.175) to

$$\frac{\partial}{\partial\tau}\left(\frac{\alpha^2}{\lambda^3}\mathbf{U}^*\right) + \frac{2\alpha}{\lambda^4}(\mathbf{E}^* + \beta\mathbf{F}^* + \gamma\mathbf{G}^*) + \frac{\partial}{\partial\beta}\left[\frac{\alpha}{\lambda^2}(-\beta\mathbf{E}^* + \mathbf{F}^*)\right] + \frac{\partial}{\partial\gamma}\left[\frac{\alpha}{\lambda^2}(-\gamma\mathbf{E}^* + \mathbf{G}^*)\right] = 0 \tag{8.177}$$

The solution is computed on a spherical surface whose nondimensional radius ($r^* = r/L$) is equal to 1. On this computational surface, $\alpha = 1$, since

$$r^* = \left[(x^*)^2 + (y^*)^2 + (z^*)^2\right]^{1/2} = \alpha$$

As a result, Eq. (8.177) can be rewritten as

$$\frac{\partial\mathbf{U}_4}{\partial\tau} + \frac{\partial\mathbf{F}_4}{\partial\beta} + \frac{\partial\mathbf{G}_4}{\partial\gamma} + \mathbf{H}_4 = 0 \tag{8.178}$$

where

$$\begin{aligned}
\mathbf{U}_4 &= \frac{\mathbf{U}^*}{\lambda^3} \\
\mathbf{F}_4 &= \frac{-\beta\mathbf{E}^* + \mathbf{F}^*}{\lambda^2} \\
\mathbf{G}_4 &= \frac{-\gamma\mathbf{E}^* + \mathbf{G}^*}{\lambda^2} \\
\mathbf{H}_4 &= \frac{2(\mathbf{E}^* + \beta\mathbf{F}^* + \gamma\mathbf{G}^*)}{\lambda^4}
\end{aligned} \tag{8.179}$$

The partial derivatives appearing in the viscous terms of $\mathbf{E}^*$, $\mathbf{F}^*$, and $\mathbf{G}^*$ are readily transformed using

$$\begin{aligned}
\frac{\partial}{\partial x^*} &= -\beta\lambda\frac{\partial}{\partial\beta} - \gamma\lambda\frac{\partial}{\partial\gamma} \\
\frac{\partial}{\partial y^*} &= \lambda\frac{\partial}{\partial\beta} \\
\frac{\partial}{\partial z^*} &= \lambda\frac{\partial}{\partial\gamma}
\end{aligned} \tag{8.180}$$

Thus the shear-stress and heat flux terms, given in Eqs. (5.47), become

$$\tau_{xx}^* = \frac{2\mu^*}{3\,\mathrm{Re}_L}(-2\beta\lambda u_\beta^* - 2\gamma\lambda u_\gamma^* - \lambda v_\beta^* - \lambda w_\gamma^*)$$

$$\tau_{yy}^* = \frac{2\mu^*}{3\,\mathrm{Re}_L}(2\lambda v_\beta^* + \beta\lambda u_\beta^* + \gamma\lambda u_\gamma^* - \lambda w_\gamma^*)$$

$$\tau_{zz}^* = \frac{2\mu^*}{3\,\mathrm{Re}_L}(2\lambda w_\gamma^* + \beta\lambda u_\beta^* + \gamma\lambda u_\gamma^* - \lambda v_\beta^*)$$

$$
\begin{aligned}
\tau_{xy}^* &= \frac{\mu^*}{\mathrm{Re}_L}(\lambda u_\beta^* - \beta\lambda v_\beta^* - \gamma\lambda v_\gamma^*) \\
\tau_{xz}^* &= \frac{\mu^*}{\mathrm{Re}_L}(\lambda u_\gamma^* - \beta\lambda w_\beta^* - \gamma\lambda w_\gamma^*) \\
\tau_{yz}^* &= \frac{\mu^*}{\mathrm{Re}_L}(\lambda v_\gamma^* + \lambda w_\beta^*) \\
q_x^* &= \frac{\mu^*}{(\gamma-1)M_\infty^2\,\mathrm{Re}_L\,\mathrm{Pr}}(-\beta\lambda T_\beta^* - \gamma\lambda T_\gamma^*) \\
q_y^* &= \frac{\mu^*}{(\gamma-1)M_\infty^2\,\mathrm{Re}_L\,\mathrm{Pr}}\lambda T_\beta^* \\
q_z^* &= \frac{\mu^*}{(\gamma-1)M_\infty^2\,\mathrm{Re}_L\,\mathrm{Pr}}\lambda T_\gamma^*
\end{aligned}
\tag{8.181}
$$

Note that the Reynolds number Re_L remains in the expressions for shear stress and heat flux. This Reynolds number is evaluated using

$$
\mathrm{Re}_L = \frac{\rho_\infty V_\infty L}{\mu_\infty} \tag{8.182}
$$

where L is the radius of the spherical surface where the solution is computed. As a consequence, solutions of the CNS equations depend directly on the position ($r = L$) where they are computed. This is different from inviscid solutions, which are independent of r and, thus, truly conical.

An analysis by Rasmussen and Yoon (1990) has shown that the boundary layer computed on a circular cone with the CNS equations is thinner than would be computed with the complete Navier-Stokes equations. Nevertheless, the CNS equations are very useful in providing approximate starting solutions for PNS calculations of flows over pointed bodies.

The CNS equations can be solved using the same "time-dependent" algorithms that are applied in Chapter 9 to the 2-D compressible Navier-Stokes equations. Thus we will postpone our discussion of numerical schemes for the CNS equations until then. In closing, it should be remembered that the CNS equations are a very approximate form of the complete Navier-Stokes equations, and as such, they should not be used for flow problems where a high degree of accuracy is required.

PROBLEMS

8.1 Verify Eq. (8.8).

8.2 Derive Eqs. (8.9)–(8.11).

8.3 Reduce the thin-layer equations in Cartesian coordinates to the set of boundary equations that are valid at a no-slip wall ($y = 0$). Assume the wall is held at a constant temperature of T_w.

8.4 Reduce the thin-layer equations written in the transformed coordinate system [Eqs. (8.9)–(8.11)] to the set of boundary equations that are valid at a no-slip wall ($\eta = 0$). Assume the wall is held at a constant temperature of T_w.

8.5 Obtain Eq. (8.15) from Eq. (5.19).

8.6 Obtain Eq. (8.16) from Eq. (5.19).

8.7 Obtain Eq. (8.17) from Eq. (5.31).

8.8 Obtain Eq. (8.23) from Eq. (8.17).

8.9 Derive the compressible laminar boundary-layer equations starting with Eqs. (8.14)–(8.17). Note that in the boundary-layer region, $\Delta^2 \sim O(1)$ and $(\Delta/\delta^*)^2 \gg 1$.

8.10 Apply the thin-layer approximation to Eqs. (8.37)–(8.39) and show that they are equivalent to Eqs. (8.40), (8.10), and (8.11).

8.11 Verify that Eq. (8.44) is equivalent to Eq. (8.43).

8.12 Show that the eigenvalues of Eq. (8.44) are given by Eq. (8.46).
Hint: $|\lambda[I] - [A_1]^{-1}[B_1]| = |[A_1]^{-1}||\lambda[A_1] - [B_1]|$.

8.13 Derive Eq. (8.47).

8.14 Verify Eqs. (8.48) and (8.49).

8.15 Derive Eq. (8.50).

8.16 For the flow conditions,

$$M_x = 0.6$$

$$\frac{\mathrm{Re}}{L} = \frac{\rho u}{\mu} = \frac{1000}{m}$$

$$\gamma = 1.4$$

$$\mathrm{Pr} = 0.72$$

solve Eq. (8.50), and show that all the roots will be real and positive if $\omega = 0.4$, which satisfies Eq. (8.52).

8.17 Repeat Prob. 8.16 with $\omega = 0.5$, and show that at least one root of Eq. (8.50) will *not* be real and positive.

8.18 If all the eigenvalues of Eq. (8.50) are real, show that these eigenvalues are positive, provided that the conditions given by Eqs. (8.51) and (8.52) are satisfied.

8.19 Place an ω in front of the streamwise pressure gradient term in both the streamwise momentum equation and the energy equation, and evaluate the condition that must be satisfied in order for Eq. (8.44) to remain hyperbolic if $\omega < 1$. You may assume that $v \ll u$.

8.20 Linearize the following terms using Eq. (8.61):

(*a*) $u^{m+1}_{i+1,j,k} v^{m+1}_{i+1,j,k}$

(*b*) $(u^{m+1}_{i+1,j,k})^2 v^{m+1}_{i+1,j,k}$

(*c*) $(u^{m+1}_{i+1,j,k})^3 v^{m+1}_{i+1,j,k}$

(*d*) $u^{m+1}_{i+1,j,k} v^{m+1}_{i+1,j,k} w^{m+1}_{i+1,j,k}$

(*e*) $u^{m+1}_{i+1,j,k} (v^{m+1}_{i+1,j,k})^2 w^{m+1}_{i+1,j,k}$

8.21 Derive the expression for the Jacobian $\partial \mathbf{E}^*/\partial \mathbf{U}$ given by Eq. (8.78).

8.22 Derive the expression for the Jacobian $\partial \mathbf{F}/\partial \mathbf{U}$ given by Eq. (8.79).

8.23 Derive the expression for the Jacobian $\partial \mathbf{G}/\partial \mathbf{U}$ given by Eq. (8.80).

8.24 If ω can be approximated by

$$\omega \simeq \gamma M_x^2$$

derive the expression for the Jacobian $\partial \mathbf{E}^*/\partial \mathbf{U}$ that results when ω is no longer assumed independent of $\mathbf{U}$.

8.25 Derive the expression for the Jacobian $\partial \mathbf{F}_v/\partial \mathbf{U}$ given by Eq. (8.84).

8.26 Derive the expression for the Jacobian $\partial \mathbf{G}_v/\partial \mathbf{U}$ given by Eq. (8.85).

8.27 The elements of the matrix $[C]_k$ in Eq. (8.96) can be represented by $(c_{lm})_k$, where $l = 1, 2, \ldots, 5$ and $m = 1, 2, \ldots, 5$. Determine the element $(c_{24})_k$.

8.28 Determine the element $(c_{32})_k$ in Prob. 8.27.

8.29 Determine the element $(c_{43})_k$ in Prob. 8.27.
8.30 The elements of the matrix $[B]_k$ in Eq. (8.96) can be represented by $(b_{lm})_k$, where $l = 1, 2, \ldots, 5$ and $m = 1, 2, \ldots, 5$. Determine the element $(b_{24})_k$.
8.31 Determine the element $(b_{43})_k$ in Prob. 8.30.
8.32 Determine the elements $(a_{33})_k$, $(b_{33})_k$, and $(c_{33})_k$ of the matrices $[A]_k$, $[B]_k$, and $[C]_k$ in Eq. (8.96).
8.33 Apply the difference formula given in Eq. (8.70) to the 2-D PNS equation,

$$\frac{\partial \mathbf{E}^*}{\partial x} + \frac{\partial \mathbf{P}}{\partial x} + \frac{\partial \mathbf{F}}{\partial y} = 0$$

and develop a solution algorithm like that given by Eqs. (8.92)–(8.95) for the 3-D PNS equation.
8.34 Derive the expressions for the cell-face-area vectors given in Eq. (8.104).
8.35 Verify Eqs. (8.105) and (8.106).
8.36 Starting with the x momentum Navier-Stokes equation [Eq. (5.19)], show how this equation is reduced and write out the resulting x momentum equation for the following simplified sets of fluid dynamic equations. Assume that the streamwise flow is in the x direction, while the body surface is in the x-z plane.

(a) thin-layer Navier-Stokes (TLNS) equations
(b) reduced Navier-Stokes (RNS) equations
(c) PNS equations
(d) PNS equations with thin-layer approximation
(e) three-dimensional steady boundary-layer equations
(f) Euler equations

8.37 Repeat Prob. 8.36 for the y momentum Navier-Stokes equation.
8.38 Repeat Prob. 8.36 for the Navier-Stokes energy equation [Eq. (5.25)]. You may ignore all body forces and external heat transfer.
8.39 Work out the details for a velocity correction procedure for the 3-D parabolic procedure for an incompressible flow in a rectangular channel. Use both the $\hat{\phi}$ potential and p' methods. Employ a staggered grid.
8.40 Write the y momentum equation in finite-difference form for the PPNS model following the strategy outlined in Section 8.4.3 for the x momentum equation.
8.41 Prove that the formulation described for the Poisson equation for pressure in the PPNS model satisfies the constraint

$$\iint S_p \, dx \, dy = \oint \frac{\partial p}{\partial n} \, dC$$

8.42 Suggest a way that the PPNS procedure might be extended to 3-D flows.
8.43 Explain how the velocity boundary conditions can be implemented for a boundary that is a line of symmetry (such as the centerline of a 2-D channel) when a staggered grid is used for the PPNS momentum equations. Explain in terms of the Thomas algorithm.
8.44 The incompressible partially parabolized Navier-Stokes momentum equations are given below for a flow predominantly in the positive x direction:

$$\underbrace{u\frac{\partial u}{\partial x}}_{\text{term C}} + v\frac{\partial u}{\partial y} = \underbrace{-\frac{1}{\rho}\frac{\partial p}{\partial x}}_{\text{term A}} + \nu\frac{\partial^2 u}{\partial y^2}$$

$$\underbrace{u\frac{\partial v}{\partial x}}_{\text{term B}} + v\frac{\partial v}{\partial y} = -\frac{1}{\rho}\frac{\partial p}{\partial y} + \nu\frac{\partial^2 v}{\partial y^2}$$

The equations are to be solved by a coupled space-marching fully implicit scheme. Assume that the unknowns are to be solved at the $i + 1$ marching station, $k + 1$ marching sweep.

(a) Explain how term A is to be treated in the discretization. Give an appropriate difference representation.

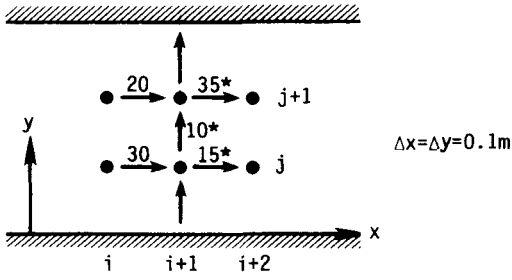

Figure P8.1

(*b*) Use Newton linearization to obtain a representation for term B that is linear in the unknown values of u and v.

(*c*) Give a difference representation for term C that is appropriate for use in a small region of recirculation where $u < 0$. Apply Newton linearization.

8.45 The partially parabolized Navier-Stokes equations are being solved on a uniform staggered grid for a steady laminar incompressible flow by the method described in the text. Provisional velocities (in m/s) have been obtained at the $i + 1$ marching level, and these are indicated by an asterisk in Fig. P8.1. Use the velocity potential method to determine velocity corrections that must be added to the three provisional velocities so that mass is conserved. Note that velocities on the upper and lower boundaries are fixed by the boundary conditions to be zero (no slip), so that no corrections are needed for these.

8.46 Suggest an implicit discretization scheme to implement a coupled space-marching procedure for the PPNS equations given by Eqs. (8.155)–(8.159) for subsonic applications. Use Newton linearization. Explain how the linear equations can be solved.

8.47 Suggest appropriate boundary conditions for solving the PPNS equations given by Eqs. (8.155)–(8.159) by an implicit scheme on a rectangular domain for the following problems. State the conditions needed when the viscous term in the y momentum equation is (1) included; (2) omitted.

(*a*) developing flow in a 2-D channel

(*b*) flow over a flat plate of finite length

8.48 Apply the transformation

$$\alpha = x^*$$

$$\beta = \frac{y^*}{x^*}$$

$$\gamma = \frac{z^*}{x^*}$$

$$\tau = t^*$$

to Eq. (8.173) and derive the "conical" Navier-Stokes equations that can be used to compute a solution at the station $x = L$, where $\alpha = x^* = 1$.